ELECTROMECHANICS OF DIELECTRIC PARTICLES IN DIELECTRIC LIQUIDS ACTED ON BY A MICROELECTRODE ARRAY

A Dissertation

by

CHEONG SOO SEO

Submitted to the Office of Graduate Studies of
Texas A&M University
in partial fulfillment of the requirements for the degree of

DOCTOR OF PHILOSOPHY

December 2005

Major Subject: Aerospace Engineering

ELECTROMECHANICS OF DIELECTRIC PARTICLES IN DIELECTRIC LIQUIDS ACTED ON BY A MICROELECTRODE ARRAY

A Dissertation

by

CHEONG SOO SEO

Submitted to the Office of Graduate Studies of
Texas A&M University
in partial fulfillment of the requirements for the degree of

DOCTOR OF PHILOSOPHY

Approved by:

Chair of Committee,	James G. Boyd IV
Committee Members,	Dimitris C. Lagoudas
	John D. Whitcomb
	Won-jong Kim
Head of Department,	Helen Reed

December 2005

Major Subject: Aerospace Engineering

ABSTRACT

Electromechanics of Dielectric Particles in Dielectric Liquids Acted on by a Microelectrode Array. (December 2005)

Cheong Soo Seo, B.S. Sung Kyun Kwan University;

M.S., Sung Kyun Kwan University

Chairman of Advisory Committee: Dr. James G. Boyd IV

Arrays of microelectrodes were used to apply forces to dielectric (soda lime glass) spheres in a thin (200 micrometer thick) layer of a dielectric liquid polymer (EOPN 8021). The microelectrodes were fabricated using standard photolithographic methods of evaporating and electroplating gold onto a glass substrate. The objective is to use the electric body forces in the sphere and the electric surface tractions on the sphere to position the spheres in a microscale pattern, in this case a square array in-plane.

Three sizes of spheres were used: 30, 90, and 170 microns in diameter. The 30 micron spheres formed clusters associated with the regions of highest electric energy density, whereas single 90 micron spheres were located at the regions of highest electric energy density. The 170 micron spheres generally did not form patterns. The experiments indicated that free charges, either in the volume of the sphere and/or on the sphere surface, significantly influence the motion of the sphere.

A finite element analysis was performed to study the electro-fluid mechanics. The liquid velocity and streamlines were plotted, and the force resultants due to the liquid acting on the sphere were calculated. Also, the electric body force and surface

tractions resultants were calculated. In general, the forces on the sphere and the liquid velocity are in agreement with the experimental results.

DEDICATION

To my wife, Jennifer Yujung, family, and friends

TABLE OF CONTENTS

Page

LIST OF FIGURES

FIGURE Page

LIST OF TABLES

1. INTRODUCTION

1.1 Motivation for the Present Research

At the most fundamental level, the properties of any device depend on what materials the device is made of and how these materials are spatially arranged. With respect to composite materials, the ability to precisely control the position of various particles – dielectric, piezoelectric, non-magnetic conductors, paramagnetic, ferromagnetic, and permanent magnetic – may allow for novel material symmetries and coupling coefficients between mechanical, electrical, magnetic, optical, thermal, and transport properties in structural and biological materials, sensors, and actuators. Furthermore, relative to random microstructures, a patterned microstructure should exhibit reduced field concentrations, thereby resulting in larger threshold values, including mechanical strength, electric breakdown field, and magnetic saturation field.

The ability to control the orientation and pattern of both piezoelectric and magnetostrictive particles will enable coupling between the effective (or macroscopic) stress, electric field, and magnetic field. For example, the coupled effective constitutive response of a polymer reinforced with piezoelectric and magnetostrictive particles is given by

$$\begin{pmatrix} e \\ D \\ H \end{pmatrix} = \begin{bmatrix} S & \alpha & \beta \\ \alpha & \varepsilon & \delta \\ \beta & \delta & \frac{1}{\mu} \end{bmatrix} \begin{pmatrix} T \\ E \\ B \end{pmatrix} \tag{1.1}$$

This dissertation follows the style of *Smart Materials & Structures*.

in terms of matrix representation of tensors quantities *E*, the (3x1) electric field vector, *B*, the (3x1) magnetic field vector, *T*, the (6x1) Cauchy stress tensor, *e*, the (6x1) strain tensor, *D*, the (3x1) electric displacement vector, *H*, the (3x1) magnetic field intensity vector, *S*, (6x6) the elastic compliance tensor, ε , the (3x3) electric permittivity, μ , the (3x3) magnetic permeability, and α (6x3) and β (6x3) account for piezoelectricity and piezomagnetism, respectively.

The parameter δ (3x3) is a novel coefficient that couples the electric and magnetic fields even at low frequencies, and even for static fields. This form of static electromagnetic coupling is due to the fact that an applied *E* causes the piezoelectric particles to strain the polymeric matrix, thereby inducing a strain in the piezomagnetic particles, which induces an *H*. Similarly, an applied *B* would cause the piezomagnetic particles to strain the polymer matrix, thereby inducing a strain in the piezoelectric particles, which induces a *D*. In effect, the *E* and *B* fields are coupled at the microlevel though the strain in the polymer matrix. (Lee et al, 2005).

This static coupling should not be confused with the high-frequency coupling of *E* and *B* in Faraday's law, which couples the curl of *E* to the time rate of change of *B*, and Ampere's law, which couples the curl of *B* to the time rate of change of *E*. These Faraday/Ampere coupling effects are negligible at low frequencies. Because Faraday's law and Ampere's law are fundamental laws of nature, they are independent of the material properties. In contrast, the electro-magnetic coupling of equation (1.1) is due entirely to the properties of the multi-functional material.

Currently there is no way to affordably arrange particles and whiskers in microscale patterns in composite materials.

Although it is not proven in this dissertation, affordable microscale patterning of different types of particles in polymers may enable the design of new multifunctional materials with: (1) novel coupling between electric, magnetic, mechanical (Lee et al, 2005), thermal, and optical properties; (2) structural materials with reduced stress concentrations and therefore longer fatigue life; (3) control of residual stresses, both thermal and curing-induced; (4) simultaneous sensing with electric (magnetic) fields while actuating with magnetic (electric) fields (Lee et al, 2005); (5) controlled reflection and adsorption of electromagnetic radiation (Neekalanta, 1995) ; (6) microscale control of the poling direction of piezoelectric and permanent magnetic particles; (7) control of diffusion coefficients; (8) anisotropy of electrical conductivity; (9) control of thermal expansion and thermal conductivity; and (11) multi-functional properties in preceramic polymers which can be fired to obtain multi-functional ceramic materials.

1.2 A Proposed Composites Processing Method

It may be possible to use large arrays of programmable electrodes and electromagnets to achieve affordable micro scale positioning of particles, whiskers, and chopped fibers in polymer matrix multi-functional materials. As shown in Figure 1.1, Arrays of electrodes and electromagnets are placed above and beneath thin layers of a random particle-filled liquid polymer. Microscale variations in the electric and magnetic fields may be used to pattern the dielectric and magnetic particles, respectively. The polymer is then solidified, either frozen as a “prepreg” or cured, by heating or UV light.

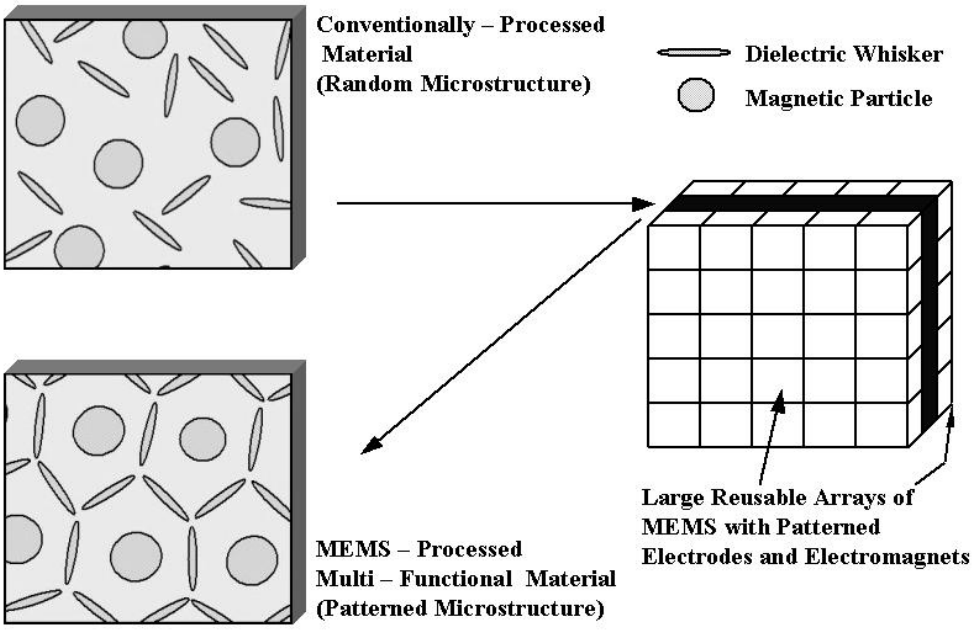

Figure 1.1 Large Reusable Arrays of Electrodes and Electromagnets Used to Pattern Particles on the Microscale

The basic scheme of particle manipulation is shown below in Figure 1.2, which shows a cross section of a thin liquid layer with arrays of electrodes and electromagnetic conductors on the top and bottom. The conducting lines are shown going into the page and out of the page. The magnetic field lines (B) curl around the conductors, and the electric field lines (E) are controlled by the electrodes. The disturbance of these fields by the particles is not indicated on the schematic.

The fabrication process of the large arrays of electrodes and electromagnets should be affordable because photolithography can be used to make massive arrays of electrodes and electromagnets with features as small as one micrometer at low unit cost.

The electrodes and electromagnets are not part of the final product, and they should be reusable.

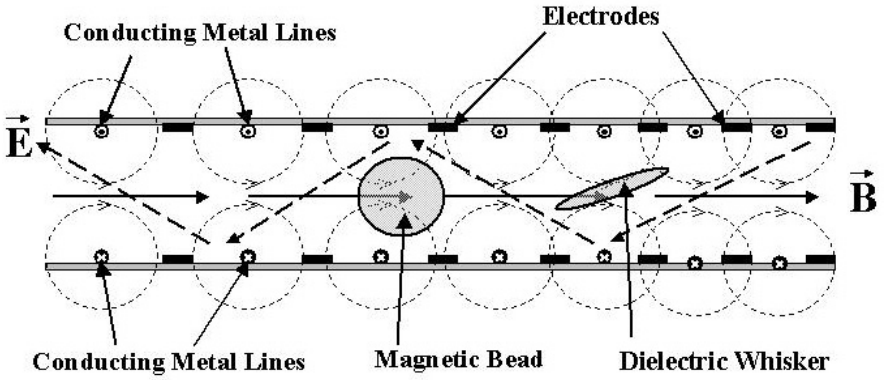

Figure 1.2 Array of Electrodes and Electromagnets

1.3 Literature Review of Dielectrophoresis and Magnetophoresis as Applied to Composite Materials Processing

Bowen et al (1993, 1994, 1995) used macroscopic unidirectional electric fields to align piezoelectric particles in a polymer melt. The dielectrophoretic effect aligns the particles in long, unidirectional chains. It was demonstrated that electric fields can be used to unidirectionally align many dielectric and piezoelectric particles, including $BaTiO_3$, $PbTiO_3$, $Pb(ZrTi)O_3$, $SrTiO_3$, $Ba_2TiSi_2O_8$, ZrO_2, TiO_2, and SiO_2, in several polymeric liquids, including polyurethane, silicone elastomer, Eccogel epoxy, Epon epoxy, and Norland optical adhesive. This work was motivated by the fact that in the early 1990s continuous fiber piezoelectric materials were not available. Now that continuous piezoelectric fibers are available there is no need to perform unidirectional

alignment of piezoelectric particles. (Rossetti et al, 2000; Janos et al, 2000; Cornejo et al, 2000). Furthermore, did not pattern the particles on the microscale.

Magnetostrictive material (Terfenol-D) is not available in fiber form. Thus in order to form quasi-fibrous magnetostrictive composites, McKnight and Carman (2000) used static, macroscopic magnetic fields to align magnetostrictive particles in liquid vinyl ester resin prior to curing the resin. Although this procedure is novel in that it is the only reported case of using magnetic fields to align magnetostrictive particles into quasi-fibers, McKnight and Carmen, like Bowen and coworkers, did not pattern the particles on the microscale.

In the last decade there has been a growing effort to manipulate biological cells and particles in micro-fluidic devices. This effort is motivated by the need to detect biowarfare agents, automate DNA analysis and cytology, and control cells for artificial tissues. Advances in microfabrication methods for MEMS have achieved micrometer precision for massively parallel fabrication, and have therefore made these micro-fluidic efforts economically feasible. Early efforts include the electrical manipulation of cells and macromolecules by Washizu and coworkers (1990, 1992) and Fuhr and Shirley (1995). Each group used electrode arrays to generate electric fields to control individual mammalian cells (approximately 30 micrometers in diameter) in a liquid. Washizu's work has demonstrated the need for accurate design of the electrode curvature with respect to the cell size in order to prevent the cell from becoming trapped in a "dead" zone. Microfabricated flow cytometry devices have recently been made (Sobek et al, 1994). These efforts are still in their early stages, they are focused on biological cells, and they use electric fields only.

Ahn and Allen (1994) electroplated conducting coils to make an electromagnet to attract magnetic beads for biochemical analysis. However, there was no attempt to pattern magnetic beads, and the results were qualitative only.

The previous studies dealt with micron-sized particles in water, but Muller and coworkers (1996) and Green et al (1995) and Green and Morgan (1997) demonstrated that dielectrophoresis can be used to manipulate viruses as small as 100 nm and latex spheres as small as 14 nm in water.

1.4 Outline of the Dissertation

The forces on particles in liquids acted on by electric and magnetic fields are reviewed in Section 2, Analytical Fundamentals. The fabrication of the electrode arrays is discussed in Section 3. Experimental results are presented in section 4, and these results are discussed and modeled in Section 5. Conclusions and recommendations for future work are presented in Section 6.

1.5 Contributions and Limitations of the Dissertation

1.5.1 Limitations of the Dissertation

For completeness and motivation of future studies, the Introduction and Analysis sections include discussions of both electric and magnetic effects. However, the experiments and discussion of results include only the electric effects, i.e. there are no magnet arrays or magnetic particles.

Commercially available finite element codes were used to study the mechanics of dielectric particles in liquids. However, there was no attempt to predict the pathlines of

the particles. This extremely complex problem would necessitate further research with an emphasis on computational fluid dynamics and finite element methods with automatic mesh regeneration to account for particle motion. Even then, the problem may be too sensitive to the initial positions of the particles to allow for meaningful predictions of particle pathlines.

1.5.2 Contributions of the Dissertation

The experimental and analytical work reported herein is evidently the first attempt to use arrays of microelectrodes to pattern particles in polymer matrix composite materials. As discussed in Section 1.1, significant technological benefits may result from the ability to pattern particles in liquid polymers.

A fabrication method was developed to make arrays of electrodes and electromagnets that are compatible with the cleaning methods used to remove liquid polymers from surfaces. Thus, the arrays should be reusable.

2. ANALYTICAL FUNDAMENTALS

2.1 Review of Forces on Particles

Particles in a liquid polymer medium experience several forces. These forces include the electromagnetic body force due to the applied electric and magnetic fields, the electro-magnetic surface traction force related to the difference in electric and magnetic fields between the particle and the liquid, the gravitational sedimentation force, and the pressure and viscous drag force from the surrounding liquid. In addition to these forces, there may exist other forces such as the force induced by the Brownian motion, the force related to the Gouy-Chapman double layer of positive and negative charge in the surrounding liquid, the Van der Waals force, etc.

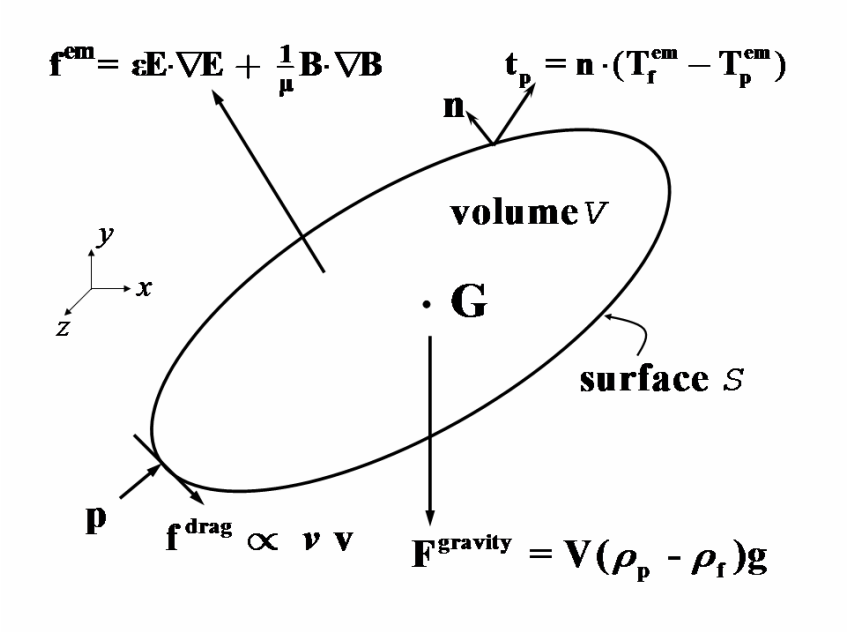

Figure 2.1 Free-Body Diagram of a Particle in a Liquid Polymer

The free-body diagram of a particle in a liquid is shown in Figure 2.1, including the viscous drag force f^{drag} per unit area, the pressure *P*, the electromagnetic body force f^{em} per unit volume, the mechanical surface traction t_p, the gravitational sedimentation force $F^{gravity}$ and the outer unit normal *n* to the particle surface. The particle is modeled as a rigid body. These forces are individually reviewed.

Although magnetic forces are not included in the experiments or discussion of results, the magnetic forces are included in this review of forces.

2.1.1 Static Pressure Forces

A static pressure acts on the particle even when the particle and the liquid have zero velocity. If the static pressure is homogeneous in the liquid, then there is no pressure resultant force on the particle. However, a gradient of the static pressure in the liquid could cause a nonzero pressure resultant force on the particle.

2.1.2 Viscous Forces

The viscous force exerted on the particle by the liquid is proportional to the liquid viscosity ν and the local relative velocity v between the particle and the liquid:

$$F^{viscous} \propto \nu v \tag{2.1}$$

For a spherical particle of radius *a*, the total viscous force is given by

$$F^{viscous} = 6\pi\nu a v \tag{2.2}$$

Two-thirds of this force is due to the tangential component of the viscous force, and one-third is due to the pressure component [White, 1991].

2.1.3 Electric and Magnetic Forces on the Particle: Dielectrophoresis

There are two types of electromagnetic forces acting on the particle, the surface traction per unit area t_p^{em} and the electromagnetic body force per unit volume f^{em}. The electromagnetic surface traction (Maugin, 1988):

$$t_p^{em} = n \cdot T_p^{em} \tag{2.3}$$

where

$$T^{em} = \varepsilon EE + \frac{1}{\mu} BB - \frac{1}{2}(\varepsilon_0 E^2 + \frac{1}{\mu} B^2) \tag{2.4}$$

ε is the electric permittivity, μ is the magnetic permeability, ε_0 is the permittivity of vacuum, μ_0 is the permeability of vacuum. The electromagnetic body force per unit volume f^{em} is due to the product of the electric and magnetic fields with the field gradients (Jackson, 1975; Maugin, 1988):

$$f^{em} = \nabla \cdot T^{em} = \varepsilon E \cdot \nabla E + \frac{1}{\mu} B \cdot \nabla B \tag{2.5}$$

t_f and t_f^{em} are mechanical surface traction per unit area and the electromagnetic surface traction in the liquid, respectively. Therefore the total force F_p acting on the particle can be calculated by integrating over the particle surface boundary

$$F_p = \int_s t_p + t_p^{em} ds = \int_s t_p ds + \int_s n? \quad {}_p^{em} ds = \int_s t_p ds + \int_V \nabla \cdot T_p^{em} dv$$
$$= \int_s t_p ds + \int_V f_p^{em} dv \tag{2.6}$$

In general, t_p is determined by the solution of the elastic problem within the body. In this case, however, the body is considered to be rigid, so t_p must be determined using the following boundary condition on S:

$$t_p + t_p^{em} = t_f + t_f^{em} \tag{2.7}$$

The electric problem is solved for t_p and t_f^{em}. First, t_f is assumed to be zero, and t_p is given by

$$t_p = t_f^{em} - t_p^{em} \tag{2.8}$$

Then, the total force on the particle can be rewritten as

$$F_p = \int_s t_p + t_p^{em} ds = \int_s (t_f^{em} - t_p^{em}) ds + \int_s n? \quad {}_p^{em} ds = \int_s (t_f^{em} - t_p^{em}) ds + \int_V \nabla \cdot T_p^{em} dv$$
$$= \int_s (t_f^{em} - t_p^{em}) ds + \int_V f_p^{em} dv \tag{2.9}$$

The traction t_f is then determined by solving the fluid mechanics problem in the liquid surrounding the particle.

Dielectrophoresis does not include forces due to an electric field acting on a free charge, either within the volume or on the particle/liquid interface. If a free charge exists within the particle, then an additional term must be added to the body force. However, if a particle/liquid interfacial free charge is present, then its effects are included implicitly in the electric surface traction.

A basic motivation for this thesis is a belief that control of the micro scale electric and magnetic fields is superior to the macro scale control used by other researchers to align particles, as reviewed in the introduction chapter. The advantages of micro-fields over macro-fields are demonstrated by contrasting two example problems as follow.

(A) *First*, consider the case of two dielectric spheres of radius *a* separated by a distance R, subjected to a far electric field *E* (Figure 2.2). The two spheres disturb the applied uniform far field *E* (macroscopic field) in such a way as to induce an attractive force between the spheres, leading to dielectrophoresis and alignment of long particle chains. The force acting between the two spheres is given by (Bowen et al 1994)

$$F^{em} = \frac{24a^6\varepsilon_f}{R^4}\left(\frac{\varepsilon_p - \varepsilon_f}{\varepsilon_p + 2\varepsilon_f}\right)E^2 \tag{2.10}$$

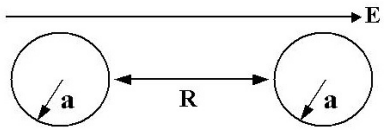

Figure 2.2 Two Dielectric Spheres under a Uniform Applied Electric Field

When this body force is in equilibrium with the viscous force on each sphere (neglecting inertial forces), the resulting relative velocity v between the liquid and the spheres is given by

$$v = \frac{4a^5\varepsilon_f}{\pi R^4 v}\left(\frac{\varepsilon_p - \varepsilon_f}{\varepsilon_p + 2\varepsilon_f}\right)E^2 \tag{2.11}$$

Consider the equilibrium speed for the case of two spheres of $BaTiO_3$ (with a relative permittivity of 1000), radius a = 10 micrometers, separated by R = 30 micrometers, in silicone with relative permittivity of 4 and a viscosity ν = 1.0 Pa-s, with $E = 1.0\times10^6$ V/m. The resulting equilibrium speed is 6 micrometers/second. This is the method of unidirectional particle alignment used by Bowen et al (1993, 1994, 1995). The maximum force on the particles is limited by the electric breakdown threshold of the liquid. The breakdown threshold is the maximum value for E that can be applied before a material's dielectric properties "break down", or fail, and the previously-dielectric material becomes an electronic conductor. Electric breakdown normally damages the material (Moulson and Herbert, 1990).

(B) *Second*, we contrast the previous problem of two spheres interacting in a uniform far field E with the case of a single sphere in an average field E and field gradient ∇E (Figure 2.3). The total electric force on a single sphere of radius a is given by the approximate solution (Jones, 1995; Giner et al, 1995),

$$F^{em} = 4\pi a^3 \varepsilon_f \left(\frac{\varepsilon_p - \varepsilon_f}{\varepsilon_p + 2\varepsilon_f} \right) E \nabla E \tag{2.12}$$

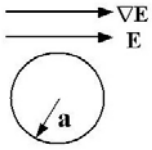

Figure 2.3. A Sphere under a Uniform Electric Field Gradient

When this force is in equilibrium with the viscous force on a sphere, the resulting relative velocity v between the liquid and the sphere is given by

$$v=\frac{2}{3}\frac{a^2}{\nu}\varepsilon_f\left(\frac{\varepsilon_p-\varepsilon_f}{\varepsilon_p+2\varepsilon_f}\right)E\nabla E \qquad (2.13)$$

Consider the equilibrium speed for the same parameters as the first problem: $BaTiO_3$ with a relative permittivity of 1000, a sphere of radius a = 10 micrometers in silicone with relative permittivity of 4 and a viscosity ν = 1.0 Pa-s, with $E = 1.0\times10^6$ V/m. Now let $\nabla E = 1.0\times10^{10}$ V/m^2. The resulting equilibrium speed is 200 micrometers/second! Thus, although the two examples use the same field E, the enormous field gradient ∇E in the second example results in a particle speed that is thirty times faster than the two-sphere interaction problem.

It is not possible to apply extremely large field gradients ∇E on the macro scale, but it <u>is</u> possible to apply extremely large field gradients on the micro scale, for the following reason: When a large field gradient ∇E is integrated over a macro distance, the resulting field E will quickly exceed the electric breakdown threshold. In contrast, an extremely large ∇E is possible on the micro scale because it need be applied only over the distance of a single unit cell of particles! Such unit cells are typically less than 100 micrometers across. Thus, integration of a large ∇E over one unit cell produces only a small field E. Note that it is E, not ∇E, that causes electric breakdown. Thus, the use of microfabricated electrodes to create enormous field gradients enables large particle velocities at fields that are safely below the breakdown threshold.

In microelectronic circuits electric fields are commonly as high as 5.0×10^7, which occurs when a potential of 5 V is dropped across a 0.1 micrometer layer of glass insulation. The field gradient $\nabla E = 1.0\times10^{10}$ V/m^2 used in the second example occurs when a field of 1.0×10^5 V/m is added or subtracted over a distance of 10.0 micrometers, well above the 1.0 micrometer limit of photolithography. Thus, it is feasible to achieve very high field gradients.

Similar equations govern the motion of magnetic particles, with the permittivity replaced by the inverse permeability, and E and ∇E replaced by B and ∇E. For a sphere of a = 10 micrometers, ν = 1.0 Pa-s, $\boldsymbol{B}$ = 0.0004 T, ∇B = 40.0 T/m, the equilibrium speed of the sphere is 10 micrometers/second. A B of 0.0004T corresponds to a location 50 micrometers from a line conductor that is carrying a high current density in a cross section of 15 square micrometers.

The dielectrophoresis and magnetophoresis forces are unchanged if the polarity of the boundary conditions are reversed. For example, changing all 10V boundary conditions to -10V and all -10V to 10V will not alter the dielectrophoresis force. The proof is as follows: The Gauss law for a linear dielectric material with homogeneous permittivity can be solved for the electric potential using the method of separation of variables. This leads to a series solution for the electric potential in terms of a summation of the product of constant coefficients multiplied by spatial eigenfunctions. The boundary conditions appear only in the integrals that give the coefficients in the series. When the series solution for the electric potential is substituted into the equations for the dielectrophoresis force, both the body force and the surface traction, it can be

seen that this force is a quadratic function of the coefficients. Therefore, changing the sign of the coefficients does not change the sign of the dielectrophoresis force.

Because the direction of the dielectrophoresis force is invariant under a reversal of the polarity of the boundary potential, dielectrophoresis can be achieved with either DC or AC applied voltages. AC voltages are often used for the following reason: many applications of dielectrophoresis are for an aqueous environment. In water, a potential difference exceeding approximately 1.3V leads to electrolysis, a phenomena in which the liquid water molecule is split into hydrogen and oxygen gas molecules. This is undesirable in dielectrophoresis applications. However, if a high frequency AC voltage is used, the voltage threshold for electrolysis is higher than 1.3V. Liquid polymers do not undergo electrolysis, so it is not necessary to use AC voltages in this thesis work.

Dielectrophoresis can be either positive or negative dielectrophoresis. In positive dielectrophoresis, $\varepsilon^p > \varepsilon^f$, and particles are attracted to electric field intensity maxima and repelled from minima. In negative dielectrophoresis, $\varepsilon^p < \varepsilon^f$, and particles are attracted to electric field intensity minima and repelled from maxima.

Note that increasing the permittivity of the particle does not increase the force proportionally. In fact, the force is limited to the range

$$-0.5 \leq \left(\frac{\varepsilon_p - \varepsilon_f}{\varepsilon_p + 2\varepsilon_f} \right) \leq 1.0 \tag{2.14}$$

Compare the case of a soda lime glass particle (relative permittivity = 7.3) and a $BaTiO_3$ particle (relative permittivity = 1000) in a typical polymer resin (relative permittivity =

4). The dielectric force on the $BaTiO_3$ particle is only 4.6 times the dielectric force on the soda lime glass particle.

2.1.4 Sedimentation (Gravity) Forces

The net sedimentation force on the particle, which is due to the gravity, is given by

$$F^{gravity} = V(\rho_p - \rho_f)g \tag{2.15}$$

where V is the particle volume, ρ_p and ρ_f are the densities of the particle and fluid, and g is the gravitational acceleration.

2.1.5 Interfacial Charge and Electroosmosis

A body force exists on a free charge in the presence of an electric field. The naturally occurring ionization between polar liquids such as water and many materials, especially glass (SiO_2), leads to a local free charge near the water/glass interface. When an electric field is applied, the water flows, a phenomenon known as electroosmosis (Russel et al, 1989). Electroosmosis is a complicating factor in electrochemical processes such as electrophoretic separations, but electroosmosis is less significant with nonpolar liquids such as polymeric liquids.

2.1.6 Other Forces

Brownian motion is the random motion of particles due to the impact of thermally excited molecules from the surrounding liquid. This Brownian speed

(Batchelor 1976) is inversely proportional to the product of the particle radius and liquid viscosity, i.e. $(1/\mu a)$ 1/(a). However, for particles larger than 1 micrometer in a polymer liquid, which typically has a minimum viscosity of 1 Pa-s, the Brownian forces are many orders of magnitude smaller than the electric and magnetic forces applied by MEMS.

Particles in polar solutions develop a "Gouy-Chapman" double layer of positive and negative charge in the surrounding liquid. These charge clouds surround each particle, and the net force between particles is repulsive. The forces act over a distance of tens of nanometers. Charge clouds are more pronounced in aqueous and ionic solutions, and are of less importance in nonpolar liquids such as liquid polymers (Russel et al, 1989). The charge cloud forces are also much smaller than the electric and magnetic forces applied by MEMS.

Dispersion forces, also called van der Waals forces, between particles in solution arise due to the permanent dipoles in molecules or the fluctuating dipoles induced by photons. These are inevitably attractive, and vary as a/R^2, the particle radius divided by the square of the distance between particles. A multiplicative factor, the Hammaker constant, is normally small enough such that the dispersion forces are significant only for extremely close particles, i.e. for R=10nm. Fortunately, polymers prevent the particles from coming this close together and therefore stabilize particulate solutions against particle agglomeration (flocculation) (Russel et al, 1989).

2.2 A Single Particle in a Uniform Field with No Surface Free Charge Has Zero Body Force and Zero Surface Traction Resultant

Consider an isotropic particle of radius R in an externally applied field

$E_{ext}=k\bar{E}_{ext}$ that is uniform other than where it is disturbed by the particle. The center of the sphere is the origin of the coordinate system. The general solution of Laplace's equation in terms of Legendre polynomials P_n is given by

$$\phi_f = \sum_{n=0}^{\infty}\left(A_n r^n + \frac{B_n}{r^{n+1}}\right)P_n(\cos\theta) \tag{2.16a}$$

$$\phi_p = \sum_{n=0}^{\infty}\left(C_n r^n + \frac{D_n}{r^{n+1}}\right)P_n(\cos\theta) \tag{2.16b}$$

The boundary conditions are:

$$\left(\phi_f\right)_{r\to\infty} = -\bar{E}_{ext} z = -\bar{E}_{ext} r(\cos\theta) \tag{2.17}$$

$$\left(\phi_f\right)_{r=R} = \left(\phi_p\right)_{r=R} \tag{2.18}$$

$$\varepsilon_f\left(\frac{d\phi_f}{dr}\right)_{r=R} = \varepsilon_p\left(\frac{d\phi_p}{dr}\right)_{r=R} \tag{2.19}$$

At the center of the sphere *(r=0),* ϕ_p must not have a singularity.

Because of the first boundary condition and the fact that the Legendre functions are linearly independent, all coefficients A_n are zero except A_1, which has the value $A_1=-E_{ext}$. Because of the fourth boundary condition, all coefficients D_n are zero.

Therefore

$$\phi_f = \sum_{n=0}^{\infty}\frac{B_n}{r^{n+1}}P_n(\cos\theta) - \bar{E}_{ext} r\cos\theta \tag{2.20a}$$

$$\phi_p = \sum_{n=0}^{\infty} C_n r^n P_n(\cos\theta) \tag{2.20b}$$

Applying the second and third boundary condition to (2.20a) and (2.20b), we have for any of *n* except *n=1*:

$$\frac{B_n}{R^{n+1}} = C_n R^n \tag{2.21a}$$

$$-\varepsilon_f (n+1)\frac{B_n}{R^{n+2}} = \varepsilon_p n C_n R^{n-1} \tag{2.21b}$$

From (2.21a) and (2.21b) it follows that $B_n = 0$ and $C_n = 0$ for all values of *n* except *n*=1. When *n*=1,

$$\frac{B_1}{R^2} - \bar{E}_{ext} R = C_1 R \tag{2.22a}$$

$$\varepsilon_f \left(\frac{2B_1}{R^3} + \bar{E}_{ext} \right) = -\varepsilon_p C_1 \tag{2.22b}$$

Hence:

$$B_1 = \frac{\varepsilon_p - \varepsilon_f}{\varepsilon_p + 2\varepsilon_f} R^3 \bar{E}_{ext} \tag{2.23a}$$

$$C_1 = \frac{3\varepsilon_f}{2\varepsilon_f + \varepsilon_p} \bar{E}_{ext} \tag{2.23b}$$

Therefore the potential in the fluid and the particle are given by

$$\phi_f = \left(\frac{\varepsilon_p - \varepsilon_f}{\varepsilon_p + 2\varepsilon_f} \frac{R^3}{r^3} - 1 \right) \bar{E}_{ext} z \tag{2.24a}$$

$$\phi_p = -\frac{3\varepsilon_f}{2\varepsilon_f + \varepsilon_p} \bar{E}_{ext} z \tag{2.24b}$$

Which gives the following electric fields:

$$E_f = \left(\frac{\varepsilon_p - \varepsilon_f}{\varepsilon_p + 2\varepsilon_f} \frac{R^3}{r^3} - 1 \right) \bar{E}_{ext} k \tag{2.25a}$$

$$E_p = -\frac{3\varepsilon_f}{2\varepsilon_f + \varepsilon_p} \bar{E}_{ext} k \tag{2.25b}$$

The electric field is uniform in the particle, so the electric body force vanishes in the particle. At the surface of the sphere, r=R, and $E_p = E_f$, i.e. the electric field is continuous. Therefore, the electric surface traction vanishes at every point on the surface of the sphere. Therefore, there is no electric force on the particle.

2.3 A Single Particle in a Uniform Field with a Nonzero Surface Free Charge Has Zero Body Force but Nonzero Surface Traction Resultant

Consider an isotropic particle of radius R in an externally applied field $E_{ext} = k\bar{E}_{ext}$ that is uniform other than where it is disturbed by the particle. The particle carries a uniform surface free charge density q^{surf} . The total electric field at any point is given by the sum of the field E_{ext} and the field that is due to the disturbance by the particle. The field disturbance by the particle has two contributions: one as discussed in Section 2.2, and one due to the surface free charge. The field due to the surface charge is given by,

$$E_{out}^{surf} = \frac{q^{surf} R^2}{\varepsilon^f r^2} r \text{ , outside sphere} \tag{2.26a}$$

$$E_{in}^{surf} = 0 \text{ , inside sphere} \tag{2.26b}$$

These fields are added to (2.25) and the sum is used to calculate the electric body force in the particle and the electric surface traction on the particle surface. The sum of (2.25b) and (2.26b) is spatially uniform, so there is no electric body force in the particle. The surface traction is given by applying Cauchy's rule to equation (2.8)

$$t_p = n \cdot \left(\overset{f}{T}^{em} - \overset{p}{T}^{em} \right) \tag{2.27}$$

In index notation,

$$T_{ij}^{em} = \varepsilon E_i E_j - \frac{1}{2} \varepsilon_0 E_k E_k \delta_{ij} \tag{2.28}$$

For any infinitesimal surface *n*,

$$\mathrm{t}_x^{em} = \mathrm{n}_x \left(\overset{f}{T}_{xx}^{em} - \overset{p}{T}_{xx}^{em} \right) + \mathrm{n}_y \left(\overset{f}{T}_{yx}^{em} - \overset{p}{Ty}_{yx}^{em} \right) \pm \mathrm{n}_z \left(\overset{f}{T}_{zx}^{em} - \overset{p}{T}_{zx}^{em} \right) \tag{2.29a}$$

$$\mathrm{t}_y^{em} = \mathrm{n}_x \left(\overset{f}{T}_{xy}^{em} - \overset{p}{T}_{xy}^{em} \right) + \mathrm{n}_y \left(\overset{f}{T}_{yy}^{em} - \overset{p}{Ty}_{yy}^{em} \right) \pm \mathrm{n}_z \left(\overset{f}{T}_{zy}^{em} - \overset{p}{T}_{zy}^{em} \right) \tag{2.29b}$$

$$\mathrm{t}_z^{em} = \mathrm{n}_x \left(\overset{f}{T}_{xz}^{em} - \overset{p}{T}_{xz}^{em} \right) + \mathrm{n}_y \left(\overset{f}{T}_{yz}^{em} - \overset{p}{Ty}_{yz}^{em} \right) \pm \mathrm{n}_z \left(\overset{f}{T}_{zz}^{em} - \overset{p}{T}_{zz}^{em} \right) \tag{2.29c}$$

Rewriting with E_i and E_j and surface normal vector,

$$\mathrm{t}_x^{em} = \mathrm{n}_x \left(\begin{array}{l} \varepsilon^f E_x^f E_x^f - \frac{1}{2}\varepsilon_0 \left(E_x^f E_x^f + E_y^f E_y^f + E_z^f E_z^f \right) - \varepsilon^p E_x^p E_x^p \\ + \frac{1}{2}\varepsilon_0 \left(E_x^p E_x^p + E_y^p E_y^p + E_z^p E_z^p \right) \end{array} \right) + \mathrm{n}_y \left(\varepsilon^f E_x^f E_y^f - \varepsilon^p E_x^p E_y^p \right) + \mathrm{n}_z \left(\varepsilon^f E_x^f E_z^f - \varepsilon^p E_x^p E_z^p \right) \tag{2.30a}$$

$$\mathrm{t}_y^{em} = \mathrm{n}_x \left(\varepsilon^f E_y^f E_x^f - \varepsilon^p E_y^p E_x^p \right) + \mathrm{n}_y \left(\begin{array}{l} \varepsilon^f E_y^f E_y^f - \frac{1}{2}\varepsilon_0 \left(E_x^f E_x^f + E_y^f E_y^f + E_z^f E_z^f \right) - \varepsilon^p E_y^p E_y^p \\ + \frac{1}{2}\varepsilon_0 \left(E_x^p E_x^p + E_y^p E_y^p + E_z^p E_z^p \right) \end{array} \right) + \mathrm{n}_z \left(\varepsilon^f E_y^f E_z^f - \varepsilon^p E_y^p E_z^p \right) \tag{2.30b}$$

$$\mathrm{t}_z^{em} = \mathrm{n}_x \left(\varepsilon^f E_z^f E_x^f - \varepsilon^p E_z^p E_x^p \right) + \mathrm{n}_y \left(\varepsilon^f E_z^f E_y^f - \varepsilon^p E_z^p E_y^p \right) + \mathrm{n}_z \left(\begin{array}{l} \varepsilon^f E_z^f E_z^f - \frac{1}{2}\varepsilon_0 \left(E_x^f E_x^f + E_y^f E_y^f + E_z^f E_z^f \right) - \varepsilon^p E_z^p E_z^p + \\ \frac{1}{2}\varepsilon_0 \left(E_x^p E_x^p + E_y^p E_y^p + E_z^p E_z^p \right) \end{array} \right) \tag{2.30c}$$

The surface traction resultant F^{em} is defined by,

$$F^{em} = \int_A t^{em} dA \tag{2.31a}$$

$$F_x^{em} = \int_A t_x^{em} dA \tag{2.31b}$$

$$F_y^{em} = \int_A t_y^{em} dA \tag{2.31c}$$

$$F_z^{em} = \int_A t_z^{em} dA \tag{2.31cd}$$

The total surface tractions are calculated using the software “Maple” in Appendix B and Appendix C. In Appendix B, the sphere radius is treated as a parameter, whereas in Appendix C the sphere radius is equal to 85 micrometers. The relative permittivity of the sphere is 7.3 (for soda lime glass) and the relative permittivity of the fluid is 3.98 (EPON 8021 resin).

$$F_x = 0 \tag{2.32a}$$

$$F_y = 0 \tag{2.32b}$$

$$F_z = 1.233\text{x}10^{-7} q^{surf} \overline{E}_{ext} \tag{2.32c}$$

This force is discussed in Section 5.3.2

2.4 Creeping Flow with Electric Body Forces

Even in the absence of dielectric and magnetic particles, a liquid will convect due to body forces caused by gradients in the electric and magnetic fields. We assume that the liquid is an incompressible Newtonian fluid and that the inertial forces are negligible. The equation of motion is then given by (White, 1991)

$$0 = \nabla p + v\nabla^2 v + \varepsilon E \cdot \nabla E + \frac{1}{\mu} B \cdot \nabla B \tag{2.33}$$

Where, p is the pressure and v is the fluid velocity. The incompressibility condition is,

$$\nabla \cdot \mathrm{v} = 0 \tag{2.34}$$

The electric body force is determined by solving Gauss’ law,

$$\nabla^2 \phi = 0 \tag{2.35}$$

For a homogeneous isotropic medium with no free charge, and then determining the electric field from,

$$E = -\nabla \phi \tag{2.36}$$

The electric body force is then substituted into the linear momentum equation to solve for the pressure and the three components of the velocity. Note that, although the electric body force is a nonlinear function of the electric potential (and also the electric field), both Gauss' law and the linear momentum equations are linear because the electric body force in the linear momentum equation is a specified function, the "input" to the fluid mechanics problem.

3. FABRICATION

Fabrication was initially performed in facilities at Texas A&M University. A photograph of the electrodes and electromagnets is provided in Figure 3.1. Each unit cell is 200 micrometers wide.

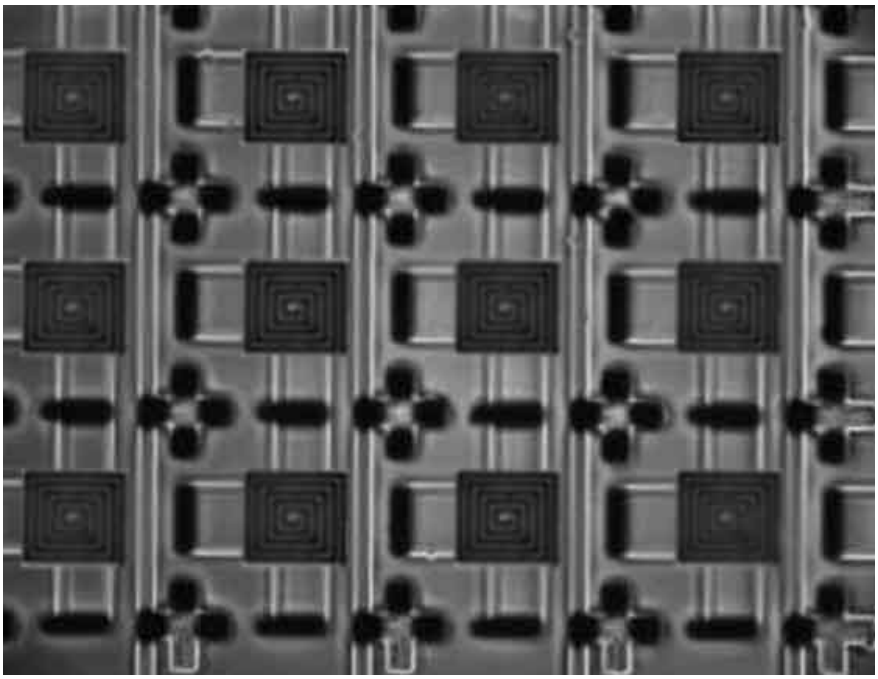

Figure 3.1 A Photograph of the Electrode and Electromagnet Arrays

A cross section of the electrodes and electromagnets is shown in Figure 3.2.

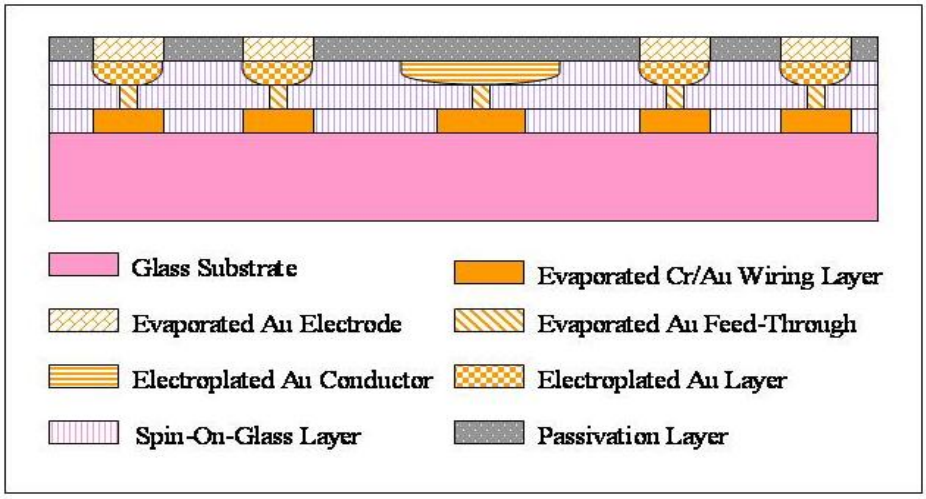

Figure 3.2 Cross Section of Electrodes and Electromagnets in the First Device Design (Not Drawn to Scale)

The fabrication process is shown in Figure 3.3. A 3 inch diameter Pyrex wafer (Corning 7740, 500μm thick) is used as a substrate material since the Pyrex is optically transparent which will allow the particles to be seen from below and electrically insulating at room temperature.

The first metal layer shown in Figure 3.4 is a wiring and electroplating seed layer. This layer is patterned using the liftoff process. A thin layer of positive photoresist is coated onto a 3 inch Pyrex wafer and patterned. An adhesion layer of 50nm of chromium is deposited by an evaporator at a rate of 1 Angstrom/second to form a chromium oxide layer, which provides strong bonding between the chromium layer and the Pyrex glass layer. One micrometer of gold is then evaporated at 1~2 Angstrom/second. Photoresist liftoff is used to pattern the Cr/Au layers. Before the Cr layer was evaporated, the Pyrex glass substrate was slightly etched with HF acid. This etching process is an isotropic process, and therefore undercuts the glass beneath the photoresist. These undercuts provide a discontinuity between the metal on the etched glass and the metal on

photoresist. As a result, the undercuts are able to promote the lift off process after Cr/Au evaporation.

Then, 1.8μm of Spin-On-Glass (SOG) is spin coated to electrically insulate (also called passivation) the metal layers. Honeywell Accuglass T512B SOG is used. With one coating process of T512B SOG, only 0.9μm can be deposited. Therefore, double coatings of the SOG are required. According to the manufacturer's technical specifications, after the SOG is spun onto the wafer at 1000rpm, the wafer should be continuously baked on hotplates at 80ºC, 150ºC, and 250ºC for one minute each. However, in our application, this procedure resulted in cracking and breaking of the wafer. Therefore, the wafer was baked in an oven at 220ºC, 50mmHg for 20 minutes. Then the SOG is cured in a nitrogen rich furnace at 425ºC.

To form the electrical connection between layers, etching of the SOG, followed by the photoresist process, metal evaporation, and liftoff process are consecutively carried out. Then another layer of SOG is formed. A gold seed layer for electroplating of gold electrodes and electromagnets is evaporated after the 3rd layer photoresist patterning and SOG etching. The SOG serves as the mold for electroplating. This electroplated layer of gold is thick enough to carry high electric current. Finally, the conductor and desired parts of the electrodes are electrically passivated SOG, so the particles and liquid polymer are exposed to electric potentials only where desired. That is, those parts of the electrodes are not passivated with SOG

All the components used in the microfabrication, such as Pyrex, SOG, chromium and gold, can withstand temperatures much higher than the maximum temperature used to process polymer. In addition, these materials can withstand the methods used to clean

the MEMS surface of residual polymer after use. The cleaning methods include wet and dry etching of residual polymer, used to “descum” or clean photoresist from CMOS components.

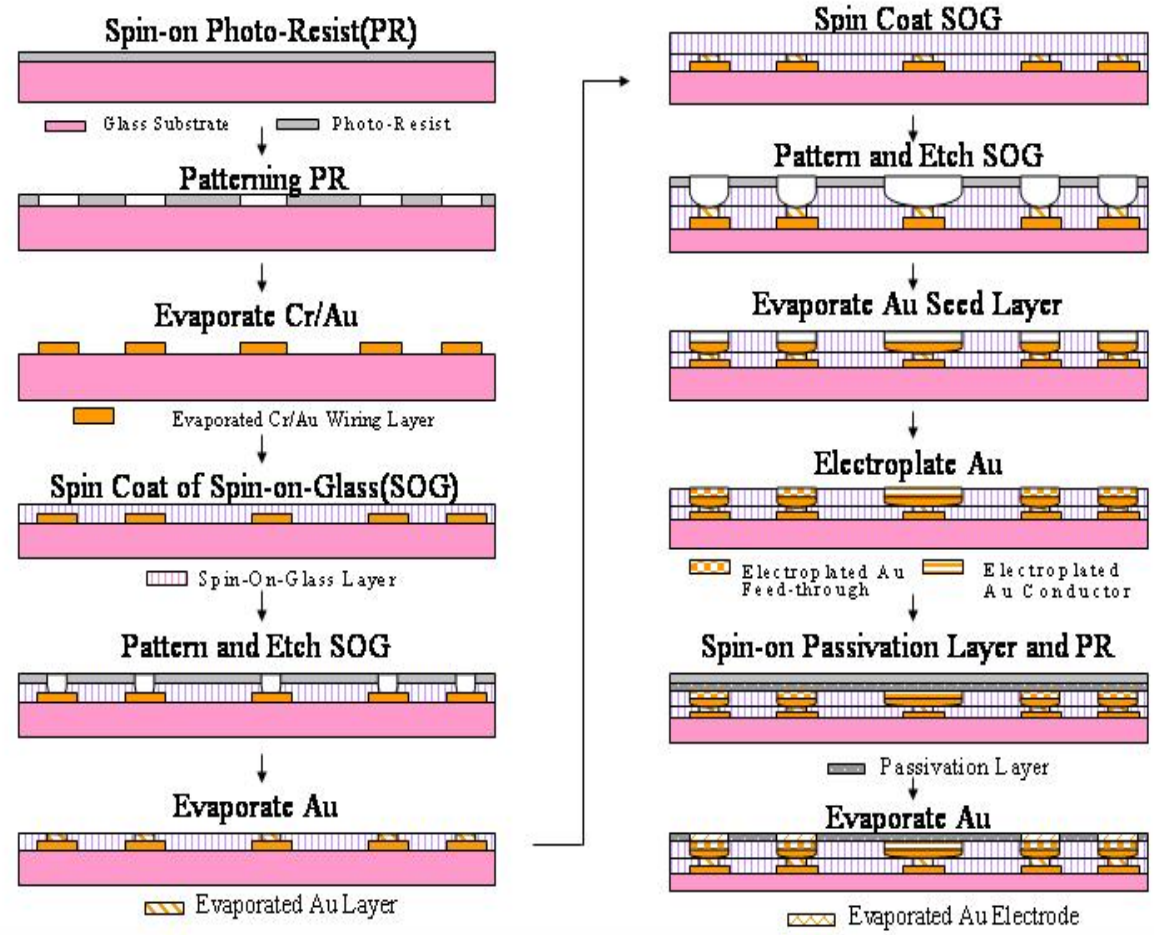

Figure 3.3 Fabrication Process of Arrays of Electrodes and Electromagnets in the First Device Design (Not Drawn to Scale)

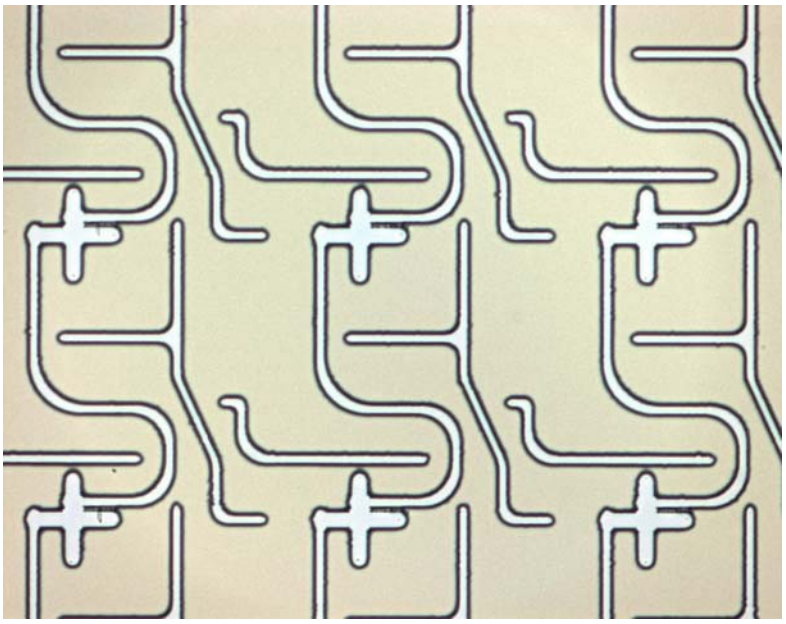

Figure 3.4 Wiring and Seed Layer

The device of Figure 3.4 had many incomplete conducting lines due to the large number of particles in the clean room. Particles can be seen in Figure 3.5.

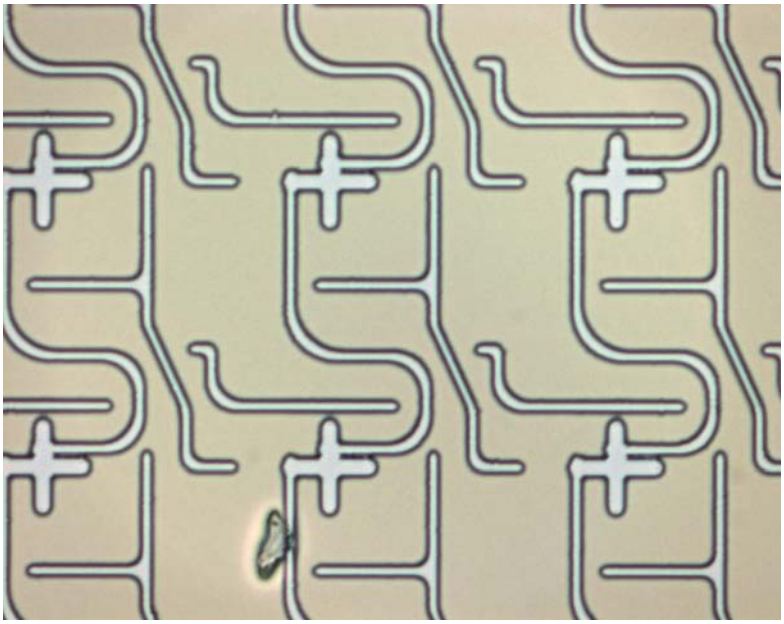

Figure 3.5 A Particle on a Conducting Line

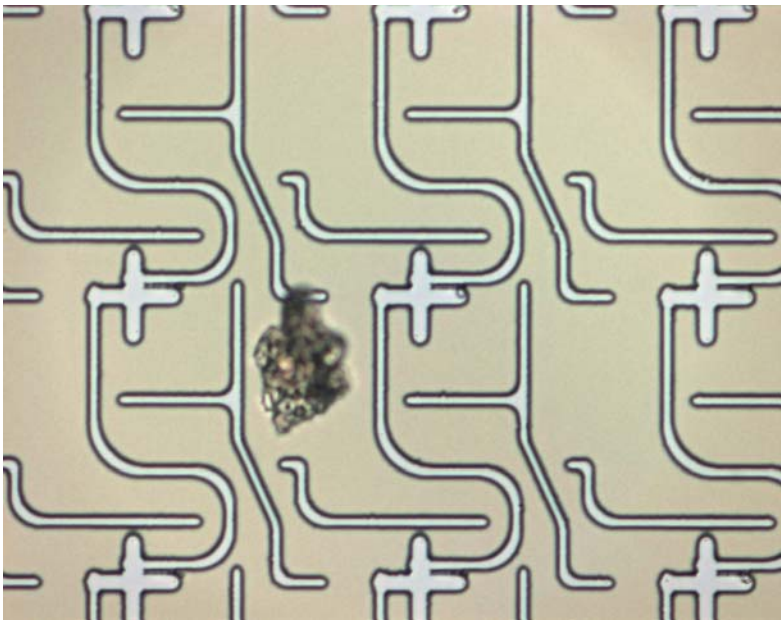

Figure 3.5 Continued

As seen in Figure 3.6, the particles damaged the conducting lines so much that the devices were not functional.

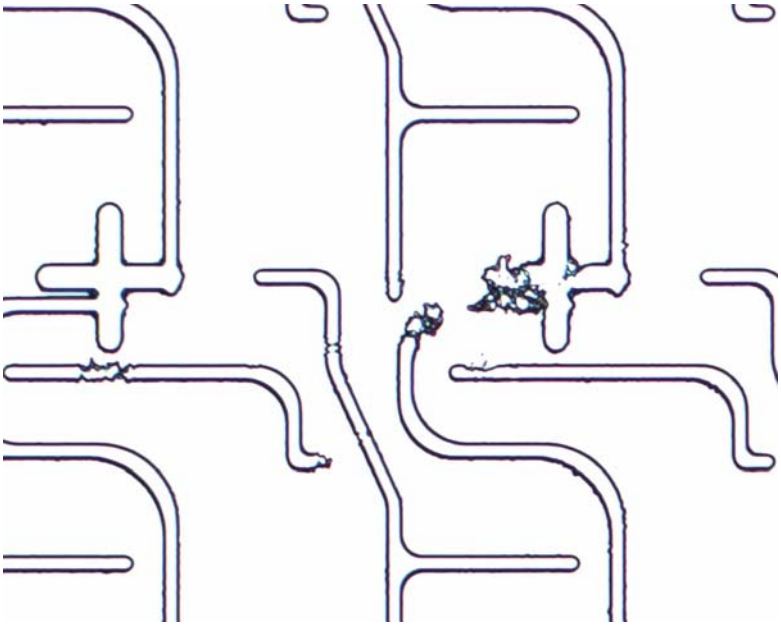

Figure 3.6 Damage to Conducting Lines

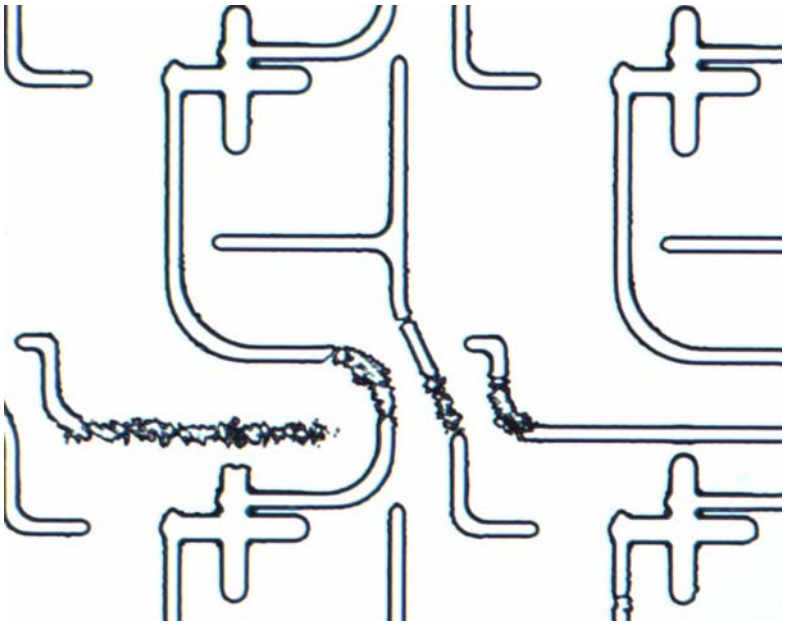

Figure 3.6 Continued

Because of these problems, the 2nd device design was made and the design has several different in-plane shapes, but the same in out-of-plane process. The fabrication of the device explained in Figure 3.7 was done at the University of Texas at Dallas. The process was modified as described below. SU-8 is a negative photosensitive epoxy. Although the 1st original device design have both electrodes and electromagnets, since the fabrication of the 1st device was not completed and available magnetic spheres are not found, only an electrode array in the 2nd device was actually made.

Only electrode arrays were used in the experiment. A three dimensional view of the electrodes is shown in Figure 3.8. Four types of electrode arrays are shown in Figure 3.9. In Figures 3.9(c) and 3.9(d), the electrodes and wiring layer are at the same level, or height out of plane. In Figures 3.9(a) and 3.9(b), the electrodes are 2.0 microns high, and

the wiring layer is 1.0 micrometer high. Picture of the fabricated devices are shown in Figure 3.10.

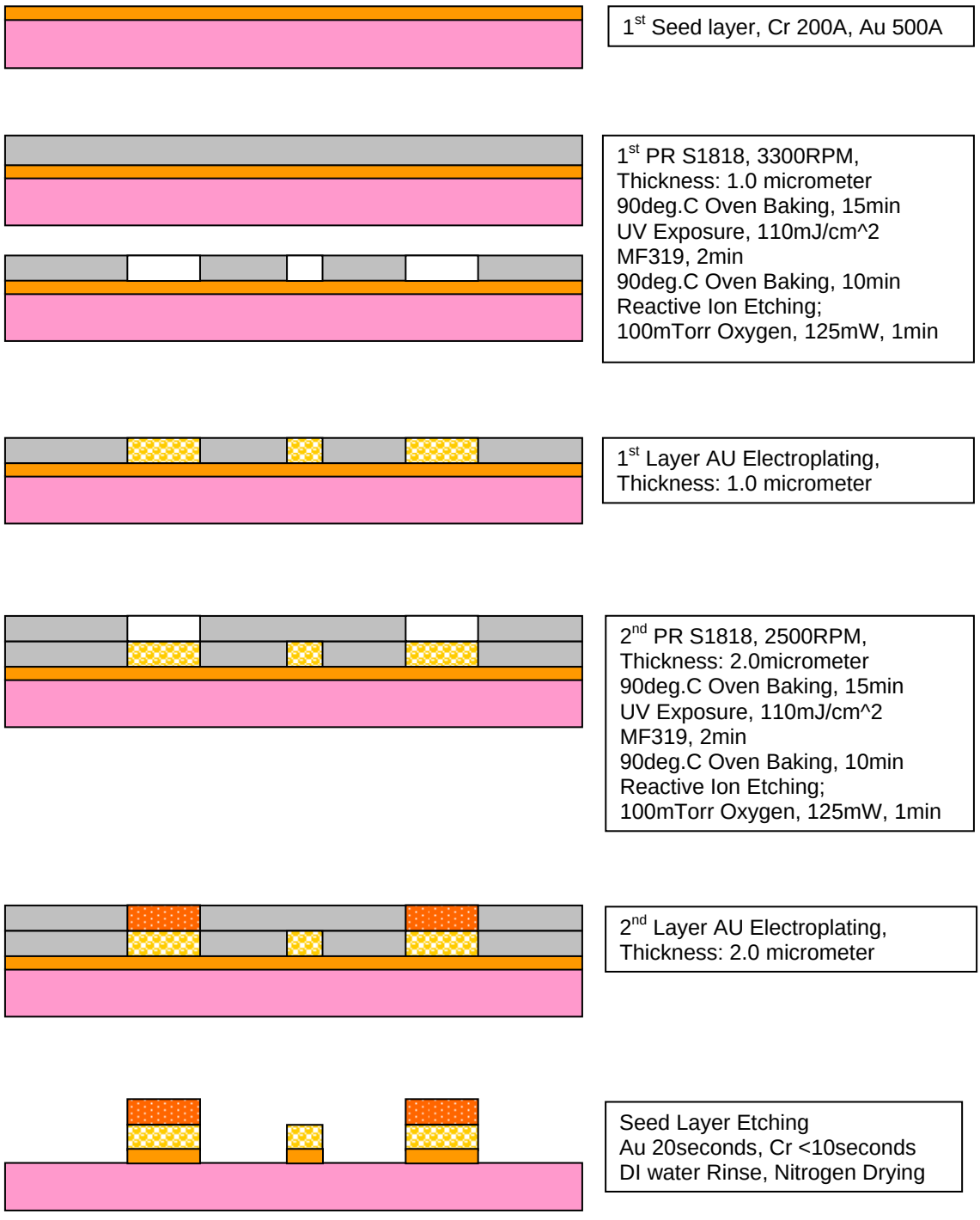

Figure 3.7 Fabrication Process

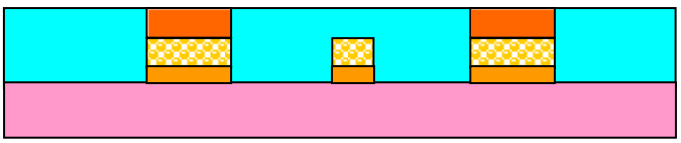

SU-8 2005 Coating, 3500rpm,
Thickness 3micrometer
Soft Bake on hotplates
65deg.C for 1min, 95deg.C for 2min
Reactive Ion Etching;
100mTorr Oxygen, 125mW, 1min

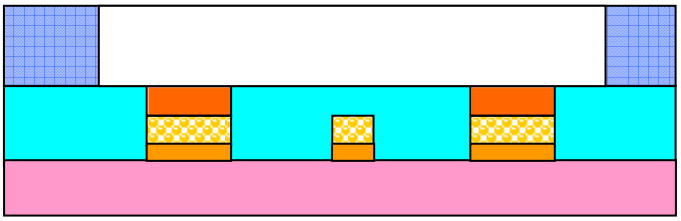

SU-8 2100 Coating, 1000rpm,
Thickness: 200micrometer
Soft Bake on hotplates
65deg.C for 5min, 95deg.C for 45min

Figure 3.7 Continued

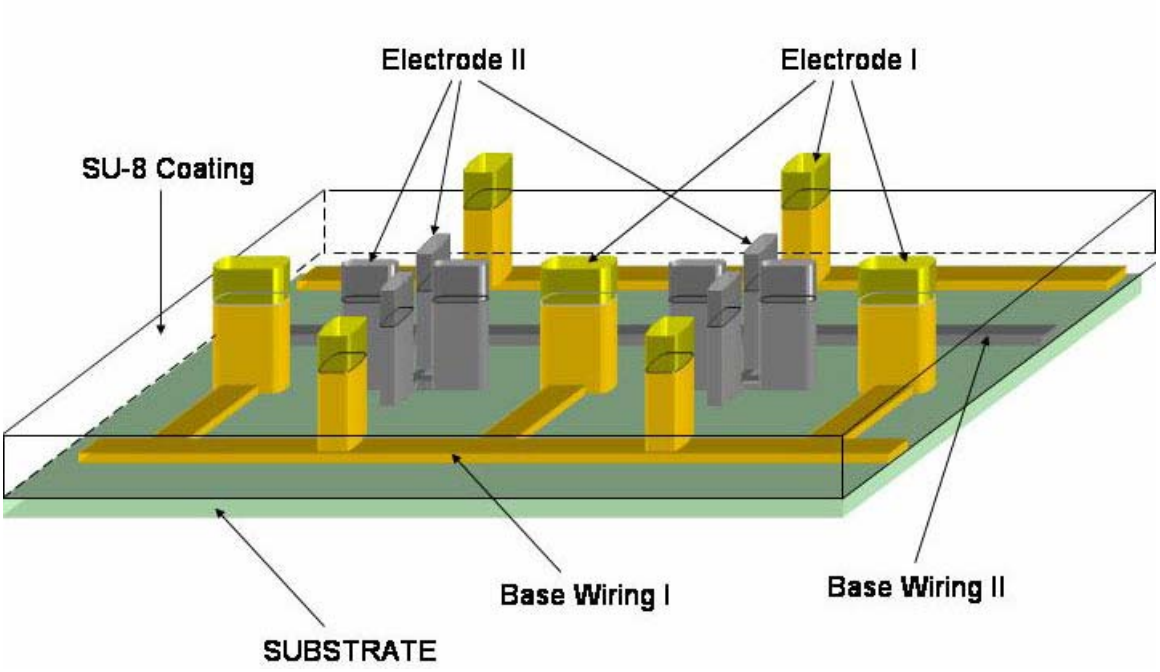

Figure 3.8 Three Dimensional View of Electrodes

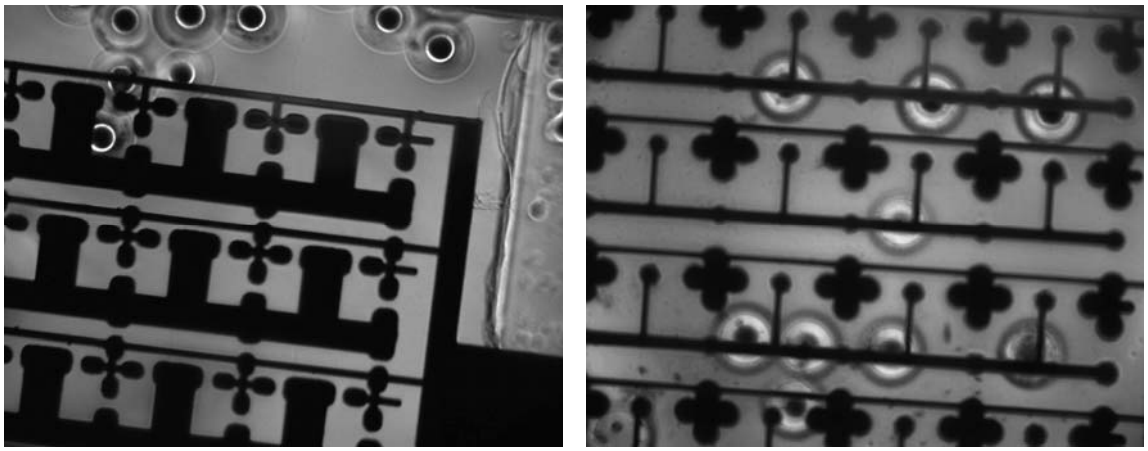

(a) Type-I **(b) Type-II**

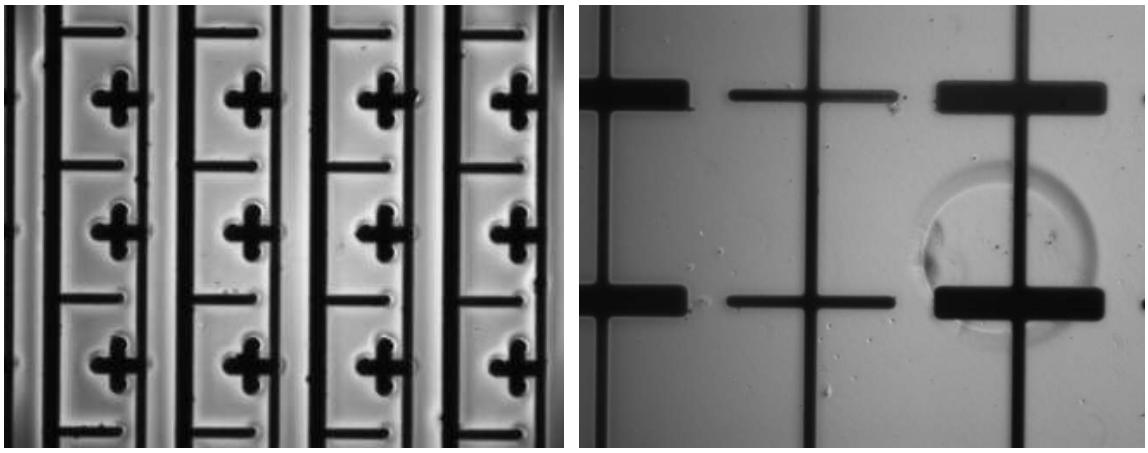

(c) Type-III **(d) Type-IV**

Figure 3.9. Four Types of Electrode Arrays

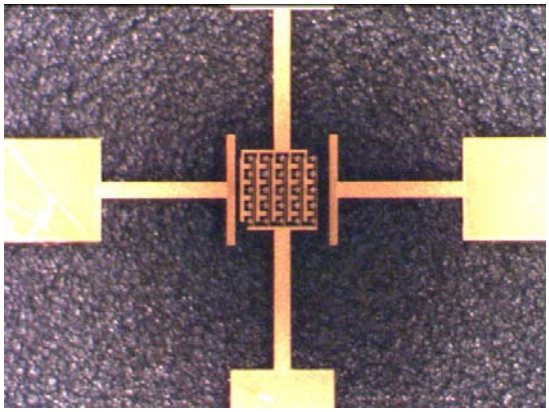

(a) 2nd Device

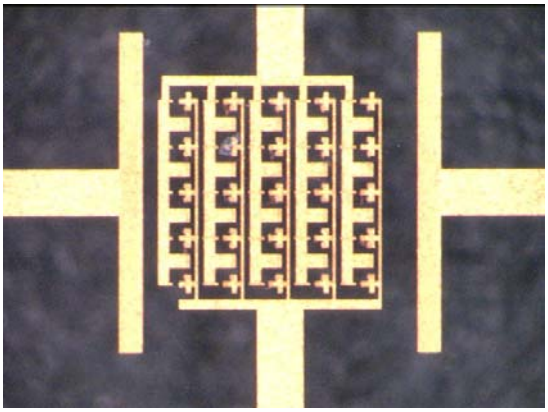

(b) 2nd Device Detail View

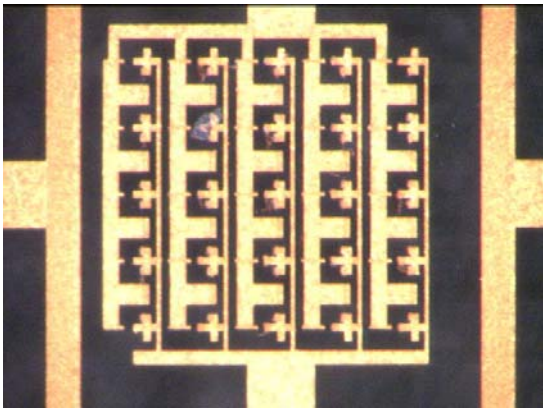

(c) 2nd Device, Electrode Type - II

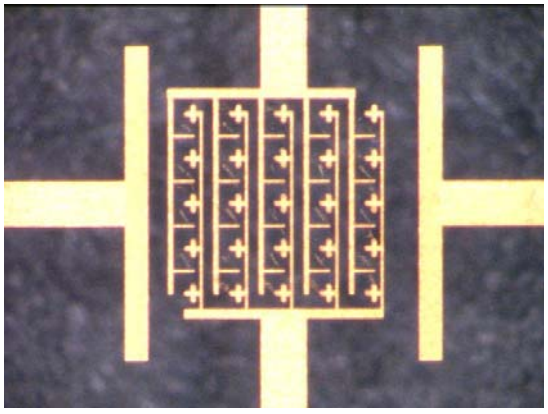

(d) 2nd Device, Electrode Type - III

Figure 3.10. Photos of Electroplated 5x5 Electrode Arrays

4. EXPERIMENAL RESULTS

4.1 Experimental Apparatus

The particles were viewed using a Carl Zeiss Axiovert 200 light microscope mounted on a vibration isolation table. The particle motion was recorded using a Carl Zeiss Axiocam HR CCD camera. Experiments were performed at room temperature. All experiments were performed using EPON 8021 resin as the liquid. The relative permittivity (or dielectric constant) is 3.98. The liquid was 200 micrometers thick, and the top of the liquid was exposed to the air environment, i.e. no cover was placed on the liquid. The particles were soda lime glass spheres, with a relative permittivity (or dielectric constant) of 7.3.

4.2 Demonstration of Patterning of 90 Micron Diameter Particles

Ninety micron diameter particles were trapped near “cloverleaf” electrodes with 200V DC applied voltage, as shown in Figure 4.1.

The next four photos shown in Figure 4.2, from the movie “90 micron patterning,” show patterning of 90 micron particles at various magnitudes of applied voltage. The particles are not patterned until the voltage reaches 250 volts, at which point some particles form approximately a square array. It is evident in the video that the particles in this square array maintain their fixed positions as other particles move around them. However, because the unit cell is so much larger than the particles, there are some non-patterned particles between the patterned particles.

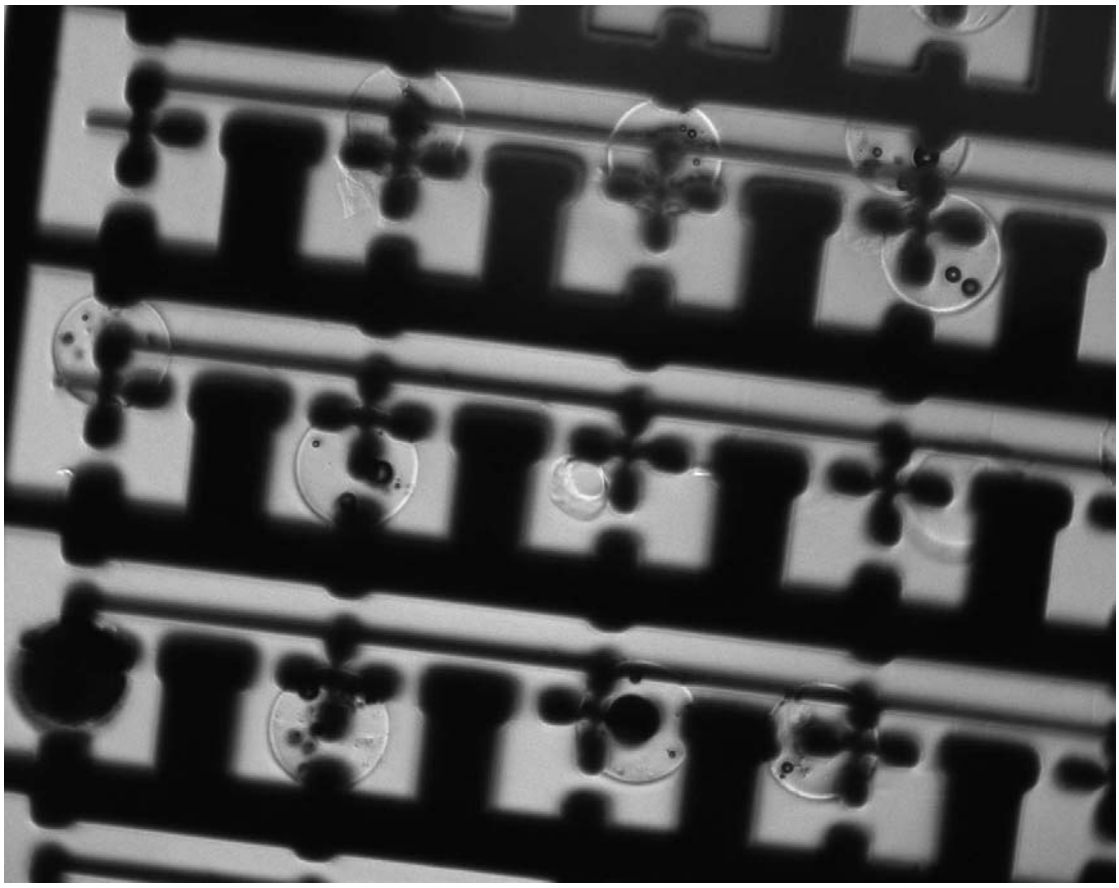

Figure 4.1 90 Micron Diameter Particles Trapped Near "Cloverleaf" Electrodes at 200V DC

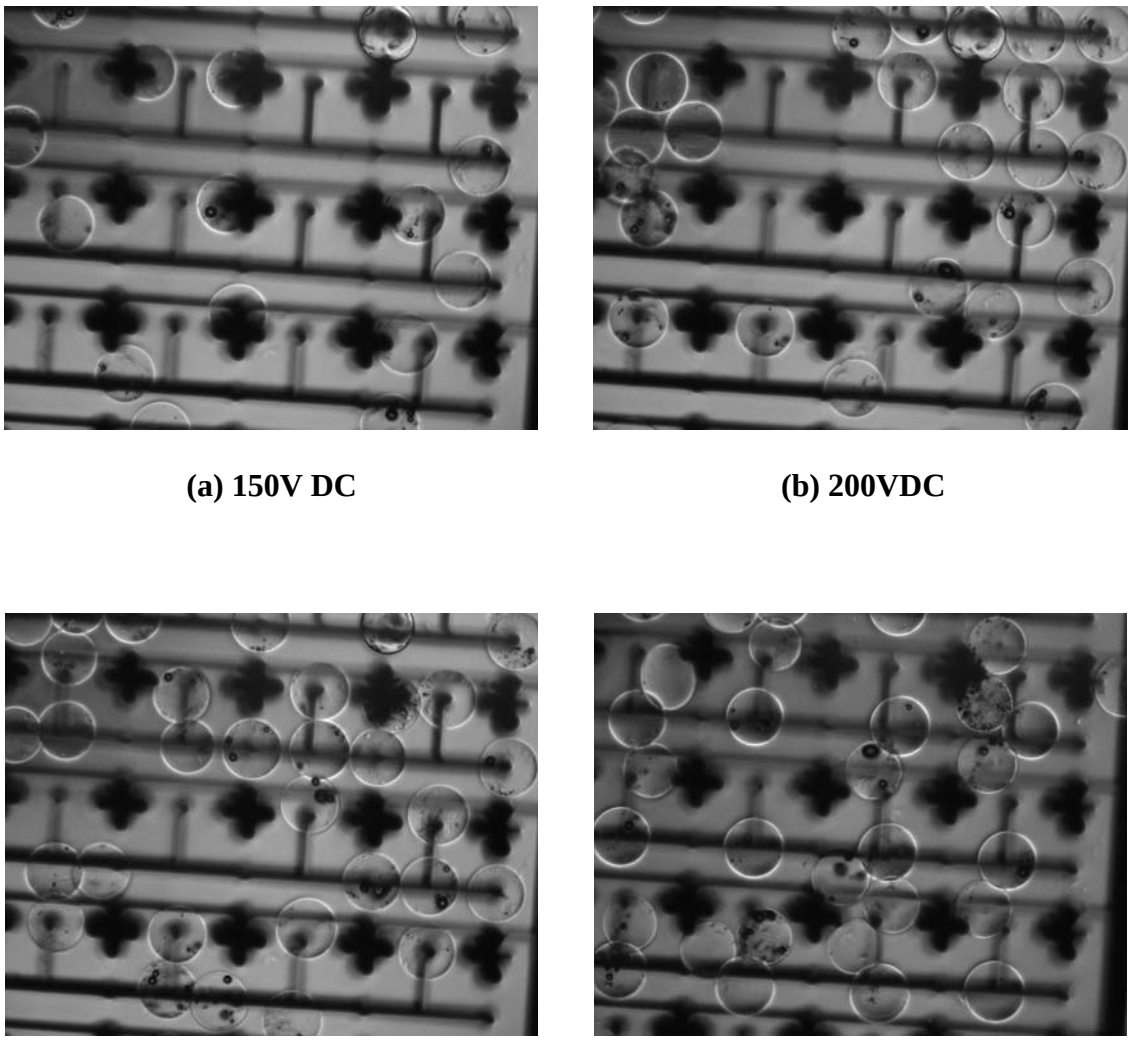

(a) 150V DC **(b) 200VDC**

(c) 200V DC **(d) 250V DC**

Figure 4.2 Patterning of 90 Micron Diameter Particles

A different electrode array, shown in the video “90 micron not patterned,” did not pattern the 90 micron particles even with applied voltages as high as 500 V. The initial and final positions of the particles are shown in Figures 4.3(a) and 4.3(b).

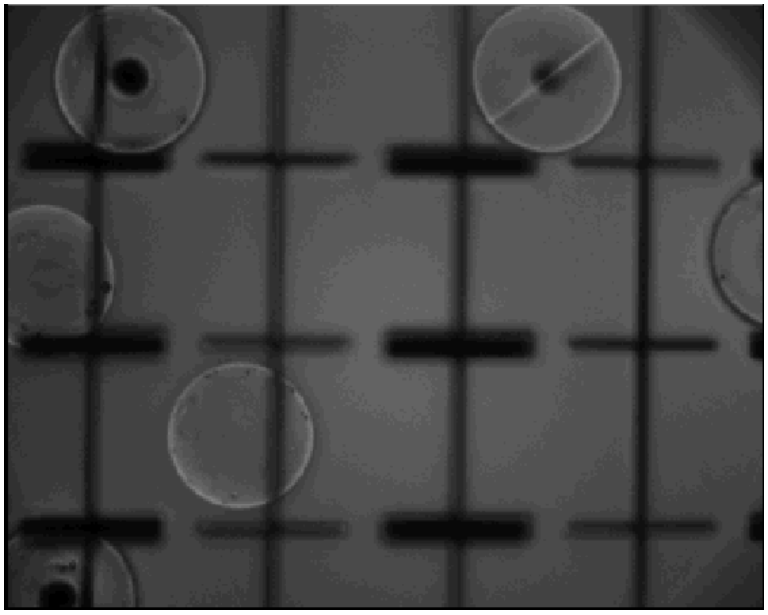

Figure 4.3 (a) 90 Micron Diameter Particles, Initial Position

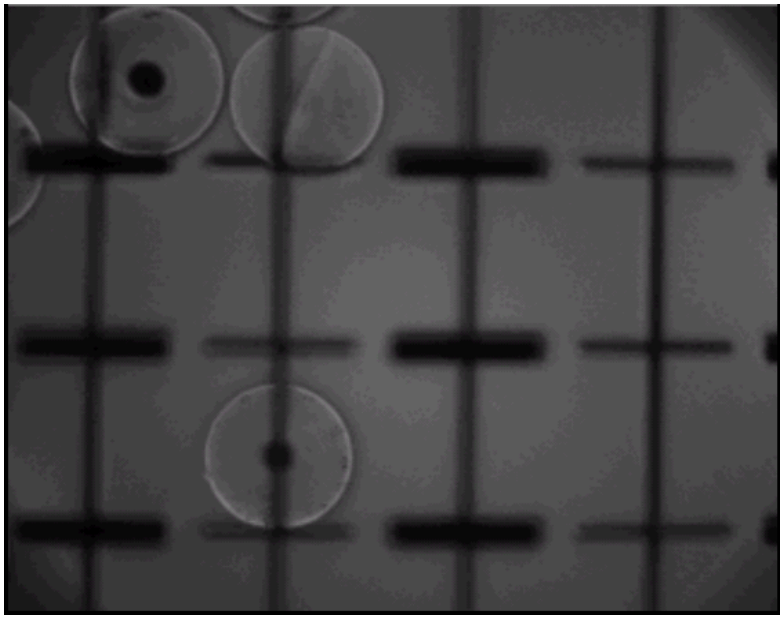

Figure 4.3 Continued. (b) 90 Micron Diameter Particles, Final Position

4.3 30 Micron Diameter Particles Do Not Form Patterns

In general, the 30 micron diameter particles did not form patterns in which single particles were located at the regions of highest energy density. The video “30 micron clusters” shows that single 30 micron particles are trapped at the regions of high energy density, and then other particles cluster around the originally trapped particles, and these clusters grow. There are no clusters in the center of the unit cells, where the energy density is low. Apparently, the particles near a cluster are influenced more by other particles than by the electrodes, which are further away than the other particles. A photograph of the initial and final particle positions of the video “30 micron clusters” is shown in Figure 4.4(a) and 4.4(b). There is a similar result shown in the video “30 micron movie.”

In the video “three 30 micron” there are three 30 micron diameter particles. Two are easily visible and one is barely visible. The voltage difference is increased from 0 to 50V in increments of 10V every 30 seconds, and then the voltage is decreased to 0 in decrements of 10V every 30 seconds. One particle is trapped at the region of highest electric energy density, but the another particle circulates around this region. This particle apparently has an impurity on it.

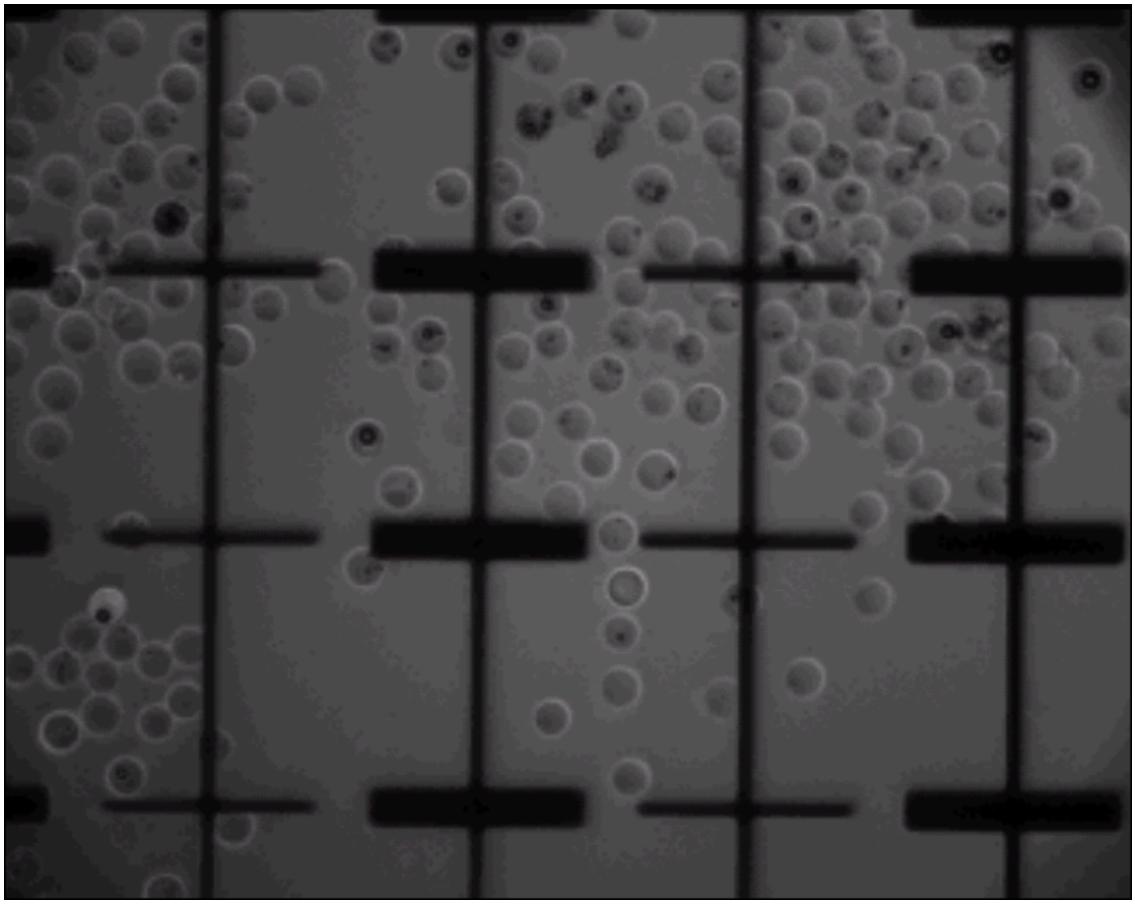

Figure 4.4 (a) 30 Micron Diameter Particles, Initial Position

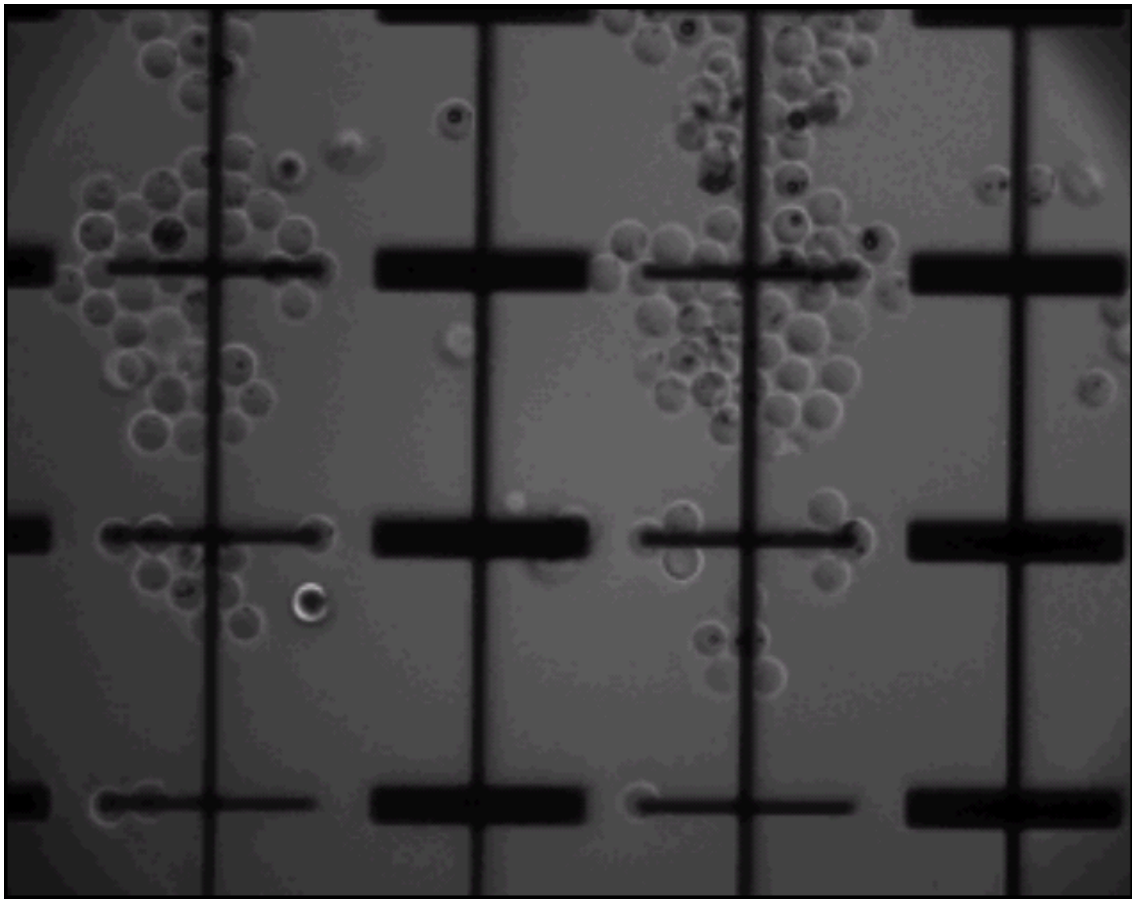

Figure 4.4 Continued. (b) 30 Micron Diameter Particles, Final Position

4.4 170 Micron Diameter Particles Rest on Asymmetric Sites

When a small number of 170 micron particles are subjected to an applied potential, they often, but not always, move to asymmetric sites on the electrodes.

The 170 micron diameter particles did not form a regular pattern. The 170 micron particles are generally not centered on the regions of high energy density.

However, a small number of 170 micron spheres can be separated from one another, as shown in the video “two 170 micron particles separated,” in which two 170 micron particles in contact are separated by applying 25V.

4.5 Particle Positions Sometimes Reverse in Response to a Reversal of the Applied Voltage

The sign convention for the electrode voltage polarity is given in Figure 4.5.

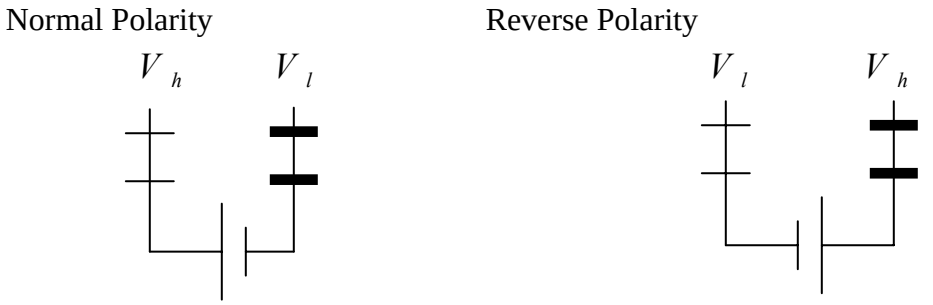

Figure 4.5 Polarity Sign Convention

A sequence of experiments was performed as described in Table 4.1. Still images from these experiments are shown in Figure 4.6. Experiments 9, 10, 11, and 13 and 14 demonstrate that the particle reversed its position when the polarity of the electric potential was reversed.

Table 4.1 Experiments with 170 Micron Diameter Particles

*IP: Initial Position, *FP: Final Position

Experi-ment No.	Applied Voltage, Polarity	Initial Position	Total Time	Remarks
1	DC 20V, Normal	Different IP*	6 min	
2	DC 15V, Normal	Different IP	6 min	
3	DC 17V, Normal	FP* of Ex.2	6 min	
4	DC 16V, Normal	FP of Ex.3	6 min	
5	DC 18V, Normal	FP of Ex.4	4 min	
6	DC 20V, Normal	FP of Ex.5	2 min	
7	DC 20V, Reverse	FP of Ex.6	6 min	
8	DC 20V, Normal	FP of Ex.7	5 min	
9	DC 23V, Normal	FP of Ex.8	6 min	
10	DC 20V, Reverse	FP of Ex.9	5 min	
11	DC 23V, Normal	FP of Ex.10	4 min	
12	DC 25V, Normal	FP of Ex.11	3 min	
13	DC 25V, Reverse	FP of Ex.12	4 min	
14	DC 25V, Normal	FP of Ex.13	5 min	
15	DC 25V, Reverse	FP of Ex.14	5 min	There is rest time of 2.5hrs between Ex. 14 and Ex. 15
16	DC 25V, Normal	FP of Ex.15	5 min	
17	DC 25V, Reverse	FP of Ex.16	5 min	
18	DC 27V, Normal	FP of Ex.17	5 min	Take a look at IP and FP
19	DC 20V, Reverse	FP of Ex. 18	5 min	Particle crossing over unitcells

Table 4.1 Continued

Experi-ment No.	Applied Voltage, Polarity	Initial Position	Total Time	Remarks
20	DC 25V, Normal	FP of Ex. 19	5 min	
21	DC 20V, Reverse	FP of Ex. 20	6 min	
22	DC 27V, Normal	FP of Ex. 21	6 min	
23	DC 25V, Reverse	FP of Ex. 22	6 min	
24	DC 25V, Normal	FP of Ex. 23	6 min	
25	DC 20V, Reverse	FP of Ex. 24	6 min	DC 20V-> DC25V for 3~5sec before Ex. 26
26	DC 25V, Normal	FP of Ex. 25	6 min	
27	DC 25V, Reverse	FP of Ex. 26	6 min	
28	DC 20V, Reverse	FP of Ex. 27	5 min	By a mistake
29	DC 25V, Normal	FP of Ex. 28	5 min	
30	DC 25V, Reverse	FP of Ex. 29	6 min	
31	DC 28V, Normal	FP of Ex. 30	6 min	
32	DC 15V, Reverse	FP of Ex. 31	6 min	DC 15V, 2.5min (doesn't move) -> 18V, 2.min -> 25V 0.5min
33	DC 28V, Normal	FP of Ex. 32	1 min	Not moved at all
34	DC 28V, Reverse	FP of Ex. 33	5 min	
35	DC 10V, Normal	FP of Ex. 34	6 min	Initial Voltage 10V->11V->13V->15V
36	DC 25V, Reverse	FP of Ex. 35		

Table 4.1 Continued

Experi-ment No.	Applied Voltage, Polarity	Initial Position	Total Time	Remarks
37	DC 5V, Normal	FP of Ex. 36	7 min	DC 12V the Particle moved DC 13V, 2min Doesn't change DV 16V, start moving => final position
38	DC 16V, Reverse	FP of Ex. 37	7 min	
39	DC 13V, Normal	FP of Ex. 38	6 min	
40	DC 13V, Reverse	FP of Ex. 39	5 min	
41	DC 11.5V, Normal	FP of Ex. 40	5 min	
42	DC 25V, Reverse	FP of Ex. 41	5 min	
43	DC 10V, Normal	FP of Ex. 42	5.5 min	
44	DC 25V, Reverse	FP of Ex. 43	3 min	
45	DC 9V, Normal	FP of Ex. 44	5 min	
46	DC 25V, Reverse	FP of Ex. 45	5 min	
47	DC 10.5V, Normal	FP of Ex. 46	5 min	
48	DC 10.5V, Reverse	FP of Ex. 47	4 min	
49	DC 9V, Normal	FP of Ex. 48	5 min	
50	DC 20V, Reverse	FP of Ex. 49	5 min	
51	DC 9V, Normal	FP of Ex. 50	5min, Infinitive	Fig. 53, after 5min Fig. 54, after 10hrs

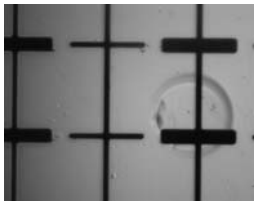
Fig.(a) Electrode Pattern

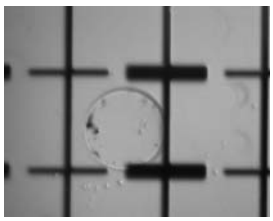
Fig.(b) IP of EX1

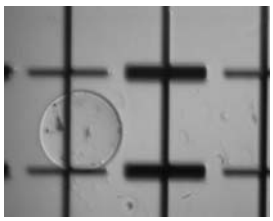
Fig.(c) FP of EX1

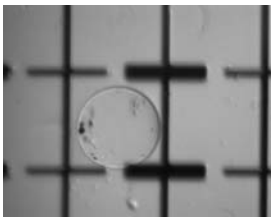
Fig.(d) IP of EX2

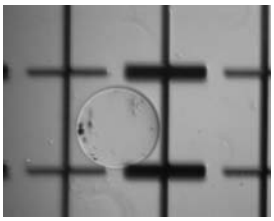
Fig.(e) FP of EX2

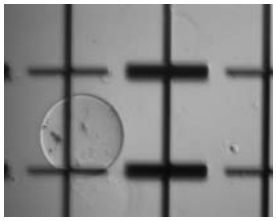
Fig.(f) FP of EX3

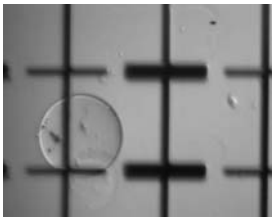
Fig.(g) FP of EX4


Fig.(h) FP of EX5

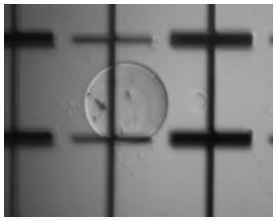
Fig.(i) FP of EX6

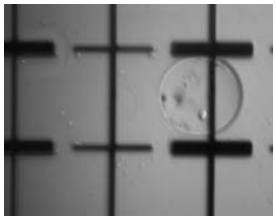
Fig.(j) FP of EX7

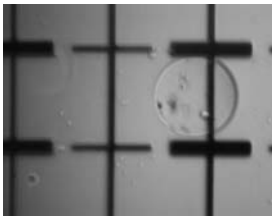
Fig.(k) FP of EX8

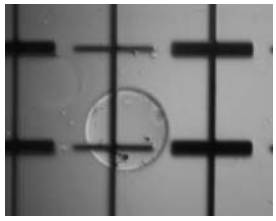
Fig.(l) FP of EX9

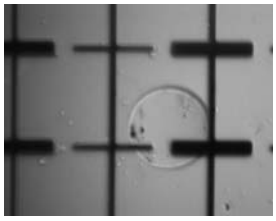
Fig.(m) FP of EX10

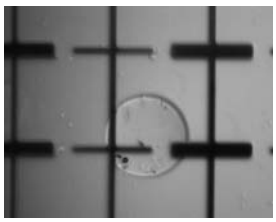
Fig.(n) FP of EX11

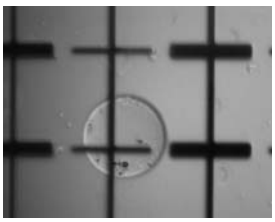
Fig.(o) FP of EX12

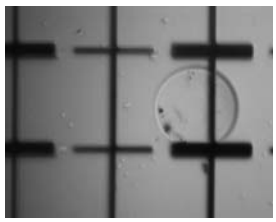
Fig.(p) FP of EX13

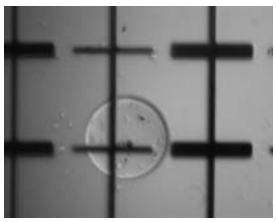
Fig.(q) FP of EX14

Figure 4.6. Experiments with 170 Micron Diameter Particles

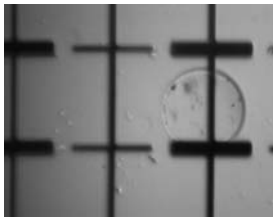
Fig.(r) FP of EX15

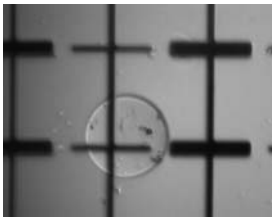
Fig.(s) FP of EX16

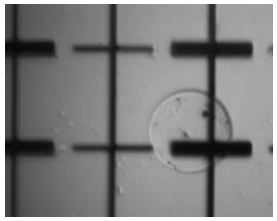
Fig.(t) FP of EX17

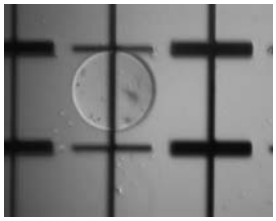
Fig.(u) FP of EX18

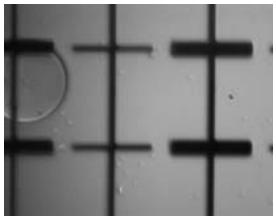
Fig.(v) FP of EX19

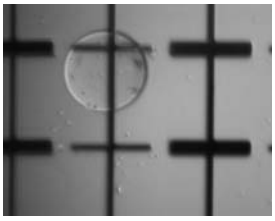
Fig.(w) FP of EX20

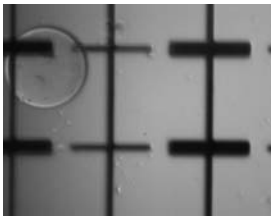
Fig.(x) FP of EX21

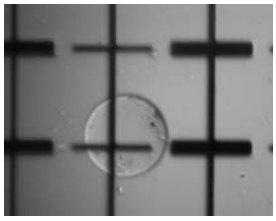
Fig.(y) FP of EX22

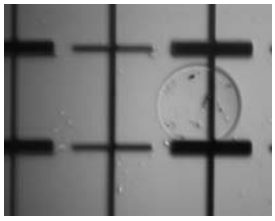
Fig.(z) FP of EX23

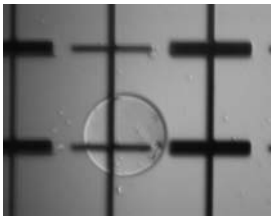
Fig.(aa) FP of EX24

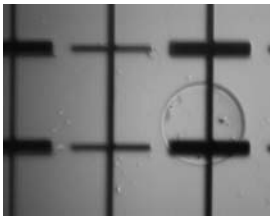
Fig.(bb) FP of EX25

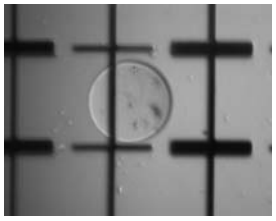
Fig.(cc) FP of EX26

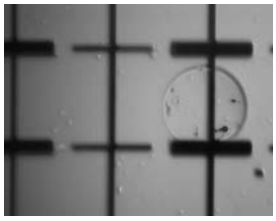
Fig.(dd) FP of EX27

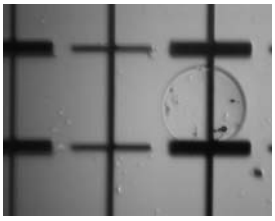
Fig.(ee) FP of EX28

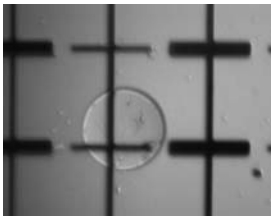
Fig.(ff) FP of EX29

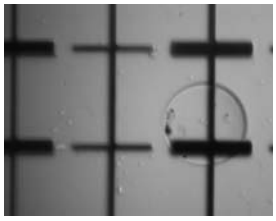
Fig.(gg) FP of EX30

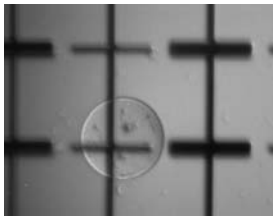
Fig.(hh) FP of EX31

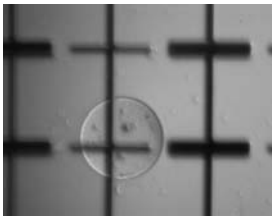
Fig.(ii) FP of EX32

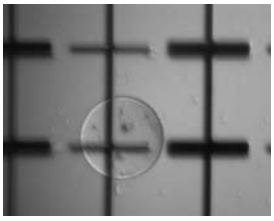
Fig.(jj) FP of EX33

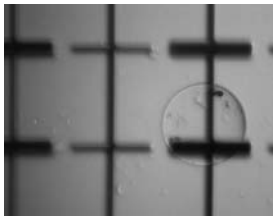
Fig.(kk) FP of EX34

Figure 4.6. Continued

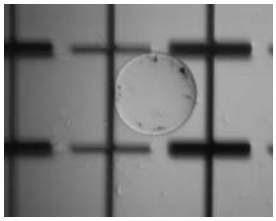
Fig.(ll) FP of EX35

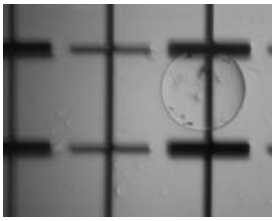
Fig.(mm) FP of EX36

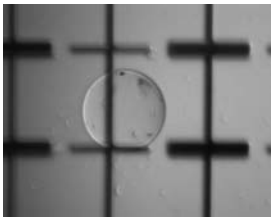
Fig.(nn) FP of EX37

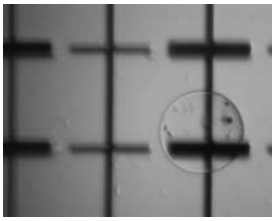
Fig.(oo) FP of EX38

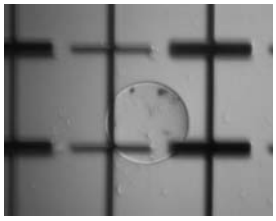
Fig.(pp) FP of EX39

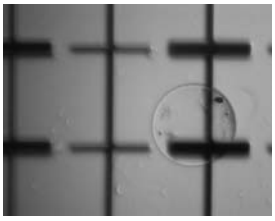
Fig.(qq) FP of EX40

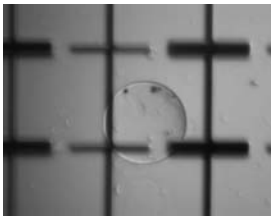
Fig.(rr) FP of EX41

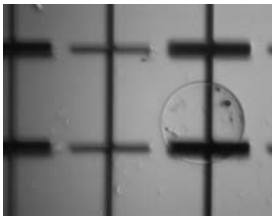
Fig.(ss) FP of EX42

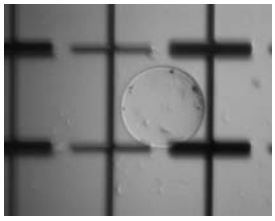
Fig.(tt) FP of EX43

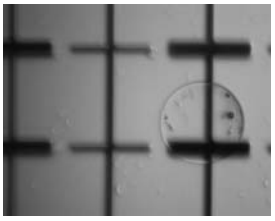
Fig.(uu) FP of EX44

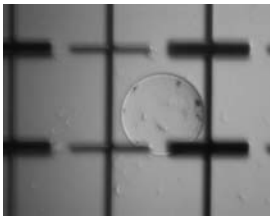
Fig.(vv) FP of EX45


Fig.(ww) FP of EX46

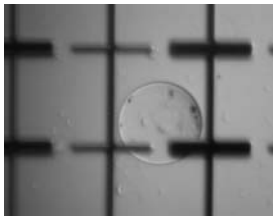
Fig.(xx) FP of EX47


Fig.(yy) FP of EX48

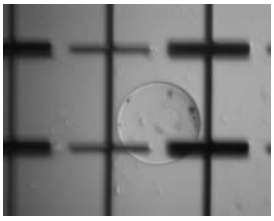
Fig.(zz) FP of EX49

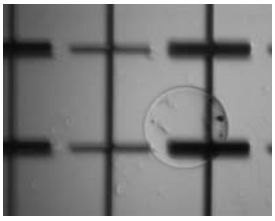
Fig.(aaa) FP of EX50

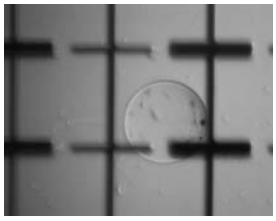
Fig.(bbb) FP of EX51-1


Fig.(ccc) FP of EX51-2

Figure 4.6. Continued

The video “particle reversal” shows a single 170 micron particle with 25V applied to the electrodes according to the sign convention of Figure 4.5. This corresponds to the initial position of Experiment 13 of Table 4.1, and is shown in Figure 4.7(a). At the end of this video (Figure 4.7(b)), the polarity is reversed, which corresponds to the beginning of the video “particle reversal continued,” which is the initial position of Experiment 14. The particle reverses its position when the polarity is reversed, Figure 4.7(c).

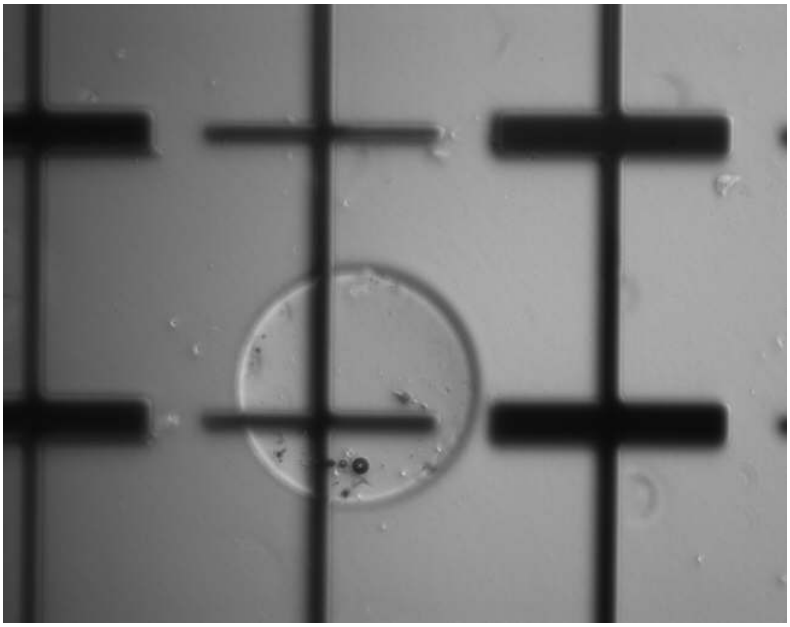

Figure 4.7 (a) Initial Position before Experiment 13. 25V with Normal Polarity

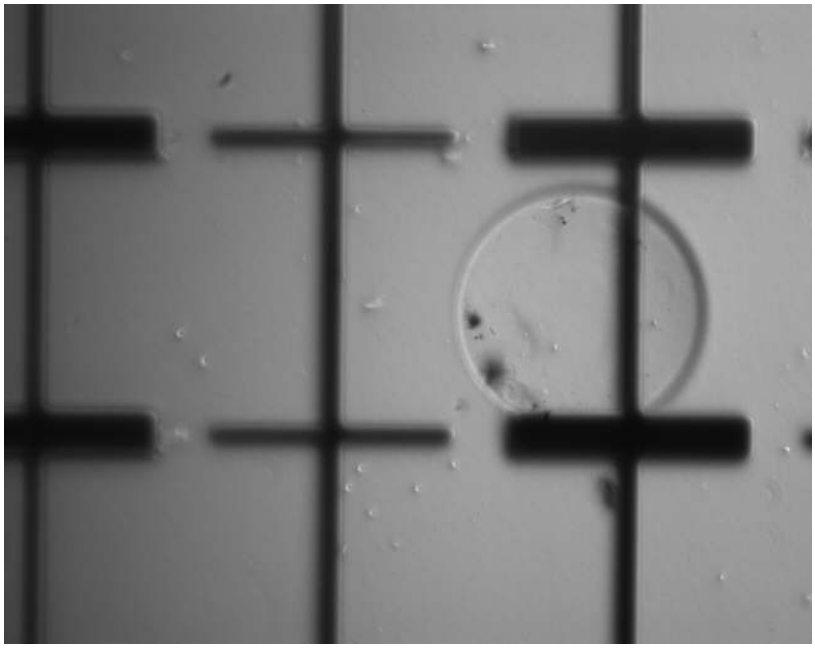

Figure 4.7 Continued. (b) Final Position after Experiment 13. Initial Position of Experiment 14. 25V with Normal Polarity

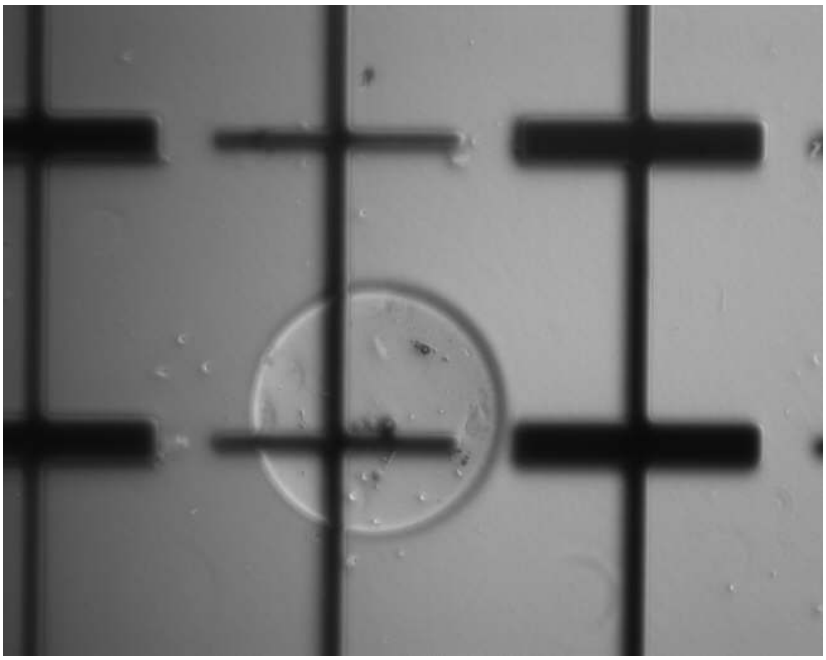

Figure 4.7 Continued. (c) Final Position after Experiment 14. 25V with Reversed Polarity

5. DISCUSSION OF RESULTS

The effect of particle size will be discussed briefly in section 5.1. The electrofluid mechanics with no particle will be discussed in detail in Section 5.2. Experiment # 14 of Table 4.1 and Figure 4.7 will be discussed in detail in Section 5.3. All finite element work reported in this section was performed using the commercially available software, “FEMLab.”

5.1 The Effect of Particle Size

The 30 micron diameter particles are attracted to the tip of the small electrodes, which is the region of highest energy density. However, only the first particles to reach the electrode tip can fit on the tip, so the particles that arrive later must contact the particles that are already at the tip. Thus, as particles attempt to reach the tip, the clusters grow.

As shown in Section 2, for a single spherical particle in a uniform electric field gradient, the dielectric force increases with the cube of the particle radius, whereas the viscous drag force increases linearly with the particle radius. Thus, the ratio of dielectric force to fluid force is greater for large particles than for small particles. For example, the ratio of the dielectric force to the fluid force is 9 times larger for the 90 micron diameter particle than for the 30 micron diameter particle. This may explain why some 30 micron diameter particles moved without ever stopping. Perhaps the electric force was never large enough to stop the 30 micron particle, which continued to move with the liquid.

5.2 Fluid Mechanics with No Particle

The fluid mechanics is performed using the finite element program “FEMLab.” The electrode array of Figure 4.6 is used in the model. Two cases are considered, one with a cover glass on the top of the liquid, and one with no cover. The boundary conditions differ for these two cases. Without a cover, the top boundary condition is a zero traction condition, whereas with a cover, the top boundary condition is a no-slip condition.

The liquid layer is 200 microns thick. A 500 micron thick Pyrex glass region is beneath the liquid layer. The region above the liquid is 500 microns thick. For the case in which there is no top cover applied, this region is air, and for the case in which there is a cover applied, this region is soda lime glass.

It is necessary to solve Gauss’ law in the bottom region, the liquid layer, and the top region. A postprocessor is used to calculate the electric body force in the liquid, and this body force is used to solve Equation (2.33).

The four sides of the unit cell are modeled as symmetry planes, meaning that there is no electric field or fluid velocity normal to the plane. A no-slip boundary condition is used where the liquid contacts the solid bottom and cover. For the case in which no cover was used, a symmetry condition is used for the liquid/air interface.

For EPON 8021 Resin, the viscosity is η=100 centipoise = 0.1 kg/(m·sec), the mass density is ρ=1.1×10^{3}kg/m^3, and the relative permittivity (or dielectric constant) is 3.98.

Eleven thousand, six hundred ninety five quadratic elements are used, and the number of degrees of freedom is 53,616.

5.2.1 With a Cover

The electric body field and electric body force distributions are shown in Figures 5.1 and 5.2, respectively. The maximum energy density is 1,1417 J/M^3 and occurs at the end of the small electrode. The velocity is shown in Figure 5.3, and the streamlines are shown in Figure 5.4, and in Figure 5.5 the liquid speed in the center of the x-y plane is plotted as a function of z. The maximum liquid speed is 88.2 microns per second. In the center of the unit cell the speed is 2.64 microns/second.

5.2.2 With No Cover

For the case in which there is no cover on the liquid, Figures 5.6 – 5.8, the maximum liquid speed is 88.5 microns per second. In the center of the unit cell the speed is 2.42 microns per second. In general, the cover has very little effect on the dynamics of the liquid.

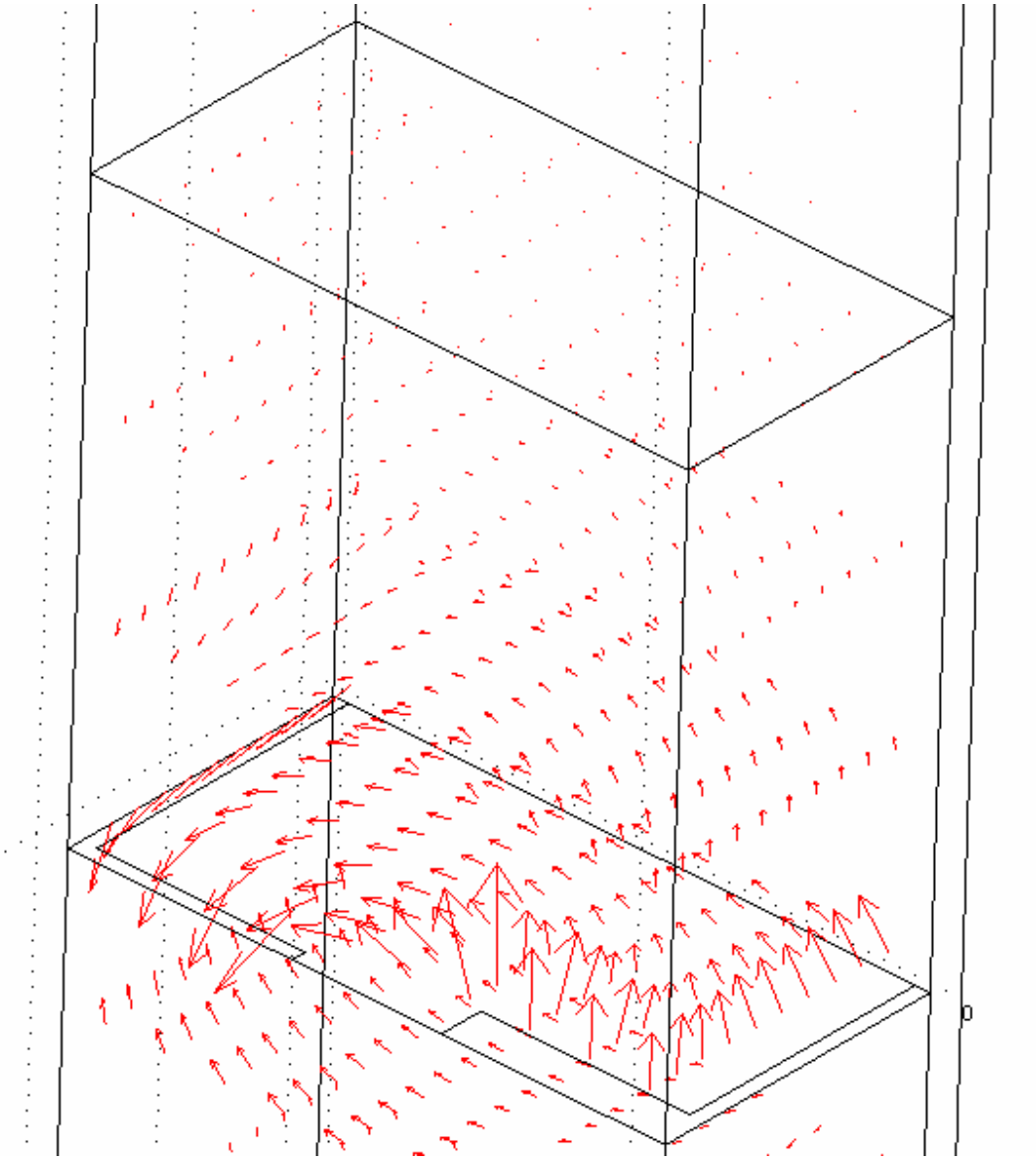

Figure 5.1. One Unit Cell with a Cover. Electric Field

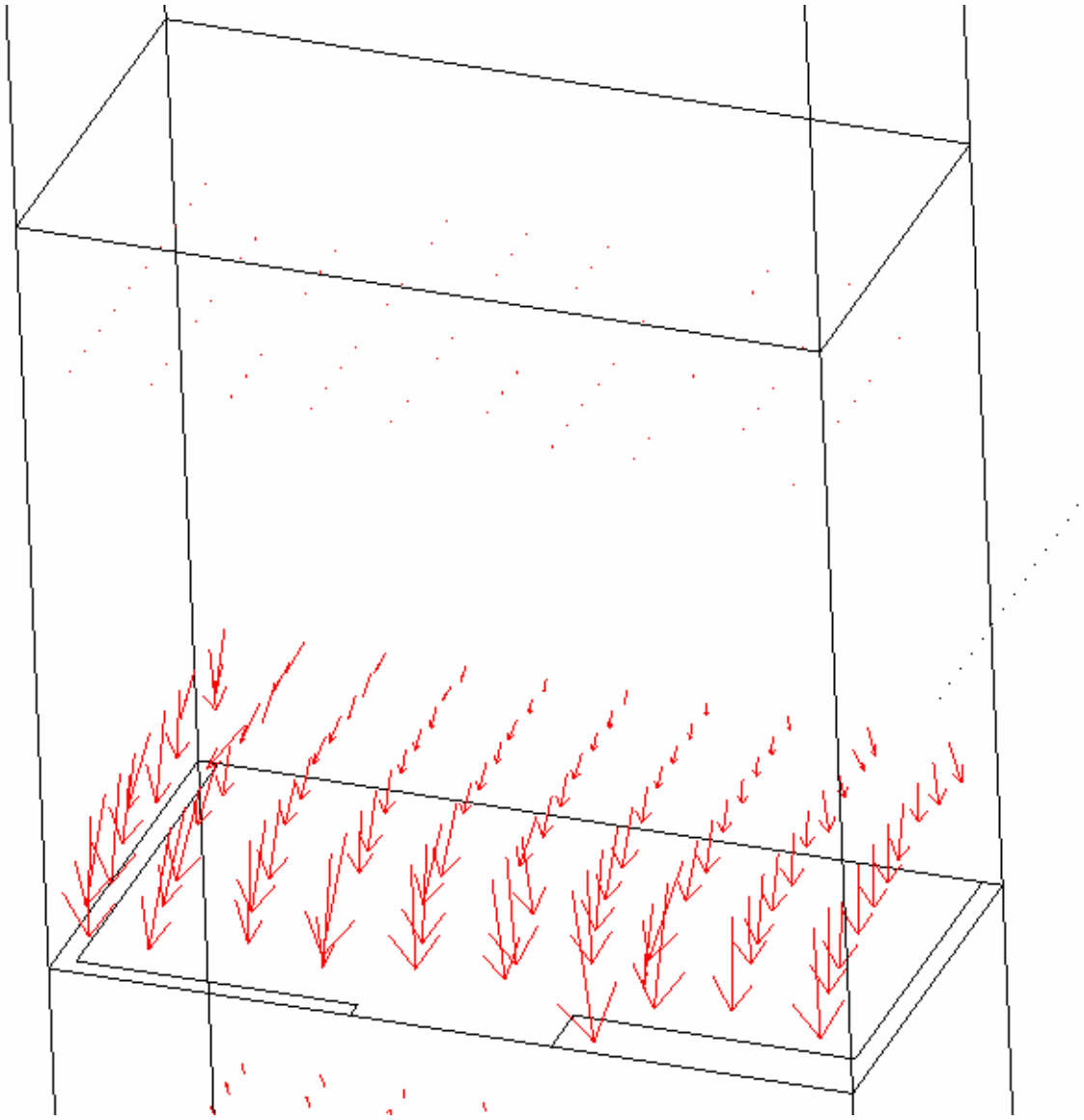

Figure 5.2. One Unit Cell with a Cover. Electric Body Force

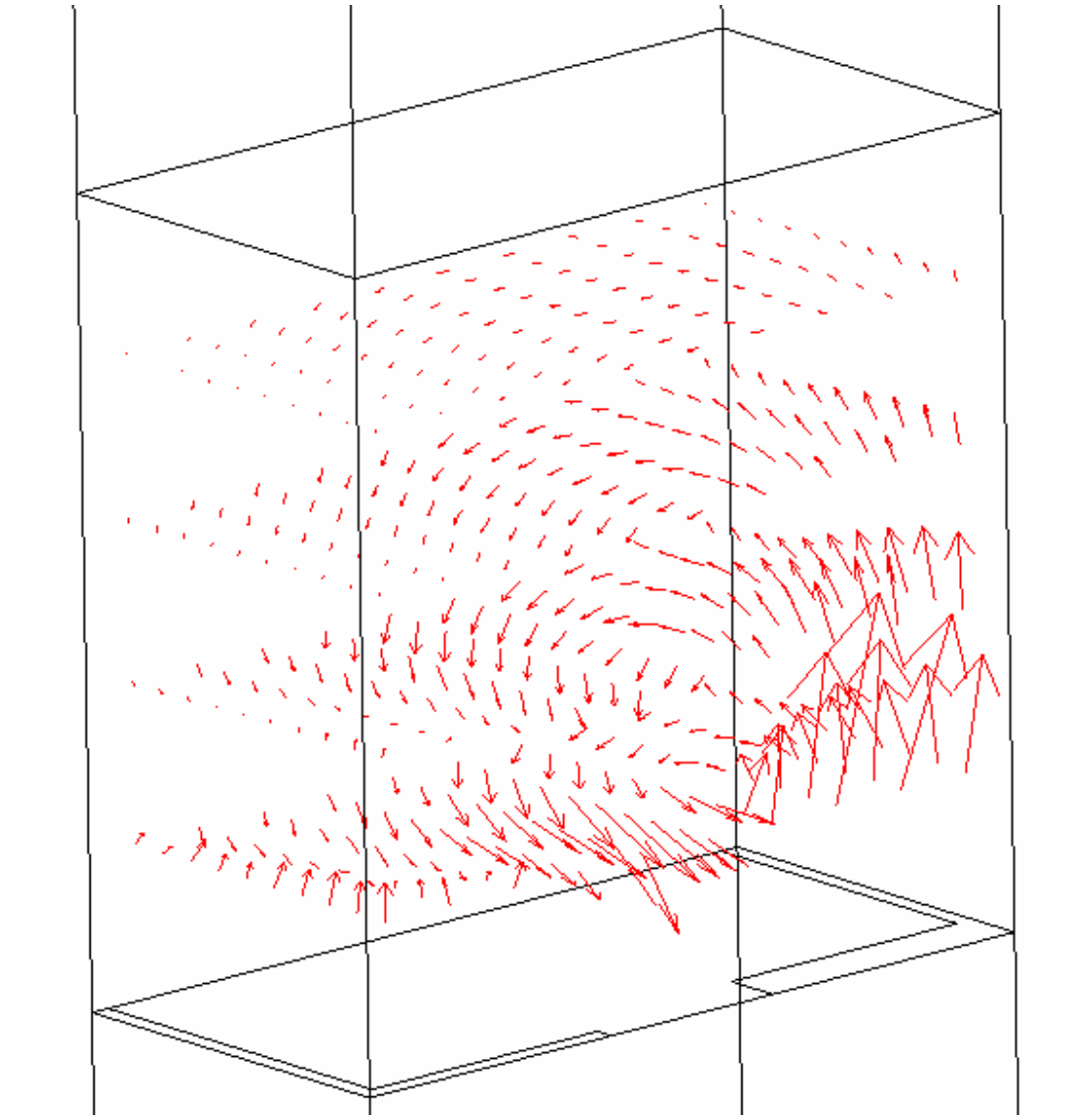

Figure 5.3. One Unit Cell with a Cover. Liquid Velocity

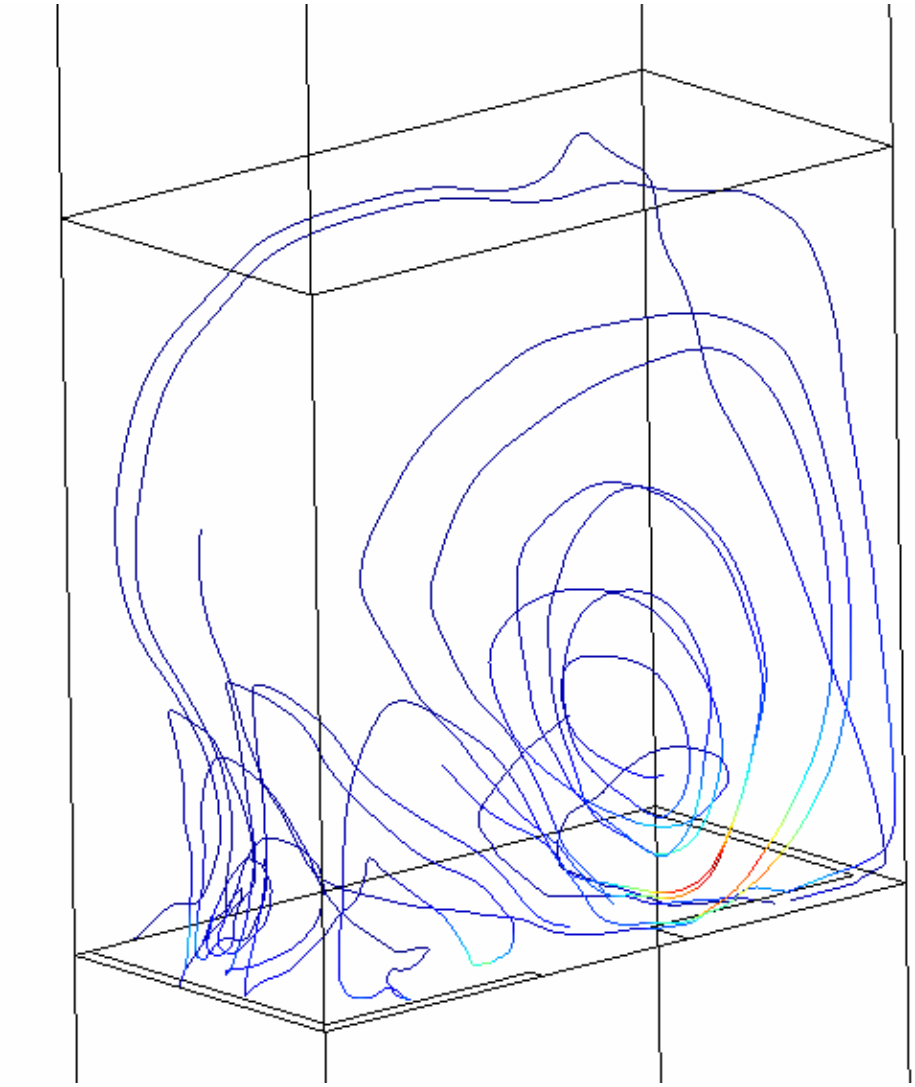

Figure 5.4. One Unit Cell with a Cover. Streamlines

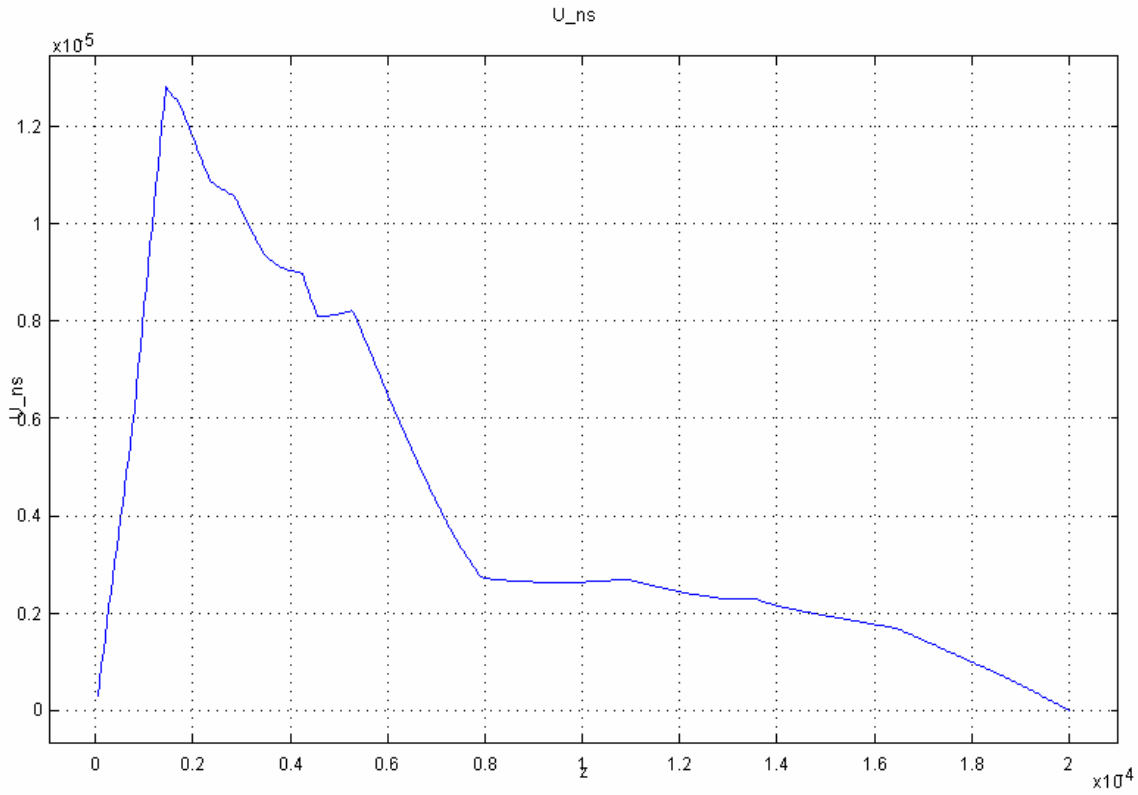

Figure 5.5. One Unit Cell with a Cover. Liquid Speed in the Center of the x-y Plane as a Function of z Difference from the Electrode Plane

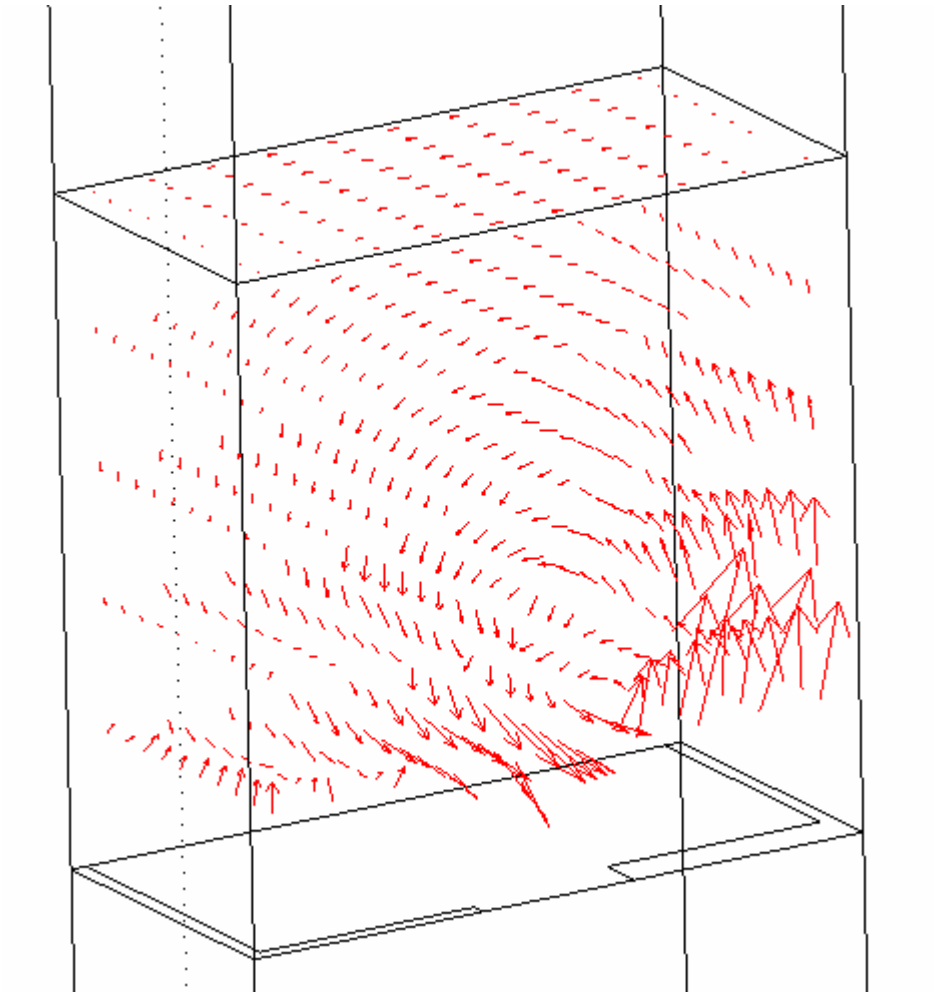

Figure 5.6. Arrow Plot for Liquid Velocity in One Unit Cell with No Cover

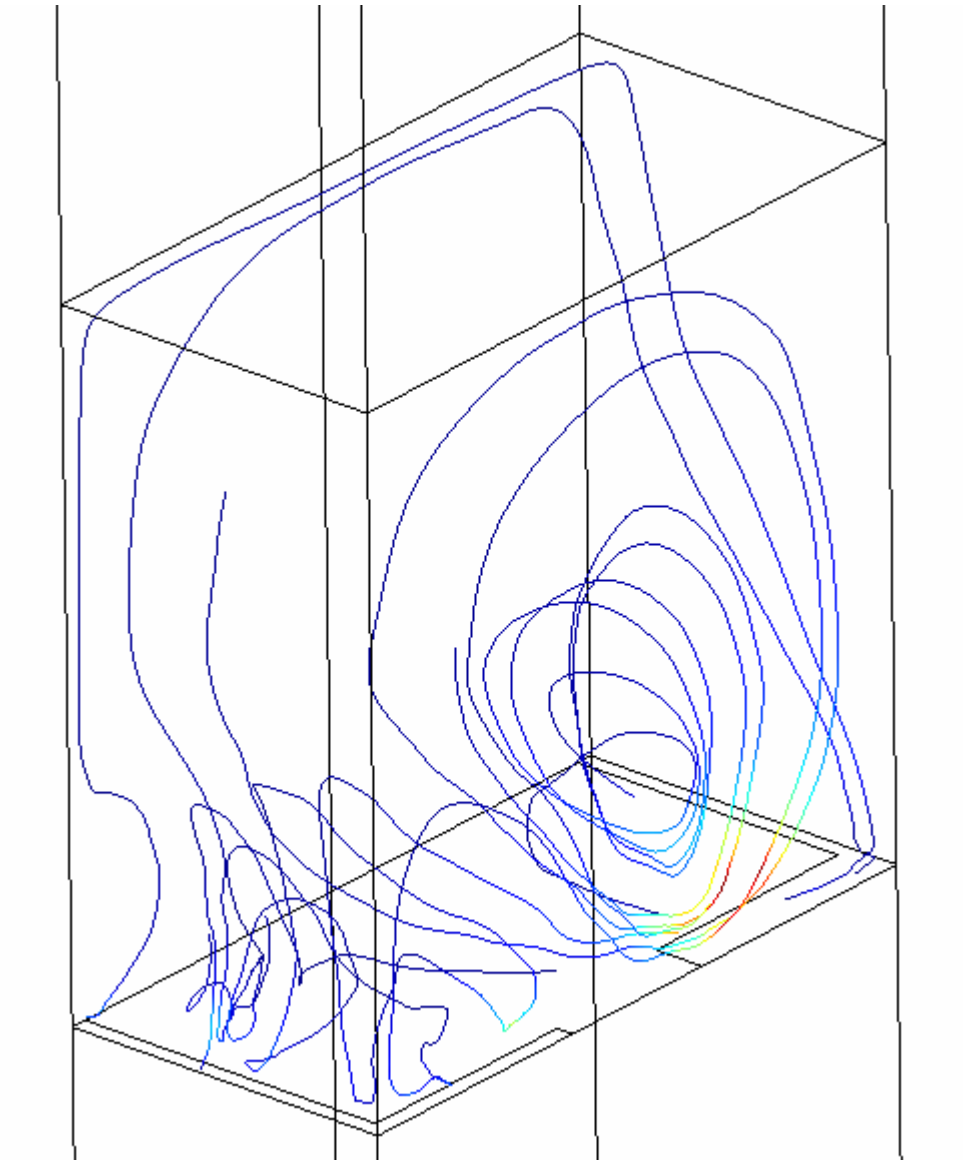

Figure 5.7. Streamlines Plot in One Unit Cell with No Cover

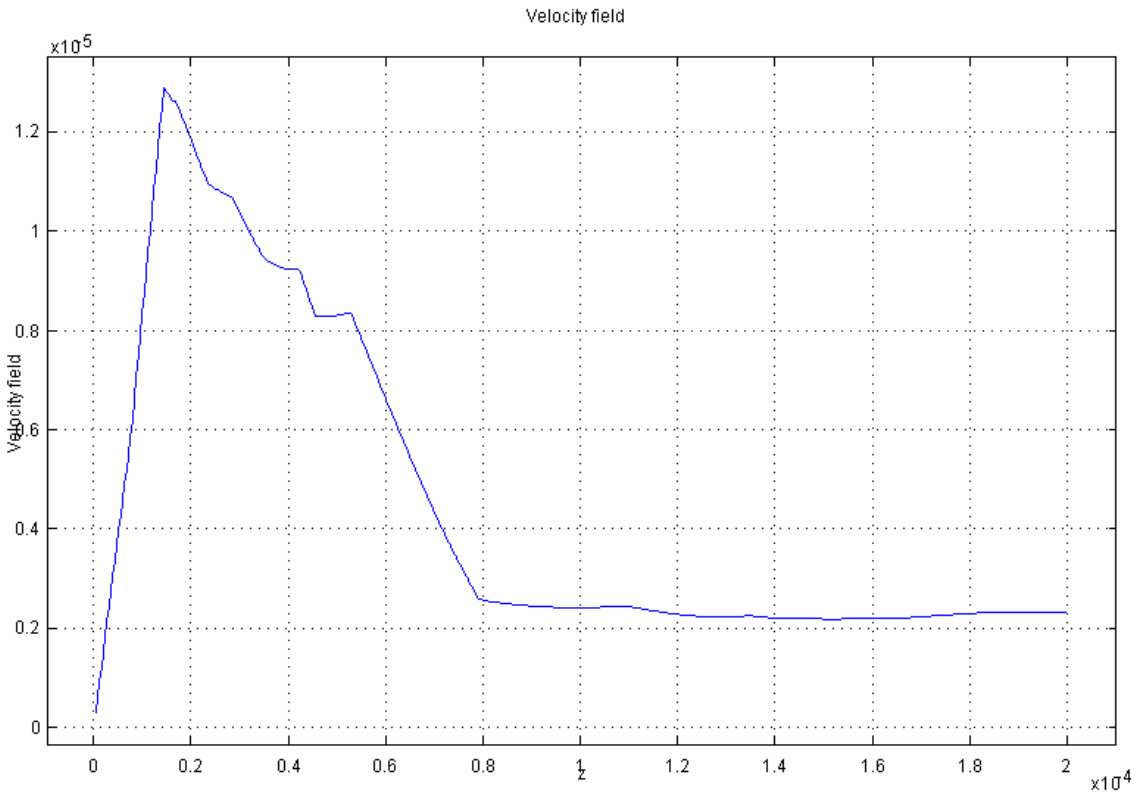

Figure 5.8. Liquid Speed in the Center of the x-y Plane as a Function of z for One Unit Cell with No Cover

5.3 Discussion of Experiment #14

An understanding of the particle dynamics can best be obtained by studying a specific boundary value problem. The final position of Experiment #14 (Figures 4.1 and 4.7) is chosen for the study.

The finite element model shown in Figure 5.9 consists of four unit cells. The liquid layer is 200 microns thick. A 500 micron thick Pyrex glass region is the bottom. The top region consists of air that is 500 microns thick.

The four sides of the unit cell are modeled as symmetry planes.

The coordinate origin is at the center of the unit cell in Figure 5.10. The particle is a sphere in the finite element model and appears non-spherical in Figure 5.10 due to limitations of the drawing software. In the experiment, the spherical particle has a diameter of 170 microns and is located at (25, 33, -15). The particle and the liquid are both isotropic dielectric materials.

Thirty-four thousand, four hundred sixty four quadratic elements were used, and the number of degrees of freedom is 136938.

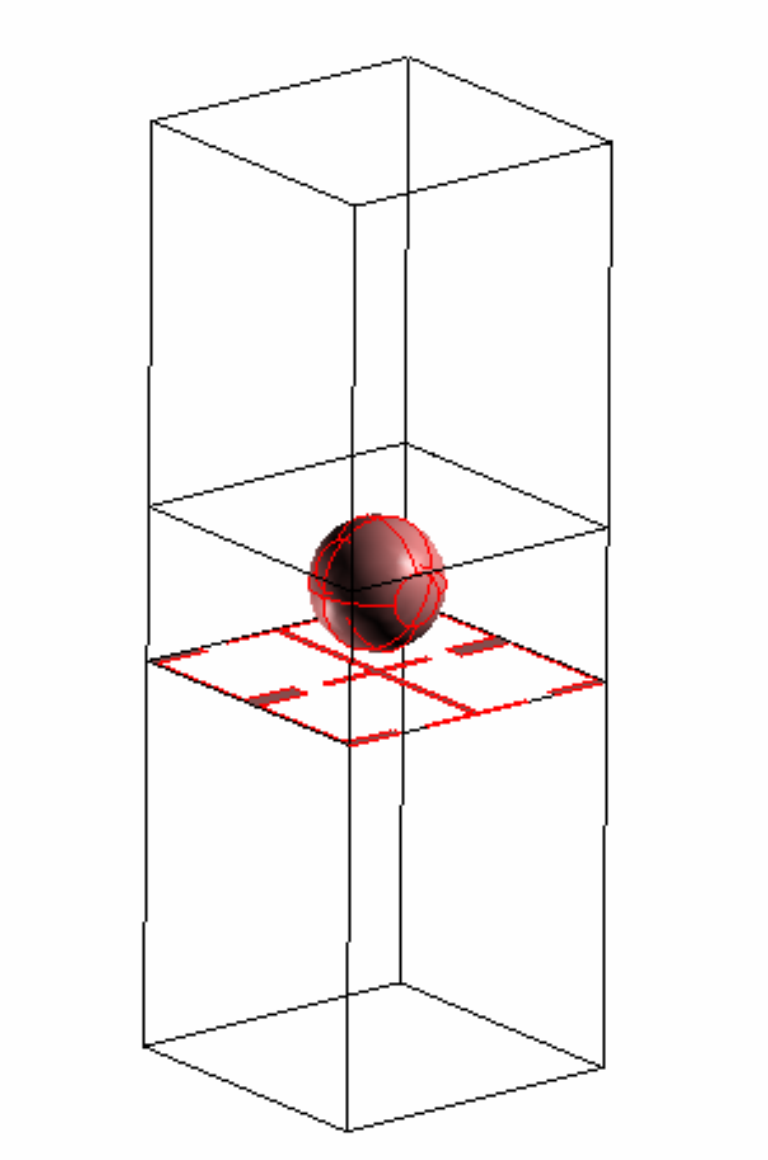

Figure 5.9 Four Unit Cell Model Used for Finite Element Analysis

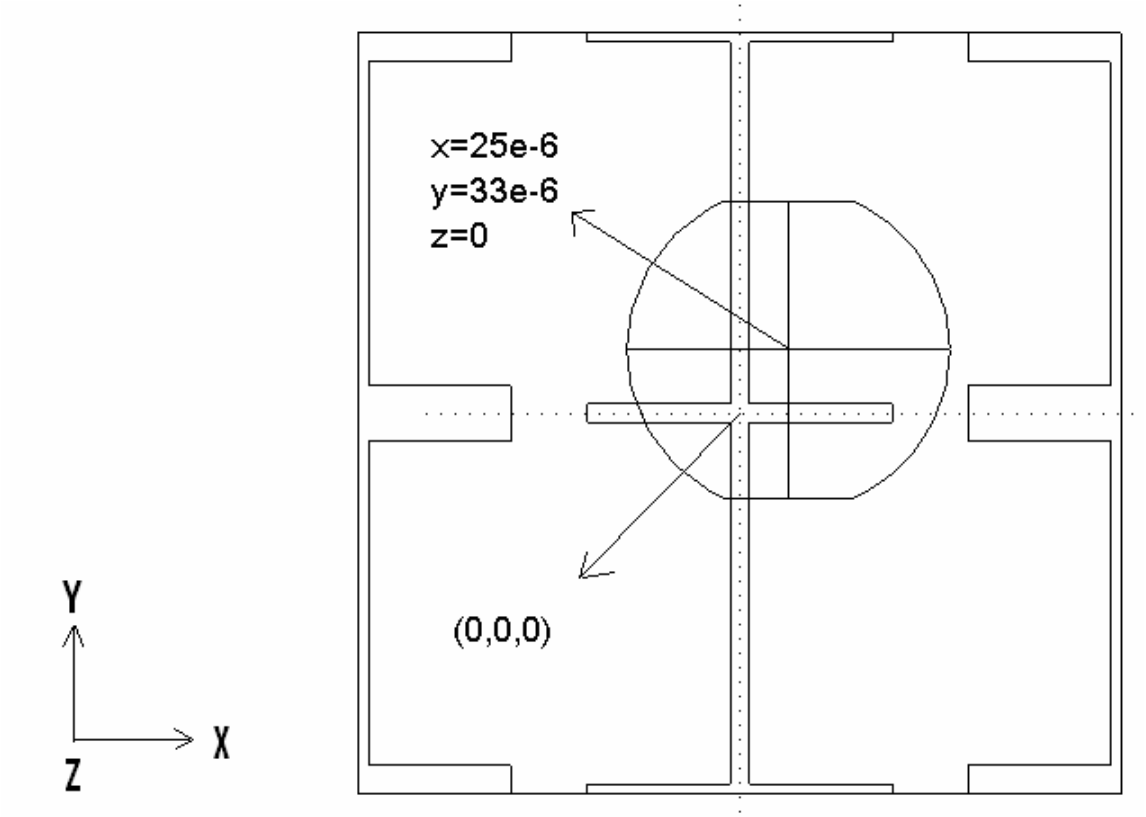

Figure 5.10 Coordinate System and Particle Location

5.3.1 Dielectric Forces

In addition to the particle location of (25, 33, -15), the finite element analysis was also performed for a particle centered at (25, 33, 0), which corresponds to the center of the liquid layer in the vertical direction. The analysis was performed for both locations because, when the particle was located on the bottom of the liquid, the finite element code did not obtain a solution. Tables 5.1 through 5.3 contain the electric body force resultant and electric traction resultant for the normal polarity.

At initial time and position, the direction of particle movement in the experiment is positive *x*, negative *y*, and positive *z*-direction. However, at final time and position, the particle movement is stopped.

Table 5.1 Electric Forces Acting on a 170 Micrometer Soda Lime Glass Sphere (Voltage Is 20V, Normal Polarity Between Electrodes, Centered at 25,33,0)

	Body Force Resultant (N)	Electric Traction Resultant (N)	Total Electric Force Resultant (N)
x-component	-1.5747×10^{-10}	-1.1123×10^{-10}	-2.6870×10^{-10}
y-component	-3.2766×10^{-10}	-2.1366×10^{-10}	-5.4123×10^{-10}
z-component	-2.6034×10^{-9}	-1.7054×10^{-9}	-4.3088×10^{-9}

Table 5.2 Electric Forces Acting on a 170 Micrometer Soda Lime Glass Sphere (Voltage Is 25V, Normal Polarity Between Electrodes, Centered at 25,33,0)

	Body Force Resultant (N)	Electric Traction Resultant (N)	Total Electric Force Resultant (N)
x-component	-2.4604×10^{-10}	-1.7379×10^{-10}	-4.1981×10^{-10}
y-component	-5.1197×10^{-10}	-3.3385×10^{-10}	-8.4582×10^{-10}
z-component	-4.0679×10^{-9}	-2.6648×10^{-9}	-6.7327×10^{-9}

Table 5.3 Electric Forces Acting on a 170 Micrometer Soda Lime Glass Sphere (Voltage Is 25V, Normal Polarity Between Electrodes, Centered at 25,33,-15)

	Body Force Resultant (N)	Electric Traction Resultant (N)	Total Electric Force Resultant (N)
x-component	-1.1728×10^{-9}	-3.0403×10^{-10}	-4.2131×10^{-10}
y-component	-1.4861×10^{-9}	-6.2904×10^{-10}	-7.7765×10^{-10}
z-component	-1.1652×10^{-8}	-1.0524×10^{-8}	-2.2176×10^{-8}

5.3.2 Effects of a Surface Free Charge

In experiments 9-11, as in 13-15, the particle reverses its position when the sign of the applied potential is reversed. Reversing the potential does not change the body force in the liquid or particle, nor does it change the surface traction on the particle. Therefore, we surmise that there is either a volume free charge or a surface free charge on the particle. The volume free charge may be due to ions diffusing from the glass, but this may be countered by the accumulation of an opposite charge on the glass surface. Accumulation of surface free charge is more likely than volume free charge.

To investigate the effect of a surface free charge, we will consider the case of a single dielectric sphere in an infinite medium. The total electric body force and surface traction are due to both the electric field caused by the surface free charge and the electric field due by the uniform applied field:

$$E_{tot}=E_{free}+E_{applied} \tag{5.1}$$

Because the particle is a dielectric, not a conductor, the surface free charge does not have to be uniformly distributed on the surface of the particle. However, we will assume a uniform distribution to simplify the analysis. As demonstrated in section 2.3, the surface free charge does not induce a field in the particle. Therefore, the field in the particle is due only to the applied field, and as demonstrated in section 2.2, the field is uniform in the particle and therefore does not produce a body force.

As shown in sections 2.2 and 2.3, both the applied field and the surface charge produce a field on the surface of the particle. The sum of these two fields must be used in calculating the electric surface tractions. Using Maple (Appendix B), the electric surface traction resultant was determined for a uniform applied field in the z direction. For a particle of radius R= 85 microns, the result is

$$F_x = 0 \tag{5.2a}$$

$$F_y = 0 \tag{5.2b}$$

$$F_z = (1.233\text{x}10^{-7})qE_{ext} \tag{5.2c}$$

In order to develop an intuitive sense of the magnitude of this force, we will compare it to the force that one would obtain if the same free charge density and applied field acted on a flat sheet of charge with an area equal to that of the sphere,

$$F_z = 4\pi R^2 qE_{ext} = 4\pi(8.5\text{x}10^{-5})^2 qE_{ext} = (9.07\text{x}10^{-8})qE_{ext} \tag{5.3}$$

and a sheet of charge with area equal to the projected area of the sphere,

$$F_z = \pi R^2 qE_{ext} = \pi(8.5\text{x}10^{-5})^2 qE_{ext} = (2.27\text{x}10^{-8})qE_{ext} \tag{5.4}$$

The magnitude of the traction resultant can also be intuitively understood by assuming that the free charge density is equal to the free charge density that would occur on a flat capacitor plate with a dielectric having the same permittivity as the liquid polymer $\varepsilon_f = 0.352\text{x}10^{-10}$:

$$q = \varepsilon_f E_{ext} \tag{5.5}$$

Equation 5.4 then becomes

$$F_z = (1.233\text{x}10^{-7})\varepsilon_f (E_{ext})^2 = (4.34\text{x}10^{-18})(E_{ext})^2 \tag{5.6}$$

Assume that $E_{ext} = 1\text{x}10^5\,\text{N/C}$, which corresponds to a voltage change of 20 volts across a distance of 200 microns. Then, the force is $F_z = 4.34\text{x}10^{-8}\,\text{N}$. This force is approximately twenty-five percent of the norm of the dielectric force resultant, $0.98\text{x}10^{-8}\,\text{N}$, obtained from the forces in Table 5.1.

5.3.3 Fluid Mechanics With a Particle

In the real experiment, the liquid experiences a body force and flows around the particle. However, in order to get an approximate estimate of the relative velocity of the liquid and the particle, let us assume that the liquid motion is due only to a moving particle. The equilibrium velocity of a spherical particle in an infinitely extended liquid can be calculated by setting the total electric force equal to the fluid drag force, as reviewed in Section 2,

$$F^{drag} = 6\pi\nu a\text{v} \tag{5.7}$$

For η=100 centipoise = 0.1 kg/(m·sec), and a particle of radius 85 microns, the total electric forces of Table 5.1 result in the following equilibrium velocity:

V_x = 16 microns/sec, V_y = 13.8 microns/sec, V_z = 57.6 microns/sec

For the finite element analysis, the particle is assumed to be fixed. When the center of the particle is located at the point (25, 33, 0) in the model, the finite element analysis gives the following values (Table 5.4) for the liquid shearing force resultant on the particle and the liquid normal (pressure) force resultant on the particle for the normal polarity.

Table 5.4 Fluid Forces Acting on a 170micrometer Soda Lime Glass Sphere (Voltage Is 25V, Normal Polarity Between Electrodes, Centered at 25,33,0)

	Liquid Shearing Force Resultant (N)	Liquid Normal (Pressure) Force Resultant (N)	Total Liquid Traction Resultant (N)
x-component	3.441×10^{-10}	-2.874×10^{-10}	5.673×10^{-11}
y-component	2.861×10^{-10}	-7.505×10^{-10}	-4.644×10^{-10}
z-component	1.979×10^{-10}	-3.768×10^{-9}	-3.5703×10^{-9}

The fluid force resultant is of the same order of magnitude as the dielectric force resultant of Table 5.2, but the fluid and dielectric forces are not in equilibrium. We surmise that the equilibrium is established by a free charge in the particle and/or on the particle surface, which is not included in the finite element analysis. Alternatively, there

could be a free charge in the liquid, and that would cause the motion of the liquid to reverse when the polarity is reversed. However, we believe it is more likely that the free charge is in or on the particle. The glass particle contains sodium ions, which are very mobile. In the presence of an electric field, these ions can diffuse according to the Nernst-Planck equation, although the diffusion should be very slow at room temperature. If the sodium ions diffuse from one part of the particle to the other, then there will be a distribution of free charge within the particle.

Finally, the lack of equilibrium between the dielectric and fluid forces when the particle is centered at (25,33,0) may be due to the fact that the particle is actually located at (25,33,-15) in the experiment, so that the fluid and dielectric forces should not be in equilibrium at (25,33,0).

6. CONCLUSIONS AND RECOMMENDATIONS FOR FUTURE WORK

6.1 Conclusions

Although the experiments demonstrated that an array of microelectrodes can be used to pattern dielectric spheres in liquid polymers, the experimental results were inconclusive. The 30 micron spheres formed clusters associated with the regions of highest electric energy density, whereas single 90 micron spheres were located at the regions of highest electric energy density. The 170 micron spheres generally did not form patterns. The experiments indicated that free charges, either in the volume of the sphere and/or on the sphere surface, significantly influence the motion of the sphere.

The experiments and analysis indicated that there may be a free charge in the particles, and/or on the particle surface, and/or in the liquid, and that this charge produces forces that significantly affect the particle dynamics.

6.2 Recommendations for Future Work

(1) The experiments suggested that there may be surface free charges on the particles. The surface free charge should be removed from the particles.

(2) The effect of the particle size relative to the unit cell of the electrode array should be studied. Patterning experiments should be conducted with one of unit cell, and particles that vary in size. For example, the ten different particle sizes could be used, beginning with a size that is 0.9 times sizes of unit cells and increasing in increments of 5%.

(3) Arrays of micromagnets or electromagnets should be used to pattern magnetic particles.

(4) Arrays of micromagnets or electromagnets and electrodes should be used to simultaneously pattern both magnetic and dielectric particles.

(5) For a liquid with no particles present, it would be interesting to determine whether electrode and magnet arrays could produce electric and magnetic body forces that sum to zero, so there would be no fluid convection even though there were electric and magnetic body forces present.

(6) The following method described in Figure 6.1 may enhance the patterning of particles. A uniform external and/or magnetic field is used to align the particles in long chains. The electrode and/or electromagnet arrays are then activated, which breaks the particle chains and patterns the particles.

Sequence in Patterning of Particles

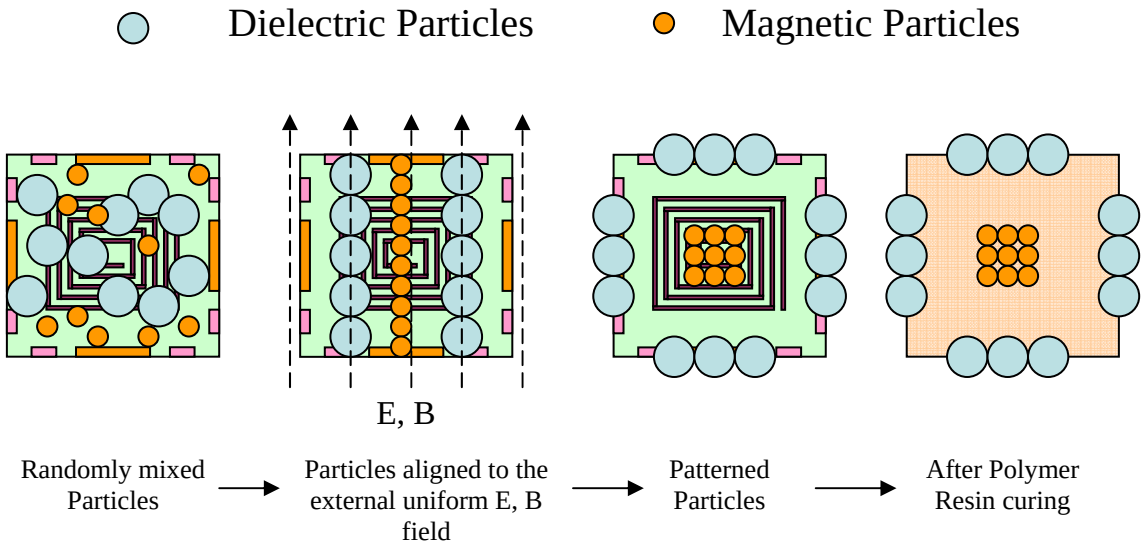

Figure 6.1 Possible Method to Pattern Particles

REFERENCES

Ahn C.H. and Allen M.G., 1994 Fully Integrated Micromachined Magnetic Particle Manipulator and Separator *Proc. IEEE Micro Electro Mechanical Systems Workshop* 91-96

Batchelor G.K. 1976 Developments in Microhydrodynamics, *Theoretical and Applied Mechanics*, W.T. Koiter, ed., (Amsterdam: North-Holland) 33-55

Bowen C. P., Shrout, T. R. and Randall, C. A. 1993 Intelligent Processing of Composite Materials *Adaptive Structures and Material Systems, (ASME)*, **AD-35** 53-62

Bowen, C. P., Bhalla, A. S., T. R., Newnham, and Randall, C. A., 1994 An Investigation of the Assembly Conditions of Dielectric Particles in Uncured Thermoset Polymer *J. Mater. Res.,* **9** (3) 781-788

Bowen C. P., Shrout T. R., Newnham R. E. and Randall C. A. 1995 Tunable Electric Field Processing of Composite Materials *J. of Intelligent Material Systems and Structures*, **6** 159-168

Cornejo I.A., Weitz G.E. and Cass R. 2000 Advanced Piezoelectric Continuous Fibers *U.S. Navy Workshop on Acoustic Transduction Materials and Devices* April 11-13

Fuhr, G. and Shirley S.G. 1995 Cell Handling and Characterization Using Micron and Submicron Electrode Arrays: State of the Art and Perspectives of Semiconductor Microtools *Journal of Micromechanics and Microengineering*, **5** (2) 77-85

Giner V., Sancho M. and Martinez G. 1995 Electromagnetic Forces on Dissipative Dielectric Media *Am. J. Phys*. **63 (**8) 749-753

Green N.G., Morgan H, Wilkinson C.D. and Milner J.J. 1995 Dielectrophoresis of Virus Particles *Proc. St Andrews Meeting of the Society for Experimental Biology* St. Andrews, UK, 77

Green N.G. and Morgan H 1997 Dielectrophoretic Separation of Nano-particles *J. Phys.D: Appl. Phys*. **30 L** 41-44

Green N.G., Morgan H and Milner J.J. 1997 Manipulation and Trapping of Submicron Bioparticles Using Dielectrophoresis *J. Biochem. Biophys. Methods* **35** 89-102

Jackson J.D. 1975 *Classical Electrodynamics*, 2nd ed., Chap.4 (New York: Wiley)

Janos B.Z., Dunn C.T. and Hagood N.W. 2000 Recent Advances in Manufacturing of Active Fiber Composites *U.S. Navy Workshop on Acoustic Transduction Materials and Devices*, April 11-13

Jones T.B. 1995 *Electromechanics of Particles* (Cambridge: Cambridge University Press)

Lee J-S, Boyd J.G. and Lagoudas D.C. 2005 Effective Properties of Three-Phase Electro-Magneto-Elastic Composites *International Journal of Engineering Science* **43** 790-825

Maugin G. 1988 *Continuum Mechanics of Electromagnetic Solids* (Amsterdam: North Holland Publishing)

McKnight G.P. and Carman G.P. 2000 Energy Absorption in Axial and Shear Loading of Particulate Magnetostrictive Composites *Smart Structures and Materials 2000: Active Materials: Behavior and Mechanics*, Christopher S. Lynch, Ed., Proceedings of SPIE, **3992** 556 -579

Moulson A.J. and Herbert J.M. 1990 *Electroceramics, Materials, Properties, Applications* (New York: Chapman & Hall)

Muller T., Gerardino A., Schnelle T., Shirley S.G., Bordoni F., DeGasperis G., Leoni R. and Fuhr G. 1996 Trapping of Micrometre and Sub-Micrometre Particles by High-Frequency Electric Fields and Hydrodynamic Forces *J. Phys D: Appl. Phys.* **29** 340-349

Rossetti G.A., Pizzochero A and Bent A.A. 2000 Progress in the Development of Active Fiber Composites *U.S. Navy Workshop on Acoustic Transduction Materials and Devices,* April 11-13

Russel W.B., Saville D.A. and Schowalter W.R. 1989 *Colloidal Dispersions* (Cambridge: Cambridge University Press)

Sobek D., Senturia S.D. and Gray M. L. 1994 Microfabricated Fused Silica Flow Chambers for Flow Cytometry 260-263, *Proc. Solid-State Sensor and Actuator Workshop* (Hilton Head Island, SC, June 13-16) pp 260-263

Washizu A., Nanba T. and Masuda S. 1990 Handling Biological Cells Using a Fluid Integrated Circuit *IEEE Transactions on Industry Applications*, **26** (2) 352-358

Washizu M. 1992 Manipulation of Biological Objects in Micromachined Structures *MicroElectro Mechanical System '92* (Travemunde, Germany) February 4-7, pp 196-201

White F.M. 1991 *Viscous Fluid Flow* (New York: McGraw-Hill, Inc.)

APPENDIX A

The dissertation includes the following video files:
“90 micron patterning”: successful patterning of 90 micron particles
“90 micron not patterned”: unsuccessful patterning of 90 micron particles
“30 micron clusters”: 30 micron particles do not pattern, but form clusters
“30 micron movie”: more evidence of the same
“three 30 micron”
“separate two 170 micron”: two 170 micron particles near together can be separated
“particle reversal”: reversing the polarity of the voltage reverses the particle position
“particle reversal continued”: more of the same

How TO Install the CODEC File to View the Videos

Codec File Name : TSCC.exe

Install Guide

Double click TSCC.exe

If you have Windows SP2, the following window will pop up.
Click Run

Click Install

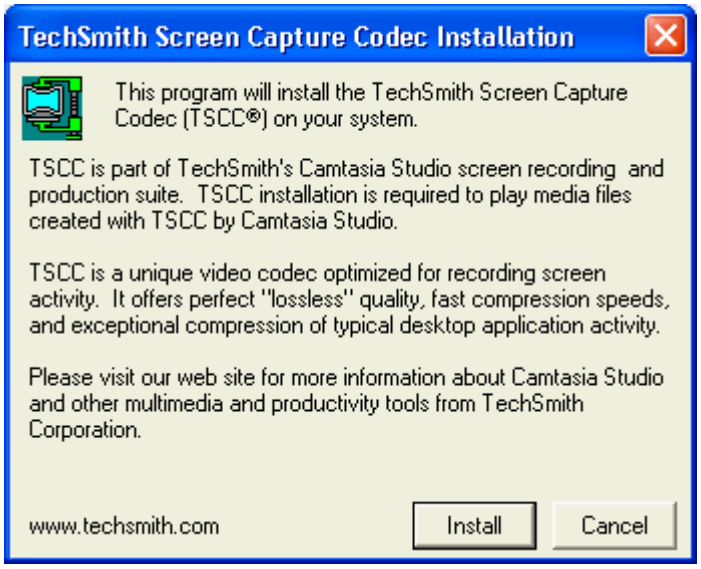

Click OK

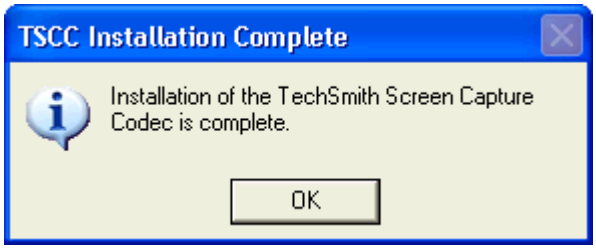

Finished

APPENDIX B

The total traction resultant on a single dielectric sphere containing a nonzero surface charge, placed in a uniform electric field, with the radius as a parameter.

The relative permittivity of the sphere is 7.3 (for soda lime glass) and the relative permittivity of the fluid is 3.98 (EPON 8021 resin).

```
> restart;
> E0:=8.854e-12;
```

$$E0 := 8.854\ 10^{-12}$$

```
> Rp:=7.3;Rf:=3.98;
```

$$Rp := 7.3$$

$$Rf := 3.98$$

```
> Ep:=Rp*E0;Ef:=Rf*E0;
```

$$Ep := 6.46342\ 10^{-11}$$

$$Ef := 3.523892\ 10^{-11}$$

```
> Efx:=C1*(x*(R^2-x^2-y^2)^0.5)/R^2+C2*x/R;
```

$$Efx := \frac{C1\ x\ (R^2 - x^2 - y^2)^{0.5}}{R^2} + \frac{C2\ x}{R}$$

```
> Efxn:=-C1*(x*(R^2-x^2-y^2)^0.5)/R^2+C2*x/R;
```

$$Efxn := -\frac{C1\ x\ (R^2 - x^2 - y^2)^{0.5}}{R^2} + \frac{C2\ x}{R}$$

```
> Efy:=C1*(y*(R^2-x^2-y^2)^0.5)/R^2+C2*y/R;
```

$$Efy := \frac{C1\ y\ (R^2 - x^2 - y^2)^{0.5}}{R^2} + \frac{C2\ y}{R}$$

```
> Efyn:=-C1*(y*(R^2-x^2-y^2)^0.5)/R^2+C2*y/R;
```

$$Efyn := -\frac{C1\ y\ (R^2 - x^2 - y^2)^{0.5}}{R^2} + \frac{C2\ y}{R}$$

```
> Efz:=C1/3*(2*R^2-3*x^2-3*y^2)/R^2+C3+C2*(R^2-x^2-y^2)^0.5/R;
```

$$Efz := \frac{C1\,(2\,R^2 - 3\,x^2 - 3\,y^2)}{3\,R^2} + C3 + \frac{C2\,(R^2 - x^2 - y^2)^{0.5}}{R}$$

> Efzn:=C1/3*(2*R^2-3*x^2-3*y^2)/R^2+C3-C2*(R^2-x^2-y^2)^0.5/R;

$$Efzn := \frac{C1\,(2\,R^2 - 3\,x^2 - 3\,y^2)}{3\,R^2} + C3 - \frac{C2\,(R^2 - x^2 - y^2)^{0.5}}{R}$$

> Epx:=0;

$$Epx := 0$$

> Epxn:=0;

$$Epxn := 0$$

> Epy:=0;

$$Epy := 0$$

> Epyn:=0;

$$Epyn := 0$$

> Epz:=C4;

$$Epz := C4$$

> Epzn:=C4;

$$Epzn := C4$$

> nx:=x/R;

$$nx := \frac{x}{R}$$

> nxn:=x/R;

$$nxn := \frac{x}{R}$$

> ny:=y/R;

$$ny := \frac{y}{R}$$

> nyn:=y/R;

$$nyn := \frac{y}{R}$$

> nz:=(R^2-x^2-y^2)^0.5/R;

$$nz := \frac{(R^2 - x^2 - y^2)^{0.5}}{R}$$

> nzn:=-(R^2-x^2-y^2)^0.5/R;

$$nzn := -\frac{(R^2 - x^2 - y^2)^{0.5}}{R}$$

> dA:=R/(R^2-x^2-y^2)^0.5;

$$dA := \frac{R}{(R^2 - x^2 - y^2)^{0.5}}$$

> dtx:=nx*(Ef*Efx*Efx-0.5*E0*(Efx*Efx+Efy*Efy+Efz*Efz)-Ep*Epx*Epx+0.5*E0*(Epx*Epx+Epy*Epy+Epz*Epz))+ny*(Ef*Efx*Efy-Ep*Epx*Epy)+nz*(Ef*Efx*Efz-Ep*Epx*Epz);

$$dtx := \frac{1}{R}\left(x\left(3.081192\ 10^{-11}\left(\frac{C1\ x\ (R^2 - x^2 - y^2)^{0.5}}{R^2} + \frac{C2\ x}{R} \right)^2 \right.\right.$$

$$- 4.4270\ 10^{-12}\left(\frac{C1\ y\ (R^2 - x^2 - y^2)^{0.5}}{R^2} + \frac{C2\ y}{R} \right)^2$$

$$\left.\left. - 4.4270\ 10^{-12}\left(\frac{C1\ (2\,R^2 - 3\,x^2 - 3\,y^2)}{3\,R^2} + C3 + \frac{C2\ (R^2 - x^2 - y^2)^{0.5}}{R} \right)^2 + 4.4270\ 10^{-12}\ C4^2 \right) \right)$$

$$+ \frac{3.523892\ 10^{-11}\ y\left(\frac{C1\ x\ (R^2 - x^2 - y^2)^{0.5}}{R^2} + \frac{C2\ x}{R} \right)\left(\frac{C1\ y\ (R^2 - x^2 - y^2)^{0.5}}{R^2} + \frac{C2\ y}{R} \right)}{R} + \frac{1}{R}\left(3.5238\backslash \right.$$

$$92\ 10^{-11}\ (R^2 - x^2 - y^2)^{0.5}\left(\frac{C1\ x\ (R^2 - x^2 - y^2)^{0.5}}{R^2} + \frac{C2\ x}{R} \right)\left(\frac{C1\ (2\,R^2 - 3\,x^2 - 3\,y^2)}{3\,R^2} + C3 \right.$$

$$\left.\left. + \frac{C2\ (R^2 - x^2 - y^2)^{0.5}}{R} \right) \right)$$

> dtxn:=nxn*(Ef*Efxn*Efxn-0.5*E0*(Efxn*Efxn+Efyn*Efyn+Efzn*Efzn)-Ep*Epxn*Epxn+0.5*E0*(Epxn*Epxn+Epyn*Epyn+Epzn*Epzn))+nyn*(Ef*Efxn*Efyn-Ep*Epxn*Epyn)+nzn*(Ef*Efxn*Efzn-Ep*Epxn*Epzn);

$$dtxn := \frac{1}{R}\left(x\left(3.081192\ 10^{-11}\left(-\frac{C1\ x\ (R^2 - x^2 - y^2)^{0.5}}{R^2} + \frac{C2\ x}{R} \right)^2 \right.\right.$$

$$\left.\left. - 4.4270\ 10^{-12}\left(-\frac{C1\ y\ (R^2 - x^2 - y^2)^{0.5}}{R^2} + \frac{C2\ y}{R} \right)^2 \right.\right.$$

$$- 4.4270\ 10^{-12}\left(\frac{C1\,(2\,R^2 - 3\,x^2 - 3\,y^2)}{3\,R^2} + C3 - \frac{C2\,(R^2 - x^2 - y^2)^{0.5}}{R} \right)^2 + 4.4270\ 10^{-12}\,C4^2 \Bigg) \Bigg)$$

$$+ \frac{3.523892\ 10^{-11}\,y\left(- \frac{C1\,x\,(R^2 - x^2 - y^2)^{0.5}}{R^2} + \frac{C2\,x}{R} \right)\left(- \frac{C1\,y\,(R^2 - x^2 - y^2)^{0.5}}{R^2} + \frac{C2\,y}{R} \right)}{R} - \frac{1}{R}$$

$$\left(3.523892\ 10^{-11}\,(R^2 - x^2 - y^2)^{0.5}\left(- \frac{C1\,x\,(R^2 - x^2 - y^2)^{0.5}}{R^2} + \frac{C2\,x}{R} \right)\left(\frac{C1\,(2\,R^2 - 3\,x^2 - 3\,y^2)}{3\,R^2} + C3 \right.\right.$$

$$\left.\left. - \frac{C2\,(R^2 - x^2 - y^2)^{0.5}}{R} \right) \right)$$

```
> dty:=nx*(Ef*Efy*Efx-Ep*Epy*Epx)+ny*(Ef*Efy*Efy-
0.5*E0*(Efx*Efx+Efy*Efy+Efz*Efz)-
Ep*Epy*Epy+0.5*E0*(Epx*Epx+Epy*Epy+Epz*Epz))+nz*(Ef*Efy*Efz-
Ep*Epy*Epz);
```

$$dty := \frac{3.523892\ 10^{-11}\,x\left(\frac{C1\,x\,(R^2 - x^2 - y^2)^{0.5}}{R^2} + \frac{C2\,x}{R} \right)\left(\frac{C1\,y\,(R^2 - x^2 - y^2)^{0.5}}{R^2} + \frac{C2\,y}{R} \right)}{R} + \frac{1}{R}\left(y\left(3.0811\backslash \right.\right.$$

$$92\ 10^{-11}\left(\frac{C1\,y\,(R^2 - x^2 - y^2)^{0.5}}{R^2} + \frac{C2\,y}{R} \right)^2 - 4.4270\ 10^{-12}\left(\frac{C1\,x\,(R^2 - x^2 - y^2)^{0.5}}{R^2} + \frac{C2\,x}{R} \right)^2$$

$$\left.\left. - 4.4270\ 10^{-12}\left(\frac{C1\,(2\,R^2 - 3\,x^2 - 3\,y^2)}{3\,R^2} + C3 + \frac{C2\,(R^2 - x^2 - y^2)^{0.5}}{R} \right)^2 + 4.4270\ 10^{-12}\,C4^2 \right) \right) + \frac{1}{R}$$

$$\left(3.523892\ 10^{-11}\,(R^2 - x^2 - y^2)^{0.5}\left(\frac{C1\,y\,(R^2 - x^2 - y^2)^{0.5}}{R^2} + \frac{C2\,y}{R} \right)\left(\frac{C1\,(2\,R^2 - 3\,x^2 - 3\,y^2)}{3\,R^2} + C3 \right.\right.$$

$$\left.\left. + \frac{C2\,(R^2 - x^2 - y^2)^{0.5}}{R} \right) \right)$$

```
dtyn:=nxn*(Ef*Efyn*Efxn-Ep*Epyn*Epxn)+nyn*(Ef*Efyn*Efyn-
0.5*E0*(Efxn*Efxn+Efyn*Efyn+Efzn*Efzn)
Ep*Epyn*Epyn+0.5*E0*(Epxn*Epxn+Epyn*Epyn+Epzn*Epzn))+nzn*(Ef*Efyn*Efzn-
Ep*Epyn*Epzn);
```

$$dtyn := \frac{3.523892\,10^{-11}\,x\left(-\frac{C1\,x\,(R^2-x^2-y^2)^{0.5}}{R^2}+\frac{C2\,x}{R}\right)\left(-\frac{C1\,y\,(R^2-x^2-y^2)^{0.5}}{R^2}+\frac{C2\,y}{R}\right)}{R}+\frac{1}{R}\left(y\right.$$

$$\left(3.081192\,10^{-11}\left(-\frac{C1\,y\,(R^2-x^2-y^2)^{0.5}}{R^2}+\frac{C2\,y}{R}\right)^2\right.$$

$$-4.4270\,10^{-12}\left(-\frac{C1\,x\,(R^2-x^2-y^2)^{0.5}}{R^2}+\frac{C2\,x}{R}\right)^2$$

$$\left.-4.4270\,10^{-12}\left(\frac{C1\,(2R^2-3x^2-3y^2)}{3R^2}+C3-\frac{C2\,(R^2-x^2-y^2)^{0.5}}{R}\right)^2+4.4270\,10^{-12}\,C4^2\right)\left.\right)-\frac{1}{R}$$

$$\left(3.523892\,10^{-11}\,(R^2-x^2-y^2)^{0.5}\left(-\frac{C1\,y\,(R^2-x^2-y^2)^{0.5}}{R^2}+\frac{C2\,y}{R}\right)\left(\frac{C1\,(2R^2-3x^2-3y^2)}{3R^2}+C3\right.\right.$$

$$\left.\left.-\frac{C2\,(R^2-x^2-y^2)^{0.5}}{R}\right)\right)$$

> dtz:=nx*(Ef*Efz*Efx-Ep*Epz*Epx)+ny*(Ef*Efz*Efy-Ep*Epz*Epy)+nz*(Ef*Efz*Efz-Ep*Epz*Epz-0.5*E0*(Efx*Efx+Efy*Efy+Efz*Efz)+0.5*E0*(Epx*Epx+Epy*Epy+Epz*Epz));

$$dtz := \frac{1}{R}\left(3.523892\,10^{-11}\,x\left(\frac{C1\,x\,(R^2-x^2-y^2)^{0.5}}{R^2}+\frac{C2\,x}{R}\right)\left(\frac{C1\,(2R^2-3x^2-3y^2)}{3R^2}+C3\right.\right.$$

$$\left.\left.+\frac{C2\,(R^2-x^2-y^2)^{0.5}}{R}\right)\right)+\frac{1}{R}\left(3.523892\,10^{-11}\,y\left(\frac{C1\,y\,(R^2-x^2-y^2)^{0.5}}{R^2}+\frac{C2\,y}{R}\right)\left(\right.\right.$$

$$\left.\left.\frac{C1\,(2R^2-3x^2-3y^2)}{3R^2}+C3+\frac{C2\,(R^2-x^2-y^2)^{0.5}}{R}\right)\right)+\frac{1}{R}\left((R^2-x^2-y^2)^{0.5}\left(3.081192\,10^{-11}\right.\right.$$

$$\left(\frac{C1\,(2\,R^2 - 3\,x^2 - 3\,y^2)}{3\,R^2} + C3 + \frac{C2\,(R^2 - x^2 - y^2)^{0.5}}{R} \right)^2 - 6.02072\ 10^{-11}\ C4^2$$

$$- 4.4270\ 10^{-12} \left(\frac{C1\,x\,(R^2 - x^2 - y^2)^{0.5}}{R^2} + \frac{C2\,x}{R} \right)^2 - 4.4270\ 10^{-12} \left(\frac{C1\,y\,(R^2 - x^2 - y^2)^{0.5}}{R^2} + \frac{C2\,y}{R} \right)^2 \Bigg) \Bigg)$$

```
> dtzn:=nxn*(Ef*Efzn*Efxn-Ep*Epzn*Epxn)+nyn*(Ef*Efzn*Efyn-
Ep*Epzn*Epyn)+nzn*(Ef*Efzn*Efzn-Ep*Epzn*Epzn-
0.5*E0*(Efxn*Efxn+Efyn*Efyn+Efzn*Efzn)+0.5*E0*(Epxn*Epxn+Epyn*Epyn+Epzn*Epzn));
```

$$dtzn := \frac{1}{R} \left(3.523892\ 10^{-11}\ x \left(- \frac{C1\,x\,(R^2 - x^2 - y^2)^{0.5}}{R^2} + \frac{C2\,x}{R} \right) \left(\frac{C1\,(2\,R^2 - 3\,x^2 - 3\,y^2)}{3\,R^2} + C3 - \frac{C2\,(R^2 - x^2 - y^2)^{0.5}}{R} \right) \right) + \frac{1}{R} \left(3.523892\ 10^{-11}\ y \left(- \frac{C1\,y\,(R^2 - x^2 - y^2)^{0.5}}{R^2} + \frac{C2\,y}{R} \right) \left(\frac{C1\,(2\,R^2 - 3\,x^2 - 3\,y^2)}{3\,R^2} + C3 - \frac{C2\,(R^2 - x^2 - y^2)^{0.5}}{R} \right) \right) - \frac{1}{R} \left((R^2 - x^2 - y^2)^{0.5} \left(3.081192\ 10^{-11} \left(\frac{C1\,(2\,R^2 - 3\,x^2 - 3\,y^2)}{3\,R^2} + C3 - \frac{C2\,(R^2 - x^2 - y^2)^{0.5}}{R} \right)^2 - 6.02072\ 10^{-11}\ C4^2 - 4.4270\ 10^{-12} \left(- \frac{C1\,x\,(R^2 - x^2 - y^2)^{0.5}}{R^2} + \frac{C2\,x}{R} \right)^2 - 4.4270\ 10^{-12} \left(- \frac{C1\,y\,(R^2 - x^2 - y^2)^{0.5}}{R^2} + \frac{C2\,y}{R} \right)^2 \right) \right)$$

```
> xmin:=-(R^2-y^2)^0.5;
```

$$xmin := -(R^2 - y^2)^{0.5}$$

```
> xmax:=(R^2-y^2)^0.5;
```

$$xmax := (R^2 - y^2)^{0.5}$$

```
> ymin:=-(R^2-x^2)^0.5;
```

$$ymin := -(R^2 - x^2)^{0.5}$$

```
> ymax:=(R^2-x^2)^0.5;
```

$$ymax := (R^2 - x^2)^{0.5}$$

> Ixx:=int(dA*dtx,x=xmin..xmax);

$$Ixx := 0.$$

> Ixy:=int(Ixx,y=-R..R);

$$Ixy := 0.$$

> Iyx:=int(dA*dty,y=ymin..ymax);

$$Iyx := 0.$$

> Iyy:=int(Iyx,x=-R..R);

$$Iyy := 0.$$

> Izx:=int(dA*dtz,x=xmin..xmax);

$$Izx := \int_{-(R^2 - y^2)^{0.5}}^{(R^2 - y^2)^{0.5}} \frac{1}{(R^2 - x^2 - y^2)^{0.5}} \left(R \left(\frac{1}{R} \left(3.523892\ 10^{-11} x \left(\frac{C1\ x\ (R^2 - x^2 - y^2)^{0.5}}{R^2} + \frac{C2\ x}{R} \right) \left(\frac{C1\ (2\ R^2 - 3\ x^2 - 3\ y^2)}{3\ R^2} + C3 + \frac{C2\ (R^2 - x^2 - y^2)^{0.5}}{R} \right) \right) + \frac{1}{R} \left(3.523892\ 10^{-11} y \left(\frac{C1\ y\ (R^2 - x^2 - y^2)^{0.5}}{R^2} + \frac{C2\ y}{R} \right) \left(\frac{C1\ (2\ R^2 - 3\ x^2 - 3\ y^2)}{3\ R^2} + C3 + \frac{C2\ (R^2 - x^2 - y^2)^{0.5}}{R} \right) \right) + \frac{1}{R} \left((R^2 - x^2 - y^2)^{0.5} \left(3.081192\ 10^{-11} \left(\frac{C1\ (2\ R^2 - 3\ x^2 - 3\ y^2)}{3\ R^2} + C3 + \frac{C2\ (R^2 - x^2 - y^2)^{0.5}}{R} \right)^2 - 6.02072\ 10^{-11}\ C4^2 - 4.4270\ 10^{-12} \left(\frac{C1\ x\ (R^2 - x^2 - y^2)^{0.5}}{R^2} + \frac{C2\ x}{R} \right)^2 - 4.4270\ 10^{-12} \left(\frac{C1\ y\ (R^2 - x^2 - y^2)^{0.5}}{R^2} + \frac{C2\ y}{R} \right)^2 \right) \right) \right) \right) dx$$

> Izy:=int(Izx,y=-R..R);

$$Izy := \int_{-R}^{R} \int_{-(R^2 - y^2)^{0.5}}^{(R^2 - y^2)^{0.5}} \frac{1}{(R^2 - x^2 - y^2)^{0.5}} \left(R \left(\frac{1}{R} \left(3.523892\ 10^{-11}\, x \left(\frac{C1\, x\, (R^2 - x^2 - y^2)^{0.5}}{R^2} + \frac{C2\, x}{R} \right) \left(\frac{C1\, (2\, R^2 - 3\, x^2 - 3\, y^2)}{3\, R^2} + C3 + \frac{C2\, (R^2 - x^2 - y^2)^{0.5}}{R} \right) \right) + \frac{1}{R} \left(3.523892\ 10^{-11}\, y \left(\frac{C1\, y\, (R^2 - x^2 - y^2)^{0.5}}{R^2} + \frac{C2\, y}{R} \right) \left(\frac{C1\, (2\, R^2 - 3\, x^2 - 3\, y^2)}{3\, R^2} + C3 + \frac{C2\, (R^2 - x^2 - y^2)^{0.5}}{R} \right) \right) + \frac{1}{R} \left((R^2 - x^2 - y^2)^{0.5} \left(3.081192\ 10^{-11} \left(\frac{C1\, (2\, R^2 - 3\, x^2 - 3\, y^2)}{3\, R^2} + C3 + \frac{C2\, (R^2 - x^2 - y^2)^{0.5}}{R} \right)^2 - 6.02072\ 10^{-11}\, C4^2 - 4.4270\ 10^{-12} \left(\frac{C1\, x\, (R^2 - x^2 - y^2)^{0.5}}{R^2} + \frac{C2\, x}{R} \right)^2 - 4.4270\ 10^{-12} \left(\frac{C1\, y\, (R^2 - x^2 - y^2)^{0.5}}{R^2} + \frac{C2\, y}{R} \right)^2 \right) \right) \right) \right) dx\, dy$$

```
> Ixxn:=int(dA*dtxn,x=xmin..xmax);
```

$$Ixxn := 0.$$

```
> Ixyn:=int(Ixxn,y=-R..R);
```

$$Ixyn := 0.$$

```
> Iyxn:=int(dA*dtyn,y=ymin..ymax);
```

$$Iyxn := 0.$$

```
> Iyyn:=int(Iyxn,x=-R..R);
```

$$Iyyn := 0.$$

```
> Izxn:=int(dA*dtzn,x=xmin..xmax);
```

$$Izxn := \int_{-(R^2 - y^2)^{0.5}}^{(R^2 - y^2)^{0.5}} \frac{1}{(R^2 - x^2 - y^2)^{0.5}} \left(R \left(\frac{1}{R} \left(3.523892\ 10^{-11} x \left(- \frac{C1\, x\, (R^2 - x^2 - y^2)^{0.5}}{R^2} + \frac{C2\, x}{R} \right) \left(\right. \right. \right. \right.$$

$$\left. \left. \frac{C1\, (2\, R^2 - 3\, x^2 - 3\, y^2)}{3\, R^2} + C3 - \frac{C2\, (R^2 - x^2 - y^2)^{0.5}}{R} \right) \right) + \frac{1}{R} \left(3.523892\ 10^{-11} y \left(\right. \right.$$

$$\left. \left. - \frac{C1\, y\, (R^2 - x^2 - y^2)^{0.5}}{R^2} + \frac{C2\, y}{R} \right) \left(\frac{C1\, (2\, R^2 - 3\, x^2 - 3\, y^2)}{3\, R^2} + C3 - \frac{C2\, (R^2 - x^2 - y^2)^{0.5}}{R} \right) \right) - \frac{1}{R} \left(\right.$$

$$(R^2 - x^2 - y^2)^{0.5} \left(3.081192\ 10^{-11} \left(\frac{C1\, (2\, R^2 - 3\, x^2 - 3\, y^2)}{3\, R^2} + C3 - \frac{C2\, (R^2 - x^2 - y^2)^{0.5}}{R} \right)^2 \right.$$

$$- 6.02072\ 10^{-11}\, C4^2 - 4.4270\ 10^{-12} \left(- \frac{C1\, x\, (R^2 - x^2 - y^2)^{0.5}}{R^2} + \frac{C2\, x}{R} \right)^2$$

$$\left. \left. - 4.4270\ 10^{-12} \left(- \frac{C1\, y\, (R^2 - x^2 - y^2)^{0.5}}{R^2} + \frac{C2\, y}{R} \right)^2 \right) \right) \right) \right) \right) \, dx$$

> Izyn:=int(Izxn,y=-R..R);

$$Izyn := \int_{-R}^{R} \int_{-(R^2 - y^2)^{0.5}}^{(R^2 - y^2)^{0.5}} \frac{1}{(R^2 - x^2 - y^2)^{0.5}} \left(R \left(\frac{1}{R} \left(3.523892\ 10^{-11} x \left(- \frac{C1\, x\, (R^2 - x^2 - y^2)^{0.5}}{R^2} + \frac{C2\, x}{R} \right) \left(\right. \right. \right. \right.$$

$$\left. \left. \frac{C1\, (2\, R^2 - 3\, x^2 - 3\, y^2)}{3\, R^2} + C3 - \frac{C2\, (R^2 - x^2 - y^2)^{0.5}}{R} \right) \right) + \frac{1}{R} \left(3.523892\ 10^{-11} y \left(\right. \right.$$

$$\left. \left. - \frac{C1\, y\, (R^2 - x^2 - y^2)^{0.5}}{R^2} + \frac{C2\, y}{R} \right) \left(\frac{C1\, (2\, R^2 - 3\, x^2 - 3\, y^2)}{3\, R^2} + C3 - \frac{C2\, (R^2 - x^2 - y^2)^{0.5}}{R} \right) \right) - \frac{1}{R} \left(\right.$$

$$(R^2 - x^2 - y^2)^{0.5}\left(3.081192\ 10^{-11}\left(\frac{C1\,(2\,R^2 - 3\,x^2 - 3\,y^2)}{3\,R^2} + C3 - \frac{C2\,(R^2 - x^2 - y^2)^{0.5}}{R} \right)^2 \right.$$

$$- 6.02072\ 10^{-11}\,C4^2 - 4.4270\ 10^{-12}\left(- \frac{C1\,x\,(R^2 - x^2 - y^2)^{0.5}}{R^2} + \frac{C2\,x}{R} \right)^2$$

$$\left. - 4.4270\ 10^{-12}\left(- \frac{C1\,y\,(R^2 - x^2 - y^2)^{0.5}}{R^2} + \frac{C2\,y}{R} \right)^2 \right) \Bigg) \Bigg) \Bigg) \Bigg)\ dx\ dy$$

> Total_Traction_X:=Ixy+Ixyn;

$Total\_Traction\_X := 0.$

> Total_Traction_Y:=Iyy+Iyyn;

$Total\_Traction\_Y := 0.$

> Total_Traction_z:=Izy+Izyn;

$$Total\_Traction\_z := \int_{-R}^{R} \int_{-(R^2 - y^2)^{0.5}}^{(R^2 - y^2)^{0.5}} \frac{1}{(R^2 - x^2 - y^2)^{0.5}} \left(R\left(\frac{1}{R}\left(3.523892\ 10^{-11}\,x\left(\frac{C1\,x\,(R^2 - x^2 - y^2)^{0.5}}{R^2} \right.\right.\right.\right.$$

$$\left. + \frac{C2\,x}{R} \right)\left(\frac{C1\,(2\,R^2 - 3\,x^2 - 3\,y^2)}{3\,R^2} + C3 + \frac{C2\,(R^2 - x^2 - y^2)^{0.5}}{R} \right) \Bigg) + \frac{1}{R}\Bigg(3.523892\ 10^{-11}\,y\Bigg($$

$$\frac{C1\,y\,(R^2 - x^2 - y^2)^{0.5}}{R^2} + \frac{C2\,y}{R} \Bigg)\left(\frac{C1\,(2\,R^2 - 3\,x^2 - 3\,y^2)}{3\,R^2} + C3 + \frac{C2\,(R^2 - x^2 - y^2)^{0.5}}{R} \right) \Bigg) + \frac{1}{R}\Bigg($$

$$(R^2 - x^2 - y^2)^{0.5}\left(3.081192\ 10^{-11}\left(\frac{C1\,(2\,R^2 - 3\,x^2 - 3\,y^2)}{3\,R^2} + C3 + \frac{C2\,(R^2 - x^2 - y^2)^{0.5}}{R} \right)^2 \right.$$

$$\left. - 6.02072\ 10^{-11}\,C4^2 - 4.4270\ 10^{-12}\left(\frac{C1\,x\,(R^2 - x^2 - y^2)^{0.5}}{R^2} + \frac{C2\,x}{R} \right)^2 \right.$$

$$- 4.4270\ 10^{-12}\left(\frac{C1\, y\,(R^2 - x^2 - y^2)^{0.5}}{R^2} + \frac{C2\, y}{R} \right)^2 \Bigg) \Bigg) \Bigg) \Bigg)\ dx\ dy + \int_{-R}^{R} \int_{-(R^2 - y^2)^{0.5}}^{(R^2 - y^2)^{0.5}} \frac{1}{(R^2 - x^2 - y^2)^{0.5}} \Bigg($$

$$R \Bigg(\frac{1}{R} \Bigg(3.523892\ 10^{-11}\, x \left(- \frac{C1\, x\,(R^2 - x^2 - y^2)^{0.5}}{R^2} + \frac{C2\, x}{R} \right) \left(\frac{C1\,(2\,R^2 - 3\,x^2 - 3\,y^2)}{3\,R^2} + C3 \right.$$

$$\left. - \frac{C2\,(R^2 - x^2 - y^2)^{0.5}}{R} \right) \Bigg) + \frac{1}{R} \Bigg(3.523892\ 10^{-11}\, y \left(- \frac{C1\, y\,(R^2 - x^2 - y^2)^{0.5}}{R^2} + \frac{C2\, y}{R} \right) \Bigg($$

$$\frac{C1\,(2\,R^2 - 3\,x^2 - 3\,y^2)}{3\,R^2} + C3 - \frac{C2\,(R^2 - x^2 - y^2)^{0.5}}{R} \Bigg) \Bigg) - \frac{1}{R} \Bigg((R^2 - x^2 - y^2)^{0.5} \Bigg(3.081192\ 10^{-11}$$

$$\left(\frac{C1\,(2\,R^2 - 3\,x^2 - 3\,y^2)}{3\,R^2} + C3 - \frac{C2\,(R^2 - x^2 - y^2)^{0.5}}{R} \right)^2 - 6.02072\ 10^{-11}\, C4^2$$

$$- 4.4270\ 10^{-12}\left(- \frac{C1\, x\,(R^2 - x^2 - y^2)^{0.5}}{R^2} + \frac{C2\, x}{R} \right)^2 - 4.4270\ 10^{-12}\left(- \frac{C1\, y\,(R^2 - x^2 - y^2)^{0.5}}{R^2} + \frac{C2\, y}{R} \right)^2$$

$$\Bigg) \Bigg) \Bigg) \Bigg)\ dx\ dy$$

APPENDIX C

The total traction resultant on a single dielectric sphere containing a nonzero surface charge, placed in a uniform electric field, with a radius equal to 85 micrometers.

The relative permittivity of the sphere is 7.3 (for soda lime glass) and the relative permittivity of the fluid is 3.98 (EPON 8021 resin).

```
> restart;
> E0:=8.854e-12;
```
$$E0 := 8.854\ 10^{-12}$$
```
> Rp:=7.3;Rf:=3.98;
```
$$Rp := 7.3$$
$$Rf := 3.98$$
```
> Ep:=Rp*E0;Ef:=Rf*E0;
```
$$Ep := 6.46342\ 10^{-11}$$
$$Ef := 3.523892\ 10^{-11}$$
```
> R:=85E-6;
```
$$R := 0.000085$$
```
> C1:=3*(Ep-Ef)/(Ep+2*Ef)*Eext;
```
$$C1 := 0.6526867629\ Eext$$
```
> C2:=q/Ef;
```
$$C2 := 2.837771419\ 10^{10}\ q$$
```
> C3:=Eext;
```
$$C3 := Eext$$
```
> C4:=3*Ef/(Ep+2*Ef)*Eext;
```
$$C4 := 0.7824377457\ Eext$$
```
> Efx:=C1*(x*(R^2-x^2-y^2)^0.5)/R^2+C2*x/R;
```
$$Efx := 9.033726822\ 10^{7}\ Eext\ x\ (7.225\ 10^{-9} - x^{2} - y^{2})^{0.5} + 3.338554611\ 10^{14}\ q\ x$$
```
> Efxn:=-C1*(x*(R^2-x^2-y^2)^0.5)/R^2+C2*x/R;
```

$$Efxn := -9.033726822\ 10^{7}\ Eext\ x\ (7.225\ 10^{-9} - x^{2} - y^{2})^{0.5} + 3.338554611\ 10^{14}\ q\ x$$

> Efy:=C1*(y*(R^2-x^2-y^2)^0.5)/R^2+C2*y/R;

$$Efy := 9.033726822\ 10^{7}\ Eext\ y\ (7.225\ 10^{-9} - x^{2} - y^{2})^{0.5} + 3.338554611\ 10^{14}\ q\ y$$

> Efyn:=-C1*(y*(R^2-x^2-y^2)^0.5)/R^2+C2*y/R;

$$Efyn := -9.033726822\ 10^{7}\ Eext\ y\ (7.225\ 10^{-9} - x^{2} - y^{2})^{0.5} + 3.338554611\ 10^{14}\ q\ y$$

> Efz:=C1/3*(2*R^2-3*x^2-3*y^2)/R^2+C3+C2*(R^2-x^2-y^2)^0.5/R;

$$Efz := 3.011242274\ 10^{7}\ Eext\ (1.4450\ 10^{-8} - 3\ x^{2} - 3\ y^{2}) + Eext + 3.338554611\ 10^{14}\ q\ (7.225\ 10^{-9} - x^{2} - y^{2})^{0.5}$$

> Efzn:=C1/3*(2*R^2-3*x^2-3*y^2)/R^2+C3-C2*(R^2-x^2-y^2)^0.5/R;

$$Efzn := 3.011242274\ 10^{7}\ Eext\ (1.4450\ 10^{-8} - 3\ x^{2} - 3\ y^{2}) + Eext - 3.338554611\ 10^{14}\ q\ (7.225\ 10^{-9} - x^{2} - y^{2})^{0.5}$$

> Epx:=0;

$$Epx := 0$$

> Epxn:=0;

$$Epxn := 0$$

> Epy:=0;

$$Epy := 0$$

> Epyn:=0;

$$Epyn := 0$$

> Epz:=C4;

$$Epz := 0.7824377457\ Eext$$

> Epzn:=C4;

$$Epzn := 0.7824377457\ Eext$$

> nx:=x/R;

$$nx := 11764.70588\ x$$

> nxn:=x/R;

$$nxn := 11764.70588\ x$$

> ny:=y/R;

$$ny := 11764.70588\ y$$

> nyn:=y/R;

$$nyn := 11764.70588\ y$$

> nz:=(R^2-x^2-y^2)^0.5/R;

$$nz := 11764.70588\ (7.225\ 10^{-9} - x^{2} - y^{2})^{0.5}$$

> nzn:=-(R^2-x^2-y^2)^0.5/R;

$$nzn := -11764.70588\ (7.225\ 10^{-9} - x^{2} - y^{2})^{0.5}$$

> dA:=R/(R^2-x^2-y^2)^0.5;

$$dA := \frac{0.000085\ 1}{(7.225\ 10^{-9} - x^2 - y^2)^{0.5}}$$

> dtx:=nx*(Ef*Efx*Efx-0.5*E0*(Efx*Efx+Efy*Efy+Efz*Efz)-Ep*Epx*Epx+0.5*E0*(Epx*Epx+Epy*Epy+Epz*Epz))+ny*(Ef*Efx*Efy-Ep*Epx*Epy)+nz*(Ef*Efx*Efz-Ep*Epx*Epz);

$$dtx := 11764.70588\, x \left(3.081192\ 10^{-11} \left(9.033726822\ 10^{7}\, Eext x\, (7.225\ 10^{-9} - x^2 - y^2)^{0.5} + 3.338554611\ 10^{14}\, q\, x \right)^2 - 4.4270\ 10^{-12} \left(9.033726822\ 10^{7}\, Eext y\, (7.225\ 10^{-9} - x^2 - y^2)^{0.5} + 3.338554611\ 10^{14}\, q\, y \right)^2 - 4.4270\ 10^{-12} \left(3.011242274\ 10^{7}\, Eext\, (1.4450\ 10^{-8} - 3\, x^2 - 3\, y^2) + Eext + 3.338554611\ 10^{14}\, q\, (7.225\ 10^{-9} - x^2 - y^2)^{0.5} \right) \wedge 2 + 2.710248472\ 10^{-12}\, Eext^2 \right) + 4.145755293\ 10^{-7}\, y \left(9.033726822\ 10^{7}\, Eext x\, (7.225\ 10^{-9} - x^2 - y^2)^{0.5} + 3.338554611\ 10^{14}\, q\, x \right) \left(9.033726822\ 10^{7}\, Eext y\, (7.225\ 10^{-9} - x^2 - y^2)^{0.5} + 3.338554611\ 10^{14}\, q\, y \right) + 4.145755293\ 10^{-7}\, (7.225\ 10^{-9} - x^2 - y^2)^{0.5} \left(9.033726822\ 10^{7}\, Eext x\, (7.225\ 10^{-9} - x^2 - y^2)^{0.5} + 3.338554611\ 10^{14}\, q\, x \right) \left(3.011242274\ 10^{7}\, Eext\, (1.4450\ 10^{-8} - 3\, x^2 - 3\, y^2) + Eext + 3.338554611\ 10^{14}\, q\, (7.225\ 10^{-9} - x^2 - y^2)^{0.5} \right)$$

> dtxn:=nxn*(Ef*Efxn*Efxn-0.5*E0*(Efxn*Efxn+Efyn*Efyn+Efzn*Efzn)-Ep*Epxn*Epxn+0.5*E0*(Epxn*Epxn+Epyn*Epyn+Epzn*Epzn))+nyn*(Ef*Efxn*Efyn-Ep*Epxn*Epyn)+nzn*(Ef*Efxn*Efzn-Ep*Epxn*Epzn);

$$dtxn := 11764.70588\, x \left(3.081192\ 10^{-11} \left(-9.033726822\ 10^{7}\, Eext x\, (7.225\ 10^{-9} - x^2 - y^2)^{0.5} + 3.338554611\ 10^{14}\, q\, x \right)^2 - 4.4270\ 10^{-12} \left(-9.033726822\ 10^{7}\, Eext y\, (7.225\ 10^{-9} - x^2 - y^2)^{0.5} + 3.338554611\ 10^{14}\, q\, y \right)^2 - 4.4270\ 10^{-12} \left(3.011242274\ 10^{7}\, Eext\, (1.4450\ 10^{-8} - 3\, x^2 - 3\, y^2) + Eext - 3.338554611\ 10^{14}\, q\, (7.225\ 10^{-9} - x^2 - y^2)^{0.5} \right) \wedge 2 + 2.710248472\ 10^{-12}\, Eext^2 \right) + 4.145755293\ 10^{-7}\, y \left(-9.033726822\ 10^{7}\, Eext x\, (7.225\ 10^{-9} - x^2 - y^2)^{0.5} + 3.338554611\ 10^{14}\, q\, x \right) \left(\right.$$

$$-9.033726822\,10^{7}\,Eexty\,(7.225\,10^{-9}-x^{2}-y^{2})^{0.5}+3.338554611\,10^{14}\,q\,y\Big)-4.145755293\,10^{-7}$$

$$(7.225\,10^{-9}-x^{2}-y^{2})^{0.5}\Big(-9.033726822\,10^{7}\,Eextx\,(7.225\,10^{-9}-x^{2}-y^{2})^{0.5}+3.338554611\,10^{14}\,q\,x\Big)$$

$$\Big(3.011242274\,10^{7}\,Eext\,(1.4450\,10^{-8}-3\,x^{2}-3\,y^{2})+Eext-3.338554611\,10^{14}\,q\,(7.225\,10^{-9}-x^{2}-y^{2})^{0.5}$$

$$\Big)$$

```
> dty:=nx*(Ef*Efy*Efx-Ep*Epy*Epx)+ny*(Ef*Efy*Efy-
0.5*E0*(Efx*Efx+Efy*Efy+Efz*Efz)-
Ep*Epy*Epy+0.5*E0*(Epx*Epx+Epy*Epy+Epz*Epz))+nz*(Ef*Efy*Efz-
Ep*Epy*Epz);
```

$$dty := 4.145755293\,10^{-7}\,x\Big(9.033726822\,10^{7}\,Eextx\,(7.225\,10^{-9}-x^{2}-y^{2})^{0.5}+3.338554611\,10^{14}\,q\,x\Big)$$

$$\Big(9.033726822\,10^{7}\,Eexty\,(7.225\,10^{-9}-x^{2}-y^{2})^{0.5}+3.338554611\,10^{14}\,q\,y\Big)+11764.70588\,y\Big(3.0811\backslash$$

$$92\,10^{-11}\Big(9.033726822\,10^{7}\,Eexty\,(7.225\,10^{-9}-x^{2}-y^{2})^{0.5}+3.338554611\,10^{14}\,q\,y\Big)^{2}$$

$$-4.4270\,10^{-12}\Big(9.033726822\,10^{7}\,Eextx\,(7.225\,10^{-9}-x^{2}-y^{2})^{0.5}+3.338554611\,10^{14}\,q\,x\Big)^{2}-4.4270$$

$$10^{-12}\Big(3.011242274\,10^{7}\,Eext\,(1.4450\,10^{-8}-3\,x^{2}-3\,y^{2})+Eext$$

$$+3.338554611\,10^{14}\,q\,(7.225\,10^{-9}-x^{2}-y^{2})^{0.5}\Big)\,\wedge 2+2.710248472\,10^{-12}\,Eext^{2}\Big)+4.145755293\,10^{-7}$$

$$(7.225\,10^{-9}-x^{2}-y^{2})^{0.5}\Big(9.033726822\,10^{7}\,Eexty\,(7.225\,10^{-9}-x^{2}-y^{2})^{0.5}+3.338554611\,10^{14}\,q\,y\Big)$$

$$\Big(3.011242274\,10^{7}\,Eext\,(1.4450\,10^{-8}-3\,x^{2}-3\,y^{2})+Eext+3.338554611\,10^{14}\,q\,(7.225\,10^{-9}-x^{2}-y^{2})^{0.5}$$

$$\Big)$$

```
> dtyn:=nxn*(Ef*Efyn*Efxn-Ep*Epyn*Epxn)+nyn*(Ef*Efyn*Efyn-
0.5*E0*(Efxn*Efxn+Efyn*Efyn+Efzn*Efzn)-
Ep*Epyn*Epyn+0.5*E0*(Epxn*Epxn+Epyn*Epyn+Epzn*Epzn))+nzn*(Ef*Efyn*Efzn-
Ep*Epyn*Epzn);
```

$$dtyn := 4.145755293\,10^{-7}\,x\Big(-9.033726822\,10^{7}\,Eextx\,(7.225\,10^{-9}-x^{2}-y^{2})^{0.5}+3.338554611\,10^{14}\,q\,x\Big)\Big($$

$$-9.033726822\,10^{7}\,Eexty\,(7.225\,10^{-9}-x^{2}-y^{2})^{0.5}+3.338554611\,10^{14}\,q\,y\Big)+11764.70588\,y\Big(3.081192\,10^{-11}$$

$$\Big(-9.033726822\,10^{7}\,Eexty\,(7.225\,10^{-9}-x^{2}-y^{2})^{0.5}+3.338554611\,10^{14}\,q\,y\Big)^{2}$$

$$- 4.4270\ 10^{-12}\left(-9.033726822\ 10^{7}\ Eext\,x\,(7.225\ 10^{-9} - x^{2} - y^{2})^{0.5} + 3.338554611\ 10^{14}\ q\,x\right)^{2} - 4.4270\ 10^{-12}\left(3.011242274\ 10^{7}\ Eext\,(1.4450\ 10^{-8} - 3\,x^{2} - 3\,y^{2}) + Eext - 3.338554611\ 10^{14}\ q\,(7.225\ 10^{-9} - x^{2} - y^{2})^{0.5}\right) \text{^}2 + 2.710248472\ 10^{-12}\ Eext^{2}\right) - 4.145755293\ 10^{-7}\,(7.225\ 10^{-9} - x^{2} - y^{2})^{0.5}\left(-9.033726822\ 10^{7}\ Eext\,y\,(7.225\ 10^{-9} - x^{2} - y^{2})^{0.5} + 3.338554611\ 10^{14}\ q\,y\right)\left(3.011242274\ 10^{7}\ Eext\,(1.4450\ 10^{-8} - 3\,x^{2} - 3\,y^{2}) + Eext - 3.338554611\ 10^{14}\ q\,(7.225\ 10^{-9} - x^{2} - y^{2})^{0.5}\right)$$

> dtz:=nx*(Ef*Efz*Efx-Ep*Epz*Epx)+ny*(Ef*Efz*Efy-Ep*Epz*Epy)+nz*(Ef*Efz*Efz-Ep*Epz*Epz-0.5*E0*(Efx*Efx+Efy*Efy+Efz*Efz)+0.5*E0*(Epx*Epx+Epy*Epy+Epz*Epz));

$$dtz := 4.145755293\ 10^{-7}\,x\left(9.033726822\ 10^{7}\ Eext\,x\,(7.225\ 10^{-9} - x^{2} - y^{2})^{0.5} + 3.338554611\ 10^{14}\ q\,x\right)\left(3.011242274\ 10^{7}\ Eext\,(1.4450\ 10^{-8} - 3\,x^{2} - 3\,y^{2}) + Eext + 3.338554611\ 10^{14}\ q\,(7.225\ 10^{-9} - x^{2} - y^{2})^{0.5}\right) + 4.145755293\ 10^{-7}\,y\left(9.033726822\ 10^{7}\ Eext\,y\,(7.225\ 10^{-9} - x^{2} - y^{2})^{0.5} + 3.338554611\ 10^{14}\ q\,y\right)\left(3.011242274\ 10^{7}\ Eext\,(1.4450\ 10^{-8} - 3\,x^{2} - 3\,y^{2}) + Eext + 3.338554611\ 10^{14}\ q\,(7.225\ 10^{-9} - x^{2} - y^{2})^{0.5}\right) + 11764.70588\,(7.225\ 10^{-9} - x^{2} - y^{2})^{0.5}\left(3.081192\ 10^{-11}\left(3.011242274\ 10^{7}\ Eext\,(1.4450\ 10^{-8} - 3\,x^{2} - 3\,y^{2}) + Eext + 3.338554611\ 10^{14}\ q\,(7.225\ 10^{-9} - x^{2} - y^{2})^{0.5}\right) \text{^}2 - 3.685937922\ 10^{-11}\ Eext^{2} - 4.4270\ 10^{-12}\left(9.033726822\ 10^{7}\ Eext\,x\,(7.225\ 10^{-9} - x^{2} - y^{2})^{0.5} + 3.338554611\ 10^{14}\ q\,x\right)^{2} - 4.4270\ 10^{-12}\left(9.033726822\ 10^{7}\ Eext\,y\,(7.225\ 10^{-9} - x^{2} - y^{2})^{0.5} + 3.338554611\ 10^{14}\ q\,y\right)^{2}\right)$$

> dtzn:=nxn*(Ef*Efzn*Efxn-Ep*Epzn*Epxn)+nyn*(Ef*Efzn*Efyn-Ep*Epzn*Epyn)+nzn*(Ef*Efzn*Efzn-Ep*Epzn*Epzn-0.5*E0*(Efxn*Efxn+Efyn*Efyn+Efzn*Efzn)+0.5*E0*(Epxn*Epxn+Epyn*Epyn+Epzn*Epzn));

$$dtzn := 4.145755293\ 10^{-7}\,x\left(-9.033726822\ 10^{7}\ Eext\,x\,(7.225\ 10^{-9} - x^{2} - y^{2})^{0.5} + 3.338554611\ 10^{14}\ q\,x\right)\left(3.011242274\ 10^{7}\ Eext\,(1.4450\ 10^{-8} - 3\,x^{2} - 3\,y^{2}) + Eext - 3.338554611\ 10^{14}\ q\,(7.225\ 10^{-9} - x^{2} - y^{2})^{0.5}\right)$$

$$\Big) + 4.145755293\,10^{-7}\,y\Big(-9.033726822\,10^{7}\,Eext\,y\,(7.225\,10^{-9}-x^{2}-y^{2})^{0.5}+3.338554611\,10^{14}\,q\,y\Big)$$

$$\Big(3.011242274\,10^{7}\,Eext\,(1.4450\,10^{-8}-3\,x^{2}-3\,y^{2})+Eext-3.338554611\,10^{14}\,q\,(7.225\,10^{-9}-x^{2}-y^{2})^{0.5}$$

$$\Big) - 11764.70588\,(7.225\,10^{-9}-x^{2}-y^{2})^{0.5}\Big(3.081192\,10^{-11}\Big(3.011242274\,10^{7}\,Eext\,(1.4450\,10^{-8}-3\,x^{2}$$

$$-3\,y^{2})+Eext-3.338554611\,10^{14}\,q\,(7.225\,10^{-9}-x^{2}-y^{2})^{0.5}\Big)\,\text{^}2-3.685937922\,10^{-11}\,Eext^{2}$$

$$-4.4270\,10^{-12}\Big(-9.033726822\,10^{7}\,Eext\,x\,(7.225\,10^{-9}-x^{2}-y^{2})^{0.5}+3.338554611\,10^{14}\,q\,x\Big)^{2}$$

$$-4.4270\,10^{-12}\Big(-9.033726822\,10^{7}\,Eext\,y\,(7.225\,10^{-9}-x^{2}-y^{2})^{0.5}+3.338554611\,10^{14}\,q\,y\Big)^{2}\Big)$$

> xmin:=-(R^2-y^2)^0.5;

$$xmin := -(7.225\,10^{-9}-y^{2})^{0.5}$$

> xmax:=(R^2-y^2)^0.5;

$$xmax := (7.225\,10^{-9}-y^{2})^{0.5}$$

> ymin:=-(R^2-x^2)^0.5;

$$ymin := -(7.225\,10^{-9}-x^{2})^{0.5}$$

> ymax:=(R^2-x^2)^0.5;

$$ymax := (7.225\,10^{-9}-x^{2})^{0.5}$$

> Ixx:=int(dA*dtx,x=xmin..xmax);

$$Ixx := 0.$$

> Ixy:=int(Ixx,y=-R..R);

$$Ixy := 0.$$

> Iyx:=int(dA*dty,y=ymin..ymax);

$$Iyx := 0.$$

> Iyy:=int(Iyx,x=-R..R);

$$Iyy := 0.$$

> Izx:=int(dA*dtz,x=xmin..xmax);

$$Izx := \int_{-(7.225\ 10^{-9} - y^2)^{0.5}}^{(7.225\ 10^{-9} - y^2)^{0.5}} \frac{1}{(7.225\ 10^{-9} - x^2 - y^2)^{0.5}} \left(0.000085 \left(4.145755293\ 10^{-7}\, x \left(9.033726822\ 10^{7}\, Eext \right.\right.\right.$$

$$\left. x\,(7.225\ 10^{-9} - x^2 - y^2)^{0.5} + 3.338554611\ 10^{14}\, q\, x \right) \left(3.011242274\ 10^{7}\, Eext\,(1.4450\ 10^{-8} - 3\,x^2 - 3\,y^2) \right.$$

$$\left. + Eext + 3.338554611\ 10^{14}\, q\,(7.225\ 10^{-9} - x^2 - y^2)^{0.5} \right) + 4.145755293\ 10^{-7}\, y \left(9.033726822\ 10^{7}\, Eext\, y \right.$$

$$(7.225\ 10^{-9} - x^2 - y^2)^{0.5} + 3.338554611\ 10^{14}\, q\, y \left. \right) \left(3.011242274\ 10^{7}\, Eext\,(1.4450\ 10^{-8} - 3\,x^2 - 3\,y^2) \right.$$

$$\left. + Eext + 3.338554611\ 10^{14}\, q\,(7.225\ 10^{-9} - x^2 - y^2)^{0.5} \right) + 11764.70588\,(7.225\ 10^{-9} - x^2 - y^2)^{0.5}$$

$$\left(3.081192\ 10^{-11} \left(3.011242274\ 10^{7}\, Eext\,(1.4450\ 10^{-8} - 3\,x^2 - 3\,y^2) + Eext \right.\right.$$

$$\left. + 3.338554611\ 10^{14}\, q\,(7.225\ 10^{-9} - x^2 - y^2)^{0.5} \right) \text{^}2 - 3.685937922\ 10^{-11}\, Eext^2$$

$$- 4.4270\ 10^{-12} \left(9.033726822\ 10^{7}\, Eext\, x\,(7.225\ 10^{-9} - x^2 - y^2)^{0.5} + 3.338554611\ 10^{14}\, q\, x \right)^2$$

$$\left. - 4.4270\ 10^{-12} \left(9.033726822\ 10^{7}\, Eext\, y\,(7.225\ 10^{-9} - x^2 - y^2)^{0.5} + 3.338554611\ 10^{14}\, q\, y \right)^2 \right) \Bigg) \Bigg)\, dx$$

> Izy:=int(Izx,y=-R..R);

$$Izy := 563.1982626\, q^2 + 6.165596508\ 10^{-8}\, q\, Eext + 3.018869824\ 10^{-19}\, Eext^2$$

> Ixxn:=int(dA*dtxn,x=xmin..xmax);

$$Ixxn := 0.$$

> Ixyn:=int(Ixxn,y=-R..R);

$$Ixyn := 0.$$

> Iyxn:=int(dA*dtyn,y=ymin..ymax);

$$Iyxn := 0.$$

> Iyyn:=int(Iyxn,x=-R..R);

$$Iyyn := 0.$$

> Izxn:=int(dA*dtzn,x=xmin..xmax);

$$Izxn := \int_{-(7.225\ 10^{-9} - y^2)^{0.5}}^{(7.225\ 10^{-9} - y^2)^{0.5}} \frac{1}{(7.225\ 10^{-9} - x^2 - y^2)^{0.5}} \left(0.000085 \left(4.145755293\ 10^{-7}\ x \left(-9.033726822\ 10^{7}\ Eext x\ (7.225\ 10^{-9} - x^2 - y^2)^{0.5} + 3.338554611\ 10^{14}\ q\ x \right) \left(3.011242274\ 10^{7}\ Eext\ (1.4450\ 10^{-8} - 3\ x^2 - 3\ y^2) + Eext - 3.338554611\ 10^{14}\ q\ (7.225\ 10^{-9} - x^2 - y^2)^{0.5} \right) + 4.145755293\ 10^{-7}\ y \left(-9.033726822\ 10^{7}\ Eext y\ (7.225\ 10^{-9} - x^2 - y^2)^{0.5} + 3.338554611\ 10^{14}\ q\ y \right) \left(3.011242274\ 10^{7}\ Eext\ (1.4450\ 10^{-8} - 3\ x^2 - 3\ y^2) + Eext - 3.338554611\ 10^{14}\ q\ (7.225\ 10^{-9} - x^2 - y^2)^{0.5} \right) - 11764.70588\ (7.225\ 10^{-9} - x^2 - y^2)^{0.5} \left(3.081192\ 10^{-11} \left(3.011242274\ 10^{7}\ Eext\ (1.4450\ 10^{-8} - 3\ x^2 - 3\ y^2) + Eext - 3.338554611\ 10^{14}\ q\ (7.225\ 10^{-9} - x^2 - y^2)^{0.5} \right) \wedge 2 - 3.685937922\ 10^{-11}\ Eext^2 - 4.4270\ 10^{-12} \left(-9.033726822\ 10^{7}\ Eext x\ (7.225\ 10^{-9} - x^2 - y^2)^{0.5} + 3.338554611\ 10^{14}\ q\ x \right)^2 - 4.4270\ 10^{-12} \left(-9.033726822\ 10^{7}\ Eext y\ (7.225\ 10^{-9} - x^2 - y^2)^{0.5} + 3.338554611\ 10^{14}\ q\ y \right)^2 \right) \right) \right) dx$$

> Izyn:=int(Izxn,y=-R..R);

$$Izyn := -3.018869824\ 10^{-19}\ Eext^2 + 6.165596508\ 10^{-8}\ q\ Eext - 563.1982626\ q^2$$

> Total_Traction_X:=Ixy+Ixyn;

$$Total\_Traction\_X := 0.$$

> Total_Traction_Y:=Iyy+Iyyn;

$$Total\_Traction\_Y := 0.$$

> Total_Traction_z:=Izy+Izyn;

$$Total\_Traction\_z := 1.233119302\ 10^{-7}\ q\ Eext$$

VITA

Cheong Soo Seo

Permanent Address

2305 Studio Dr.

Brea, California 92821

United States of America

Personal

Date of birth: January 3, 1968

Place of birth: Seoul, Korea

Education

M.S. Mechanical Engineering (February 1992)
Sung Kyun Kwan University, Seoul, Korea

B.S. Aerospace Engineering (February 1998)
Sung Kyun Kwan University, Seoul, Korea.

Professional Experience

Graduate Research Assistant (Aug. 2000 – May 2004)
MEMS & NEMS Group, Texas A&M University, College Station, TX.
Graduate Research Assistant (May. 1999 – July 2000)
Mechanical Engineering, University of Illinois, Chicago, Il
Research Engineer (Mar. 1992 – Aug. 1998)
Electro Optic System Group, the 4^{th} R&D Division,
Agency for Defense Development, Daejeon, Korea